CONTRACT NAS8-31437

DEVELOPMENT OF A SOLAR POWERED RESIDENTIAL AIR CONDITIONER (GENERATOR OPTIMIZATION)

MARCH 1976

FINAL REPORT

PREPARED FOR:

GEORGE C. MARSHALL SPACE FLIGHT CENTER
MARSHALL SPACE FLIGHT CENTER
ALABAMA, 35812

CHRYSLER
CORPORATION

CONTRACT NAS8-31437

DEVELOPMENT OF A SOLAR POWERED RESIDENTIAL AIR CONDITIONER (GENERATOR OPTIMIZATION)

MARCH 1976

FINAL REPORT

PREPARED FOR:

GEORGE C. MARSHALL SPACE FLIGHT CENTER
MARSHALL SPACE FLIGHT CENTER
ALABAMA, 35812

Prepared By: D. J. Lowen
D. J. Lowen, Program Manager

Approved By: G. Salvador
G. Salvador, Manager
Florida Operations

CHRYSLER CORPORATION SPACE DIVISION
P. O. BOX 7806
CAPE CANAVERAL, FLORIDA 32920

NAS8-31437
FINAL REPORT

TABLE OF CONTENTS

ILLUSTRATIONS

NAS8-31437
FINAL REPORT

ABSTRACT

A commercially available 3-Ton residential Lithium Bromide (LiBr) absorption air conditioner was modified for use with lower temperature solar heated water. The modification included removal of components such as the generator, concentration control chamber, liquid trap, and separator; and the addition of a Chrysler designed generator, and an off-the-shelf LiBr-solution pump. The design goal of the modified unit was to operate with water as the heat-transfer fluid at a target temperature of 85°C (185°F), 29.4°C (85°F) cooling water inlet, producing 10.5 kW (3 tons) of cooling. Tests were performed on the system before and after modification to provide comparative data.

At elevated temperatures (96°C, 205°F), the test results show that Lithium Bromide was carried into the condenser due to the extremely violent boiling and degraded the evaporator performance. In addition, a "submergence effect" due to increased static head of the solution in the generator was observed. The submergence reduced the effective heat transfer by increasing the temperature required for boiling. The net effect is the reduction of vapor generation area within the generator. The original unmodified machine is rated (by the manufacturer) at 10.5 kW (3 tons) with 41.6 dm^3/M (11 GPM) firing water at 98.9C (210F) and 37.9 dm^3/M (10 GPM) tower water at 29.4C (85F). Its capacity decreases as the firing water temperature decreases until its capacity is 5.9 kW (1.68 tons) (manufacturer's data), at a firing water temperature of 87.8C (190F) with complete loss of cooling at a "cut-out" firing water temperature of 86.1C (187F). The test results show that, after modification, the system delivered 7 to 8 kW (2 to 2 1/3 tons) of cooling at a firing water temperature of 85C (185F) (with all other test parameters held constant) and "cut-out" did not occur until the firing water temperature reached 76.7C (170F).

INTRODUCTION

Solar powered air conditioning is provided to a residential solar demonstration site at the Marshall Space Flight Center by a commercially available lithium bromide absorption machine. It is powered with firing water which is heated by an array of solar panels and, when required, an auxiliary heater. The lithium bromide solution is circulated within the machine by thermal power. A percolator tube raises the solution to the high point of the machine from which it circulates by gravity feed.

The machine is rated at 10.5 kW (3 ton) capacity at the following conditions:

Hot Water Inlet Temperature	98.9 C	210 F
Hot Water Flow	41.6 dm^3/M	11 GPM
Hot Water Input	16.1 kW	55,000 BTUH
Air Flow	34.0 m^3/M	1200 CFM
Air Inlet Dry Bulb	26.7 C	80 F
Air Inlet Wet Bulb	19.4 C	67 F
Tower Water Inlet Temperature	29.4 C	85 F
Tower Water Flow	37.9 dm^3/M	10 GPM
Tower Water Heat Rejection	26.7 kW	91,000 BUTH

Since the conductive/convective heat losses from the solar panels depend on the panel-to-ambient temperature difference, a lower water temperature is desirable to improve the panel operating efficiency. Radiative heat losses depend on the absolute temperature raised to the fourth power which also indicates the desirability of lower panel temperatures.

A hot water inlet temperature of 85 C (185 F) was selected as an optimum compromise between raising the solar collector efficiency and the requirements of the lithium-bromide absorption cycle.

The primary purpose of this program is to design, fabricate, and install a generator and mechanical solution pump to improve the performance of the system by lowering operating temperature and maintaining system capacity. The pump has the secondary purpose of replacing the thermal percolation thereby reducing the static head on the generator to facilitate boiling.

The program includes testing the machine before and after modification to determine system performance and to obtain comparative data.

A. SYSTEM DESCRIPTION

The unmodified lithium-bromide absorption machine is shown in Figure 1. The condenser and evaporator function as they do in a compression system. The refrigerant (water) vapor is cooled and condensed by cooling water which flows in the condenser tubes. The cooling water represents an external heat sink and is from a cooling tower or well. The condenser is a conventional shell and tube heat exchanger.

The liquid refrigerant then flows through the refrigerant return line which contains a restriction. This resistance separates the relatively high pressure in the condenser from the low pressure in the evaporator and is analogous to the expansion valve of the compression cycle.

The evaporator transfers heat from the air stream to the refrigerant (water). The air is cooled and dehumidified as the refrigerant changes phase from liquid to vapor at lower pressure thereby utilizing its high latent heat of vaporization. The evaporator is constructed of externally finned tubes to improve the film coefficient of heat transfer on the air side. Internally the tubes are manifolded together to minimize the pressure drop between the evaporator and the absorber. This feature is required due to the extremely high specific volume of the refrigerant vapor.

The absorbent solution (strong lithium-bromide solution) has a high affinity for pure water and draws the vapor from the adjoining evaporator to the absorber. This absorbing of vapor into solution maintains the low pressure in the evaporator (and thus the low temperature) and is analogous to the suction inlet of a

compressor. The solution leaving the absorber is weak absorbent because it is more dilute and incapable of absorbing more vapor. The incoming strong absorbent is more concentrated in lithium-bromide and capable of absorbing refrigerant.

The absorption rate or rate of mass transfer of vapor into solution increases with low solution temperature and large surface area exposed to vapor. The absorber must be cooled, therefore, to remove the heat of dilution and the latent heat of vaporization which are released as the vapor is absorbed. Otherwise, the temperature within the absorber would rise and retard the absorption process. Cooling water is provided to the coil within the cylindrical absorber shell. The solution/vapor interface area is maximized by distributing the solution over the external surface of the water coil.

The weak absorbent passes through the liquid heat exchanger to the generator. The generator performs two functions, i. e., the refrigerant is boiled from the solution and the solution is raised or carried by the high speed vapor to the high point of the system from where it returns by gravity feed to the absorber. The boiling reclaims the refrigerant from the lithium-bromide solution. The vapor and solution are separated mechanically by an impingement type of baffled separator. The refrigerant vapor passes from the separator to the condenser to repeat its cycle of condensation, evaporation, and absorption. The hot solution, which has released the refrigerant in the generator to become

ABSORPTIVE AIR CONDITIONING SYSTEM

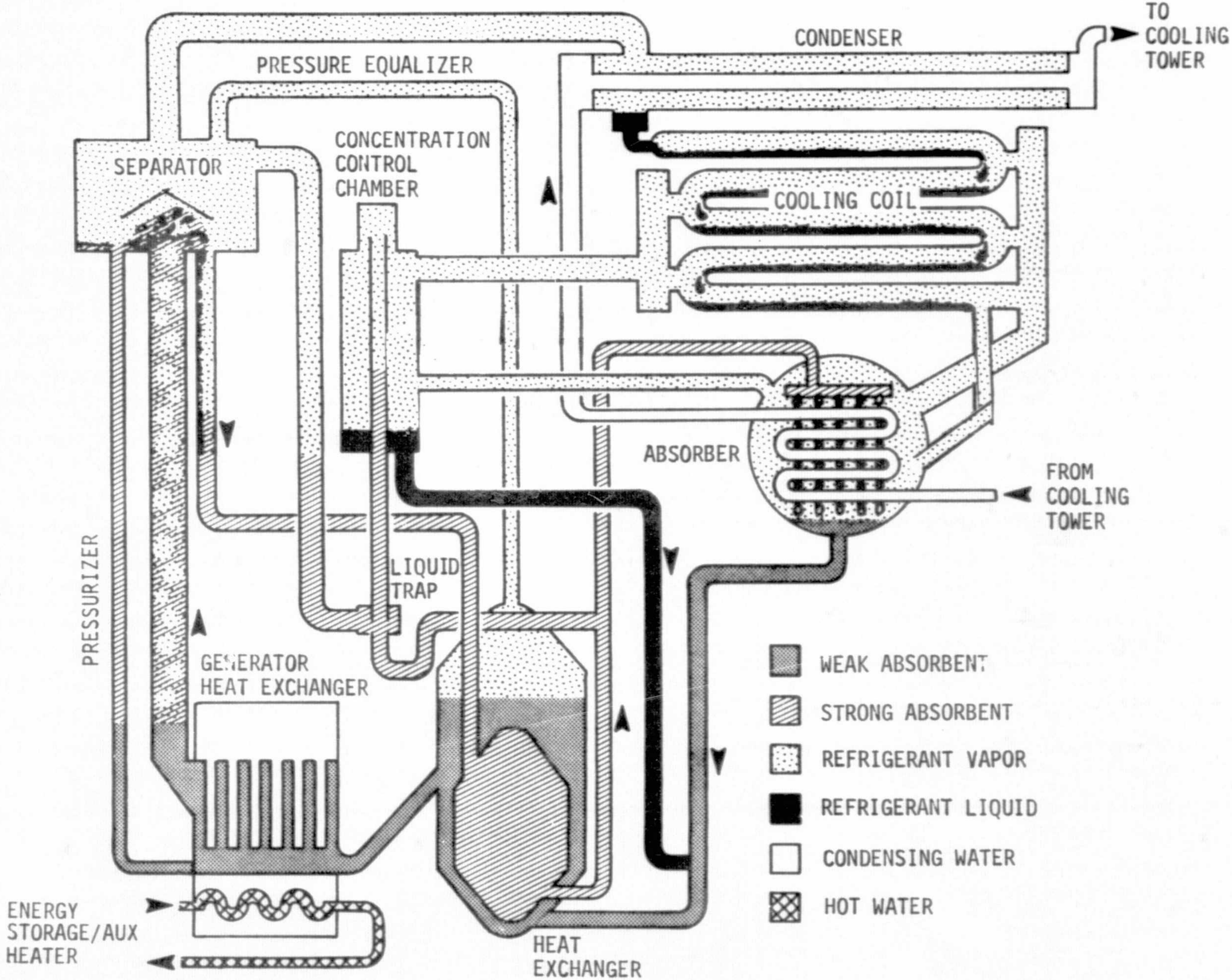

FIGURE A-1 LITHIUM BROMIDE (UNMODIFIED) ABSORPTION MACHINE

strong absorbent, returns to the absorber via the liquid heat exchanger to repeat its cycle of absorbing vapor in the absorber and releasing it in the generator. Thus, the lithium-bromide solution is a transport fluid whose function is to carry the refrigerant from the absorber to the generator where it receives the analogous "heat of compression" and "head pressure." The generator vessel contains three tube coils in parallel with the hot water in the tubes and lithium-bromide solution on the shell side.

The liquid heat exchanger is not required for system operation. Its function is to improve the system Coefficient of Performance (COP) by preheating the weak absorbent before it enters the generator, thereby reducing the generator energy requirement for sensible heating. The energy in the high temperature strong absorbent which leaves the generator is used for this purpose and the liquid heat exchanger is considered to be insulated from the ambient and any other heat source or sink.

The total head differential available for circulating the strong absorbent from the separator (highest elevation) through the liquid heat exchanger to the absorber, depends on both the static pressure difference between separator and absorber, and the elevation difference of the strong absorbent in the separator outlet line and the dripper tray in the absorber. The static pressure in the separator is established by saturation conditions in the condenser (neglecting the pressure drop in the refrigerant vapor line to the condenser) and is typically 50 to 60 mm of mercury absolute. The static pressure in the absorber (and evaporator) is determined by the absorption process and is typically 6 to 9 mm of mercury absolute.

The spill line and control chamber are not involved directly in the thermodynamic cycle. The spill line allows excess refrigerant (liquid) to be dumped

directly into the absorber and recycled through the generator. Although spillage reduces COP because energy is used in the generator to boil the refrigerant whose air conditioning capability is not utilized, the spill line is required to avoid an accumulation of liquid refrigerant which would alter the lithium-bromide concentration in the weak and strong absorbents. The spill line also allows any lithium-bromide which may have been carried past the separator into the condenser to be returned to the absorber. Gravity feed through the condenser, evaporator, and spill line allows liquid refrigerant to wash any "carry-over" back to the lithium bromide section and the machine is self-cleaning in this respect.

The control chamber serves to prevent operation when the condenser temperature is excessive, which otherwise would raise condenser and generator pressure. When the pressure is high enough to "blow" liquid from the liquid trap, a thermal switch senses hot vapor and interrupts the flow of hot water to the generator. This chamber can also be used in a heating mode to pass vapor into the evaporator which would then serve as a condenser.

The modified system is shown in Figure 2. The control chamber, separator, liquid trap, and original generator are removed. A new generator and an electrically driven solution pump are added. The generator has a separator element at the top and is designed to operate at a lower hot water inlet temperature. The pump is added to allow the generator to be raised to the level of the condenser. This reduces the static head in the generator to facilitate boiling and heat transfer.

MODIFIED ABSORPTIVE A/C SYSTEM

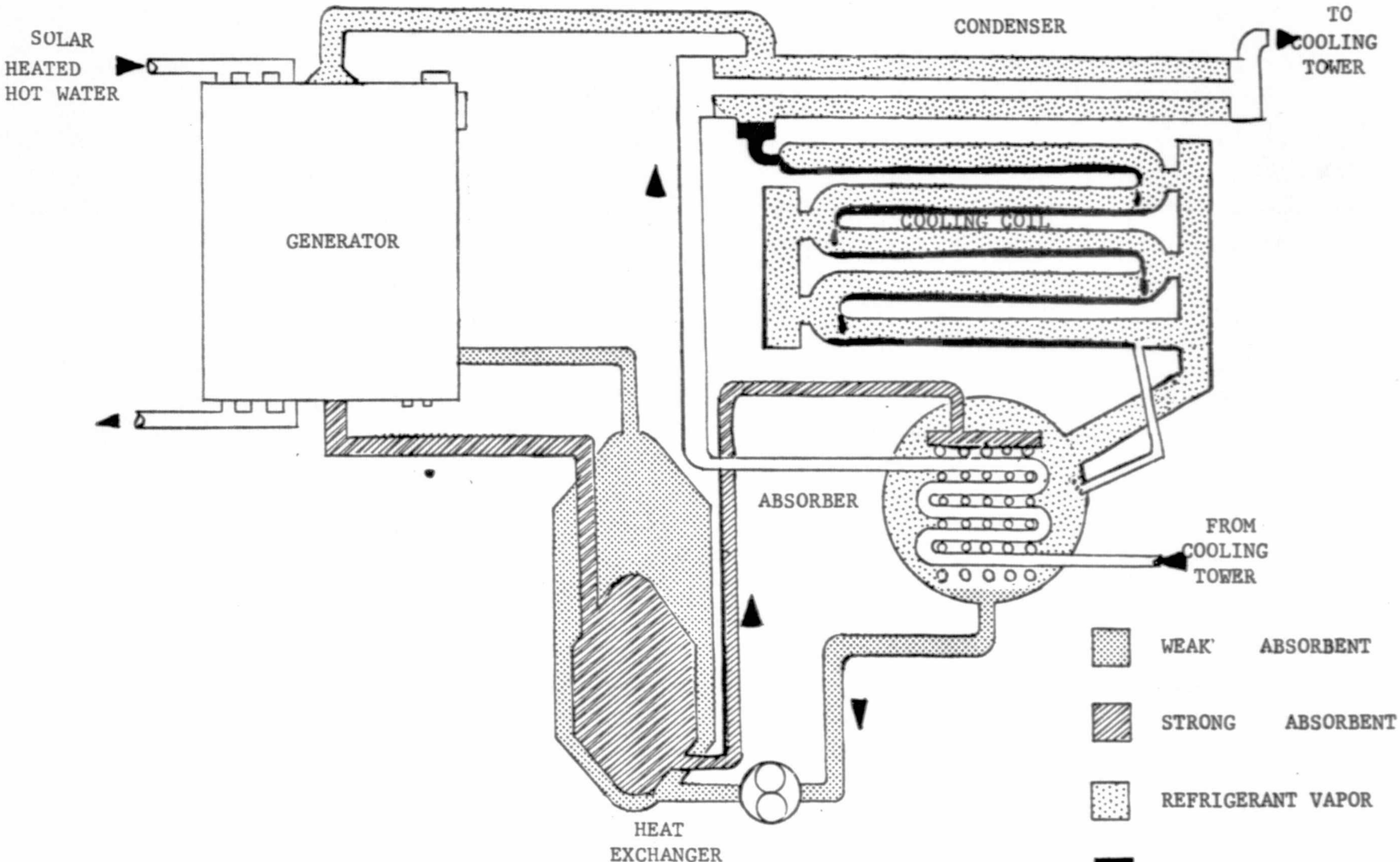

FIGURE A-2

MODIFIED LITHIUM-BROMIDE
ABSORPTION MACHINE

B. PHASE I TEST

The primary purpose of the Phase I Tests is to establish the performance of the unmodified system as the hot water inlet temperature is varied from 96.1C (205F) to "cutoff" temperature, where the unit ceases to function. The other input parameters are held constant and are listed below:

Hot Water Flow	41.6 dm^3/M	11 GPM
Air Flow	34.0 m^3/M	1200 CFM
Air Inlet Dry Bulb	26.7 C	80 F
Air Inlet Wet Bulb	19.4 C	67 F
Tower Water Inlet Temp	29.4 C	85 F
Tower Water Flow	37.9 dm^3/M	10 GPM

The secondary task is to X-ray the generator and separator to determine their configuration.

B.1 Phase I

The output temperatures (hot water outlet, air outlet dry bulb, air outlet wet bulb, tower water absorber/condenser, and tower water condenser outlet), are measured to compute the heat loads on the various components. These heat loads, listed below, are used to compute the Coefficient of Performance (COP) of the air conditioning machine and various ratios. The COP is based on the heat input to the generator.

Calculated Data

Absorber Heat Load, QABS
Condenser Heat Load, QCOND
Evaporator Heat Load, QEVAP
Generator Heat Load, QGEN

COP ≡ QEVAP/QGEN

Absorber ratio ≡ QABS/QEVAP
Condenser ratio≡ QCOND/QEVAP
Generator ratio≡ QGEN/QEVAP

The absorber, condenser, and generator heat loads are calculated from the sensible heating or cooling of water with the general relation:

$Q = (\rho F)\ C_p\ (\Delta T)$

Where - C_p = Specific heat at constant pressure - joules per kilogram degree Celsius
F = Volumetric flow ~ Cubic decimeter (liters) per minute dm^3/M (GPM)
Q = Heat load ~ Watts W (BTUH)
ΔT = Temperature difference ~ C° (F°)
ρ = Density ~ Kilogram per cubic decimeter (lbm per gallon).

F and ΔT are measured; whereas ρ and C_p are found by interpolating tabulated data* at the average water temperature within the component.

The evaporator heat load is calculated psychrometrically (see Figure B-1) using standard empirical equations and the ideal gas low (reference 5, pages 4-81, 4-82, 4-86; and reference 1, pages 99-100). The specific humidity W (mass water per unit mass of dry air) is found by assuming that both air and water vapor properties are described by the perfect gas equation.

(1) $P_vV = N_vRT$

(2) $P_aV = N_aRT$

(3) $P_a = B-P_v$

$N = W/\text{Mol.Wt.}$

Where: B = Barometric reading of atmospheric pressure
N = Number of moles
P = Pressure
R = Universal Gas Constant
T = Absolute temperature
V = Volume

a = Air
v = Vapor

Dividing equation (1) by (2) and substituting (3) for P_a, gives:

$$\frac{Pv}{B-Pv} = \frac{Nv}{Na}$$

The molecular weights of air and water are 28.97 and 18, respectively. For unit mass of dry air, therefore,

*See listed references. Density is from reference 3, page A-6; specific heat is from reference 2, page 3-123.

FIGURE B-1

TEST DATA SUMMARY

DATE:
TIME:

BAROMETRIC PRESSURE	B		IN. Hg
AIR FLOW	CFM		FT^3/MIN
ENTERING DRY BULB TEMP.	t_{edb}		°F
ENTERING WET BULB TEMP.	t_{ewb}		°F
LEAVING DRY BULB TEMP.	t_{ldb}		°F
LEAVING WET BULB TEMP.	t_{lwb}		°F
VAPOR PRESSURE @ t_{ewb} (FROM STEAM TABLE)	P_{ve}		IN. Hg
VAPOR PRESSURE @ t_{lwb} (FROM STEAM TABLE)	P_{vl}		IN. Hg
SPECIFIC HUMIDITY: $W^* = \frac{P_v}{1.609(B-P_v)}$	W_e^*		Lb H_2O/Lb DRY AIR
	W_l^*		Lb H_2O/Lb DRY AIR
$W = W^* - \frac{(0.240+0.44W^*)(t_{db}-t_{wb})}{1094+(0.44t_{db})-t_{wb}}$	W_e		Lb H_2O/Lb DRY AIR
	W_l		Lb H_2O/Lb DRY AIR
ENTHALAPY OF AIR/STEAM MIXTURE	h_{me}		BTU/Lb OF AIR
$h_m = 0.24t_{db} + W(1062+0.44t_{db})$	h_{ml}		BTU/Lb OF AIR
DENSITY OF AIR: $\rho_{la} = \frac{B-P_v}{0.7542(t_{db}+460)}$	ρ_{la}		Lb DRY AIR/FT^3
$t'_{COND} = \frac{1}{2}(t_{DEW_{IN}} + t_{DEW_{OUT}})$	$t_{DEW/IN}$		°F
	$t_{DEW/OUT}$		°F
	t'_{COND}		°F
ENTHALPY OF COND. @ t'_{COND} (FROM STEAM TABLE)	h_f		BTU/Lb
$CFM \times 60 \times \rho_l[h_{me} - h_{ml} - (W_e - W_l)h_f]$	$Q_{EVAP\,AIR}$		BTUH
HOT WATER FLOW RATE	F_{GEN}		GAL/MIN.
WATER TEMP. ENTERING GENERATOR	t_{eg}		°F
WATER TEMP. LEAVING GENERATOR	t_{lg}		°F
$t_{eg} - t_{lg}$	Δt_g		F°
SPECIFIC HEAT @ AVG. WATER TEMP. $t_{g\,AVG}$	Cp_{GEN}		BTU/Lb F°
CONSTANT ($\times 60 \times Cp_{GEN}$)	C_{GEN}		$\frac{Lb}{GAL} \cdot \frac{MIN}{HR} \cdot \frac{BTU}{Lb F°}$
$C \cdot \Delta t_g \cdot F_{GEN}$	Q_{GEN}		BTUH
COOLING TOWER WATER FLOW RATE	F_{CT}		GAL/MIN.
WATER TEMP. ENTERING (ABS)	t_{eab}		°F
WATER TEMP. LEAVING (COND)	t_{lcond}		°F
$t_{lCOND} - t_{eab}$	Δt_{CT}		F°
SPECIFIC HEAT @ AVG. WATER TEMP. $t_{CT\,AVG}$	Cp_{CT}		BTU/Lb·F°
CONSTANT ($\times 60 \times Cp_{CT}$)	C_{CT}		$\frac{Lb}{GAL} \cdot \frac{MIN}{HR} \cdot \frac{BTU}{Lb \cdot F°}$
$C_{CT} \cdot \Delta t_{CT} \cdot F_{CT}$	Q_{CT}		BTUH
$COP_{AIR} \quad \frac{Q_{EVAP}}{Q_{GEN}}$	COP_{AIR}		

FIGURE B-1

$$\frac{Pv}{B-Pv} = \frac{W^*}{18} \times \frac{28.97}{1}$$

$$W^* = \frac{Pv}{1.609\ (B-Pv)}$$

where Pv is taken as the saturation pressure at the psychometric (measured) wet bulb temperature. This assumes that the psychrometric wet bulb temperature equals the thermodynamic wet bulb temperature which is satisfactory with adequate air velocity past the wet bulb thermometer. The specific humidity (W*) then is for a mixture of dry air and saturated water vapor since Pv actually corresponds to the dewpoint temperature.

W* is corrected to the specific humidity for superheated water vapor (relative humidity <1) by writing energy and mass balances for the process of adiabatic saturation, i.e., the psychrometric wet bulb measurement process, with water supplied at the thermodynamic wet bulb temperature (reference 5, page 4-82).

An empirical relation for the enthalpy of the vapor is:

$$h_v = 1062 + 0.44\ T_{db}$$

The enthalpy of the air/vapor mixture is:

$$h_m = 0.24\ T_{db} + W\ (1062 + 0.44\ T_{db})$$

The equation for the corrected specific humidity W is then:

$$W = W^* - \frac{(0.240 + 0.44\ W^*)\ (T_{db} - T_{wb})}{1094 + (0.44\ Tdb) - T_{wb}}$$

The density of air is calculated from the Perfect Gas Equation.

The heat removed from the airstream is calculated from the enthalpy difference of entering and leaving air/vapor mixtures and the enthalpy of the condensed water vapor which is evaluated at the average drain temperature based on dewpoint temperatures.

The test schematic is shown in Figure B-2. Solar panels were simulated by hot water heaters for precise control of the hot water inlet temperature. The air in the closed Air Test Loop is reheated and humidified with an electric furnace and steam generator to provide constant inlet conditions to the evaporator.

The raw test data for Phase I are shown in Table B-1 with the test runs listed in order of decreasing hot water inlet temperature. The data are averaged from several readings. Table B-2 contains the calculated heat loads, COP, and heat ratios. The heat balances are all within 5 percent, with most of the runs falling within 3 percent.

The data were checked by noting that the condenser ratio - QCOND/QEVAP $\geqslant$ 1.05 and that the generator heat load must always exceed the absorber heat load, QGEN > QABS. The condenser ratio inequality is evaluated as follows:

Assumptions:

1. Isenthalpic expansion of refrigerant from condenser to evaporator.
2. Refrigerant at the condenser exit is saturated liquid.
3. Refrigerant at the evaporator exit is not superheated.

h_{fc} = Enthalpy of saturated liquid refrigerant at condenser exit
h_{fe} = Enthalpy of saturated liquid refrigerant at evaporator exit
h_{ge} = Enthalpy of saturated vapor refrigerant leaving evaporator
h_{sh} = Enthalpy of superheated refrigerant entering the condenser
m_r = Refrigerant flow through condenser
m_{rl} = Liquid refrigerant flow at evaporator exit (spillage)
m_{rv} = Vapor refrigerant flow at evaporator exit.

$$QCOND = m_r \; (h_{sh} - h_{fc})$$

$$QEVAP = m_{rv} \; h_{ge} + m_{rl} \, h_{fe} - m_r \, h_{fc}$$

$$\frac{QCOND}{QEVAP} = \frac{m_r \; (h_{sh} - h_{fc})}{m_{rv} \, h_{ge} + m_{rl} \, h_{fe} - m_r \, h_{fc}}$$

$$= \frac{h_{sh} - h_{fc}}{\frac{m_{rv}}{m_r} h_{ge} + \frac{m_{rl}}{m_r} h_{fe} - h_{fc}}$$

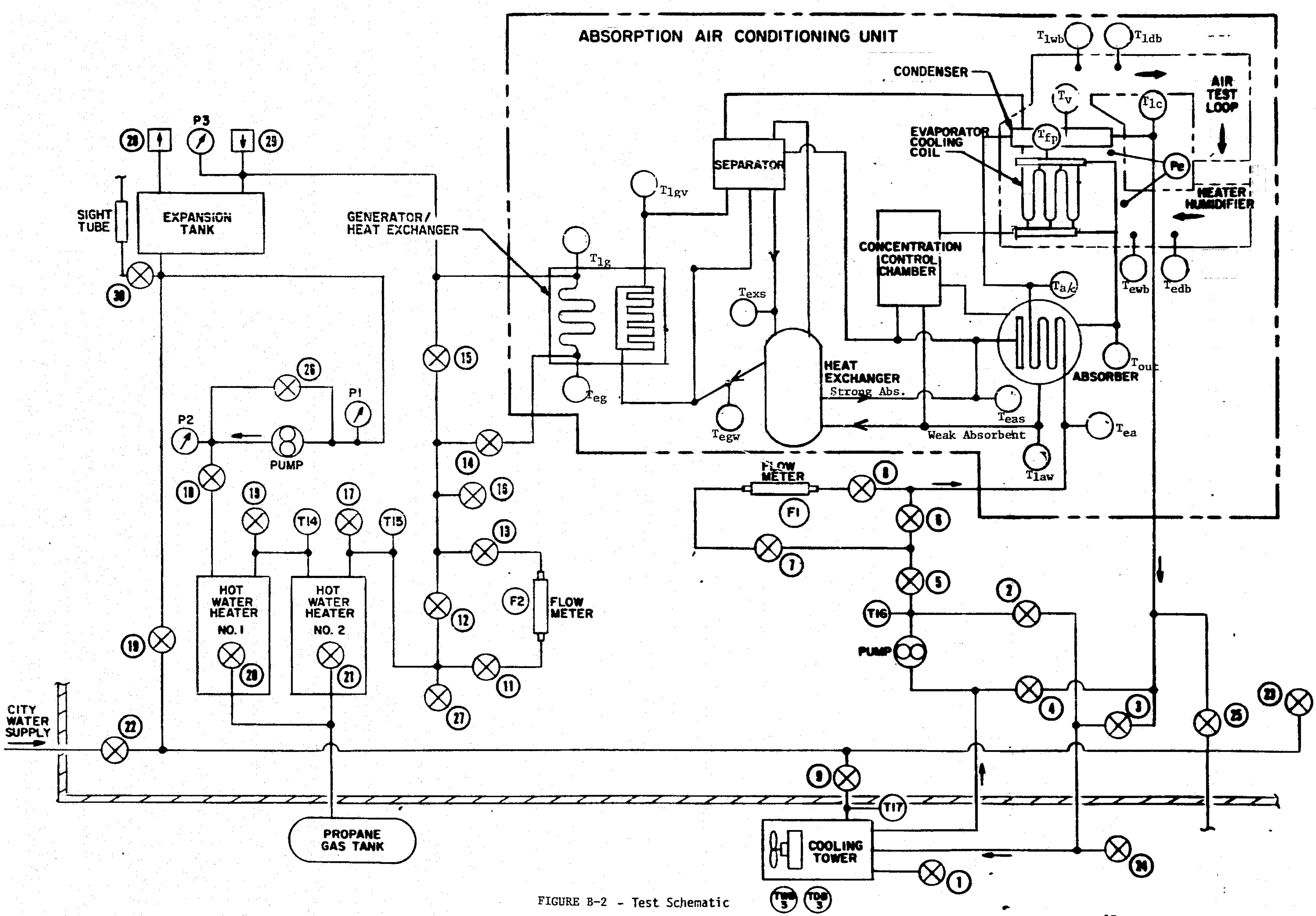

FIGURE B-2 - Test Schematic

TABLE E-1 TEST DATA XWF 501 UNITS: CONVENTIONAL & S.I.

	RUN	FLOW		AIR				HOT WTR		SOLUTION					COND		EVAP			TOWER WATER		
		HOT	TWR	T_{edb}	T_{ewb}	T_{ldb}	T_{lwb}	T_{eg}	T_{lg}	T_{eas}	T_{law}	T_{egw}	T_{lgv}	T_{exs}	T_v	T_{rr}	T_{fp}	T_{out}	SPILL	T_{ea}	$T_{a/c}$	T_{lc}
		$\frac{dm^3}{M}$	$\frac{dm^3}{M}$	°C	°C	°C	°C	°C	°C	°C	°C	°C	°C	°C	°C	°C	°C	°C		°C	°C	°C
S.I.	I-23	44.9	37.5	26.72	18.87	14.67	13.97	96.31	91.12	33.5	37.5	61.8	81.0	74.0	40.0	NOT INSTALLED PHASE I	16.5	22.0	Y	29.38	33.0	39.00
	I-25	44.9	37.5	26.69	19.31	15.09	14.44	96.20	91.21	37.0	38.5	62.0	82.2	74.0	41.0		18.0	26.0	Y	29.78	34.6	39.10
	I-21	44.9	37.5	26.30	18.36	14.18	13.60	95.97	90.93	47.0	37.0	62.5	82.0	74.5	40.0		9.4	21.7	Y	29.10	34.17	38.68
	I-24	44.9	37.5	26.91	19.16	14.65	14.05	95.96	90.91	35.0	38.0	62.0	84.2	74.0	40.0		10.0	22.5	Y	29.43	34.57	39.05
	I-26	44.9	37.5	26.64	19.42	15.08	14.51	95.15	90.38	44.2	35.0	64.1	83.7	73.5	40.0		10.6	22.4	Y	29.38	34.32	38.58
	I-27	44.9	37.5	26.66	19.30	14.94	14.41	94.41	89.79	43.5	35.0	62.2	83.0	71.0	40.0		10.0	22.0	Y	29.39	34.25	38.19
	I-31	44.9	37.5	26.58	19.34	15.28	14.28	93.35	89.05	42.5	36.0	58.5	78.0	70.0	39.4		11.1	22.7	Y	29.29	34.0	37.84
	I-28	44.9	37.5	26.64	19.28	14.67	14.06	93.29	89.09	43.5	35.0	60.0	78.5	70.5	38.9		10.0	21.5	N	29.43	34.27	37.78
	I-29	44.9	37.5	26.75	19.42	14.69	14.19	92.04	88.08	41.0	34.2	58.0	80.5	69.0	38.9		8.9	21.3	N	29.46	34.06	37.48
	I-32	44.9	37.5	26.84	19.38	15.15	14.08	91.88	87.93	41.5	32.0	62.2	80.7	69.0	38.8		9.4	21.0	N	29.28	33.89	37.32
	I-33	44.9	37.5	26.67	19.33	15.36	14.48	90.98	87.32	40.5	33.0	59.0	76.0	68.5	38.3		9.9	20.9	N	29.53	33.79	36.92
	I-30	44.9	37.5	26.68	19.39	14.89	14.43	90.90	87.29	40.0	35.5	57.0	75.0	71.0	37.8		8.9	20.9	N	29.41	33.61	36.72
	I-34	44.9	37.5	26.80	19.48	16.09	13.60	89.11	86.05	39.0	39.0	57.0	78.4	67.5	37.5		8.3	20.4	N	29.45	33.0	35.68
	I-35	44.9	37.5	26.52	19.37	16.68	13.30	88.20	85.33	39.0	39.0	61.1	77.5	65.0	36.7		10.0	20.8	N	29.43	32.9	35.70
	I-36	44.9	37.5	26.64	19.28	16.93	16.12	87.18	84.62	37.5	33.0	61.4	76.5	65.5	35.6		8.9	20.5	N	29.38	32.45	34.90
	I-37	44.9	37.5	26.85	19.37	17.92	16.52	86.35	84.13	36.0	32.0	62.4	75.9	64.0	35.6		7.8	19.5	N	29.35	32.03	34.25
		GPM	GPM	°F	°F	°F	°F	°F	°F	°F	°F	°F	°F	°F	°F		°F	°F		°F	°F	°F
CONVENTIONAL	I-23	11.9	9.9	80.10	65.97	58.41	57.15	205.4	196.0	92.3	99.5	143.2	177.8	165.2	104.0	NOT INSTALLED PHASE I	61.7	71.6	Y	84.9	91.4	102.2
	I-25	11.9	9.9	80.04	66.76	59.16	57.99	205.2	196.2	98.6	101.3	143.6	179.9	165.2	105.8		64.4	78.8	Y	85.6	94.3	102.4
	I-21	11.9	9.9	79.34	65.05	57.52	56.48	204.8	195.7	116.6	98.6	144.5	179.6	166.1	104.0		48.9	71.1	Y	84.4	93.5	101.6
	I-24	11.9	9.9	80.44	66.49	58.37	57.29	204.7	195.6	95.0	100.4	143.6	183.6	165.2	104.0		50.0	72.5	Y	84.9	94.2	102.3
	I-26	11.9	9.9	79.95	66.96	59.14	58.11	203.3	194.7	111.6	95.0	147.4	182.7	164.3	104.0		51.1	72.3	Y	84.9	93.8	101.4
	I-27	11.9	9.9	79.99	66.74	58.89	57.94	201.9	193.6	110.3	95.0	143.9	181.4	159.8	104.0		50.0	71.6	Y	84.9	93.7	100.7
	I-21	11.9	9.9	79.84	66.81	59.51	57.70	200.0	192.3	108.5	96.8	137.3	172.4	158.0	102.9		52.0	72.9	Y	84.7	93.2	100.1
	I-28	11.9	9.9	79.95	66.70	58.40	57.31	199.9	192.4	110.3	95.0	140.0	173.3	158.9	102.0		50.0	70.7	N	84.9	93.7	100.0
	I-29	11.9	9.9	80.15	66.96	58.45	57.55	197.7	190.5	105.8	93.6	136.4	176.9	156.2	102.0		48.0	70.3	N	85.0	93.3	99.5
	I-32	11.9	9.9	80.31	66.88	59.27	57.35	197.4	190.3	106.7	89.6	143.9	177.3	156.2	101.8		48.9	69.8	N	84.7	93.0	99.2
	I-33	11.9	9.9	80.01	66.79	59.65	58.07	195.8	189.2	104.9	91.4	138.2	168.8	155.3	100.9		49.8	69.6	N	85.2	92.8	98.5
	I-30	11.9	9.9	80.02	66.90	58.81	57.97	195.6	189.1	104.0	95.9	134.6	167.0	159.8	100.0		48.0	69.6	N	84.9	92.5	98.1
	I-34	11.9	9.9	80.24	67.06	60.96	56.50	192.4	186.9	102.2	102.2	134.6	173.1	153.5	99.5		46.9	68.7	N	85.0	91.4	96.2
	I-35	11.9	9.9	79.73	66.86	62.03	55.94	190.8	185.6	102.2	102.2	141.9	171.5	149.0	98.1		50.0	69.4	N	84.9	91.2	96.3
	I-36	11.9	9.9	79.95	66.70	62.48	61.01	188.9	184.3	99.5	91.4	142.5	169.7	149.9	96.1		48.0	68.9	N	84.9	90.4	94.8
	I-37	11.9	9.9	80.33	66.87	64.26	61.74	187.4	183.4	96.8	89.6	144.3	168.6	147.2	96.1		46.0	67.1	N	84.8	89.7	93.7

TABLE B-2 TEST RESULTS

	NOTES	RUN	T_{eg} C/F	T_{ea} C/F	F_{Hot} GPM/ dm^3/M	F_{Twr} GPM/ dm^3/M	QEVAP W/BTUH	QGEN W/BTUH	QABS W/BTUH	QCOND W/BTUH	COP	HT BAL	ABS RA	GEN RA
	QCOND/QEVAP = 1.213	I-23	96.31	29.38	44.9	37.5	9702	15810	12856	11769	0.61	0.965	1.325	1.629
			205.4	84.9	11.9	9.9	33125	53977	43892	40181				
	= 1.201	I-25	96.20	29.78	44.9	37.5	9715	15265	12523	11667	0.64	0.968	1.289	1.571
			205.2	85.6	11.9	9.9	33170	52118	42754	39833				
	= 1.199	I-21	95.97	29.10	44.9	37.5	9747	15346	13174	11683	0.64	0.991	1.352	1.574
			204.8	84.4	11.9	9.9	33277	52392	44978	39888				
	= 1.146	I-24	95.96	29.43	44.9	37.5	10128	15363	13360	11610	0.66	0.980	1.319	1.517
			204.7	84.9	11.9	9.9	34578	52451	45614	39637				
	= 1.114	I-26	95.15	29.38	44.9	37.5	9918	14522	12827	11049	0.68	0.977	1.293	1.464
			203.3	84.9	11.9	9.9	33863	49581	43794	37724				
	= 1.040	I-27	94.41	29.39	44.9	37.5	9818	14066	12625	10215	0.70	0.956	1.286	1.433
			201.9	84.9	11.9	9.9	33520	48024	43104	34874				
	= 1.040	I-31	93.35	29.29	44.9	37.5	9550	13094	12265	9928	0.73	0.980	1.284	1.371
			200.0	84.7	11.9	9.9	32605	44703	41875	33894				
	QEVAP = QCOND/1.05	I-28	93.29	29.43	44.9	37.5	8658	12791	12553	9091	0.64	1.009	1.450	1.477
			199.9	84.9	11.9	9.9	29561	43669	42857	31039				
	"	I-29	92.04	29.46	44.9	37.5	8563	12009	11976	8991	0.68	1.019	1.399	1.402
			197.7	85.0	11.9	9.9	29236	41000	40888	30698				
	"	I-32	91.88	29.28	44.9	37.5	8467	12053	11962	8891	0.67	1.016	1.413	1.423
			197.4	84.7	11.9	9.9	28909	41151	40841	30354				
	"	I-33	90.98	29.53	44.9	37.5	7713	11157	11067	8099	0.66	1.016	1.435	1.447
			195.8	85.2	11.9	9.9	26334	38093	37785	27651				
	"	I-30	90.90	29.41	44.9	37.5	7675	10991	10909	8059	0.67	1.016	1.421	1.432
			195.6	84.9	11.9	9.9	26205	37525	37246	27515				
	"	I-34	89.11	29.45	44.9	37.5	6617	9338	9222	6948	0.67	1.013	1.394	1.411
			192.4	85.0	11.9	9.9	22593	31882	31484	23723				
	"	I-35	88.20	29.43	44.9	37.5	6769	8748	9178	7107	0.74	1.050	1.356	1.292
			190.8	84.9	11.9	9.9	23110	29867	31336	24265				
	"	I-36	87.18	29.38	44.9	37.5	5932	7819	7967	6229	0.72	1.032	1.343	1.318
			188.9	84.9	11.9	9.9	20252	26695	27200	21265				
	"	I-37	86.35	29.35	44.9	37.5	5480	6786	6972	5755	0.77	1.037	1.272	1.238
			187.4	84.8	11.9	9.9	18711	23169	23803	19647				

The minimum value of this ratio occurs when the spillage m_{r1} is zero or negligible since $h_{ge} >> h_{fe}$. Then

$$\frac{QCOND}{QEVAP} \geqslant \frac{h_{sh} - h_{fc}}{h_{ge} - h_{fc}}$$

The inequality is valid for non zero spillage; the equality applies to the case of no-spillage. This ratio is evaluated for the case of no-spillage. Reference Run II-28, the appropriate temperatures are:

Vapor Tube Temperature	78.5C	173.3F
Condenser Shell	38.9C	102F
Evaporator Flash Point	10.0C	50F

$$\frac{QCOND}{QEVAP} \geqslant \frac{1136.9 - 70.}{1083.7 - 70.} \qquad \text{(Reference 6)}$$

$$\frac{QCOND}{QEVAP} \geqslant 1.05$$

This lower bound will be approximately constant over the range of interest.

The overall steady state heat balance equation is:

QABS + QCOND = QEVAP + QGEN

Since QCOND > QEVAP, then QGEN > QABS. These inequalities are utilized to check the data.

The psychrometric method of calculating the evaporator heat load is employed while spillage occurs. The dry bulb and wet bulb thermometers are placed where they indicate average values as calculated from a 4X6 matrix of measurements (see Figure B-3). Spilling ceases, however, below hot water inlet temperature of 93.3C (200F), which leads to thermal stratification in the air stream exit.

When the hot water inlet temperature is high enough (above 93C, 200F) to produce spillage of excess liquid refrigerant, no thermal stratification is detected in the air leaving the evaporator coil. When spillage ceases, thermal stratification is encountered due to the loss of uniform cooling across the coil, and to the

ENTERING DRY BULB TEMP.

	A °C/°F	B °C/°F	C °C/°F	D °C/°F	E °C/°F	F °C/°F
1	17.1 / 62.8	17.0 / 62.6	17.0 / 62.6	17.0 / 62.6	17.0 / 62.6	17.0 / 62.6
2	16.9 / 62.4	16.9 / 62.4	16.8 / 62.2	16.9 / 62.4	16.9 / 62.4	17.2 / 62.9
3	16.9 / 62.4	16.9 / 62.4	16.9 / 62.4	16.8 / 62.2	16.8 / 62.2	16.8 / 62.2
4	17.1 / 62.8	17.0 / 62.6	17.1 / 62.8	17.0 / 62.6	17.0 / 62.6	16.9 / 62.4

AVG. TEMP. = 16.95 °C, 62.5 °F

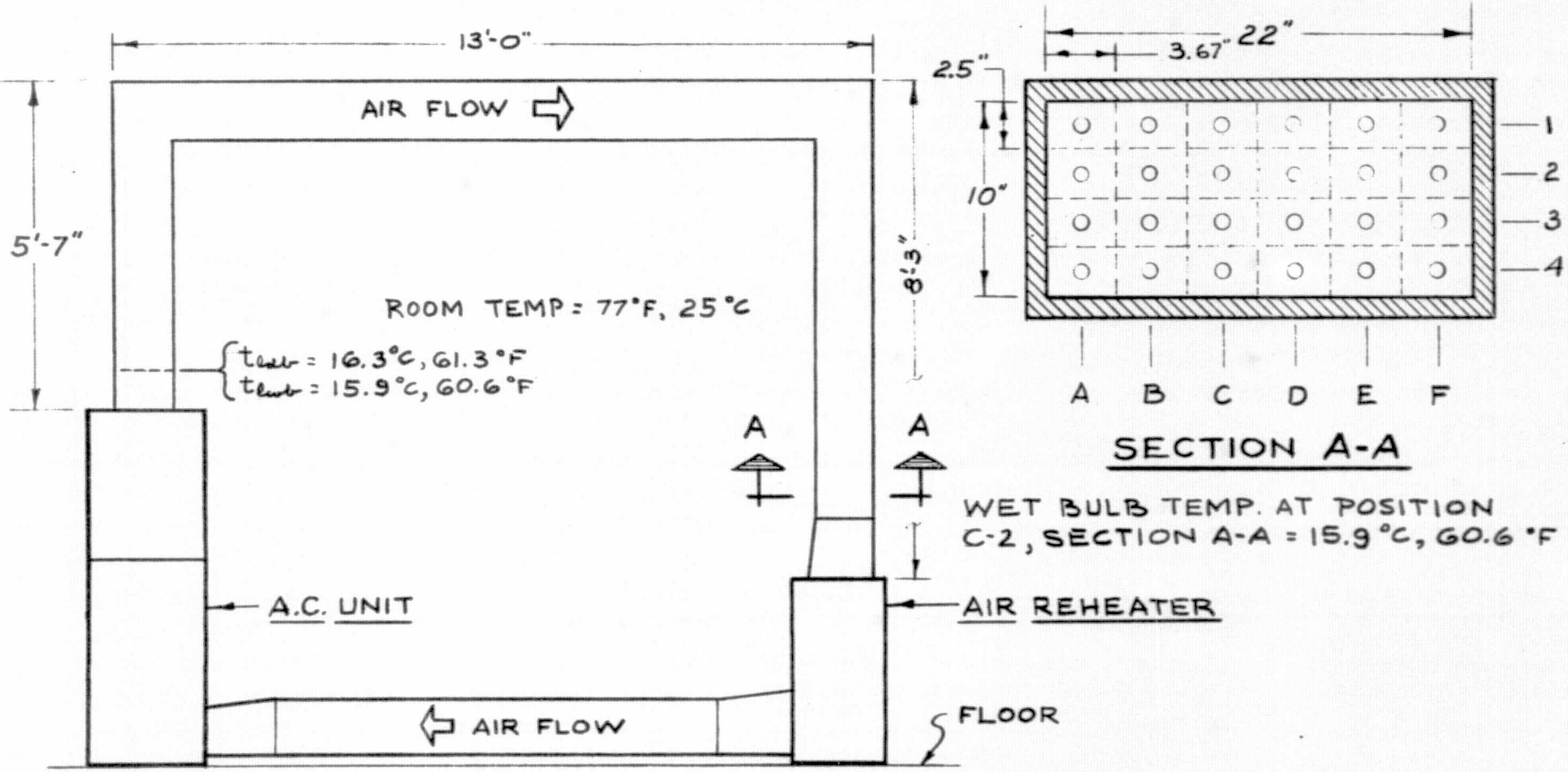

FIGURE B-3 AIR STREAM TEMPERATURE MATRIX - SPILLING

(DATA AT REHEATER INLET DUCT)

inherent flow straightening characteristics of the externally finned tubing of the evaporator. The air that flows across the bottom of the evaporator, where the refrigerant is in the vapor state, receives little cooling and is warmer than the main flow. Temperature measurements at the evaporator exit section are shown in Figure B-3 for the case of spilling; Figure B-4 shows the thermal stratification for the case of no-spillage.

The thermal stratification adversely affects the psychrometric method of calculating the evaporator heat load. When the spillage ceases, the condenser/evaporator ratio equals 1.05 and QEVAP is calculated from QCOND/1.05. This method gives good results as shown in Table B-2.

The test results (COP, QEVAP, and QGEN) are plotted as functions of hot water inlet temperature in Figures B-5, B-6, and B-7, respectively. QEVAP and QGEN decrease as the hot water inlet temperature T_{eg} decreases to the cutoff temperature. The "apparent" COP is shown dotted at those temperatures for which spillage occurs. It decreases as spillage increases because the generator is consuming energy to produce refrigerant which is only partially vaporized in the evaporator. The true COP is shown as a solid line when spillage does not occur. It rises slightly as T_{eg} decreases due to the effect of lower generator temperature on the strong absorbent concentration, and therefore on the thermal energy required to disassociate the water from the solution.

An error analysis is shown in Appendix A. It is based on data from the last run and shows that the test data are less than the root-mean-square error which is the expected error due to instrumentation.

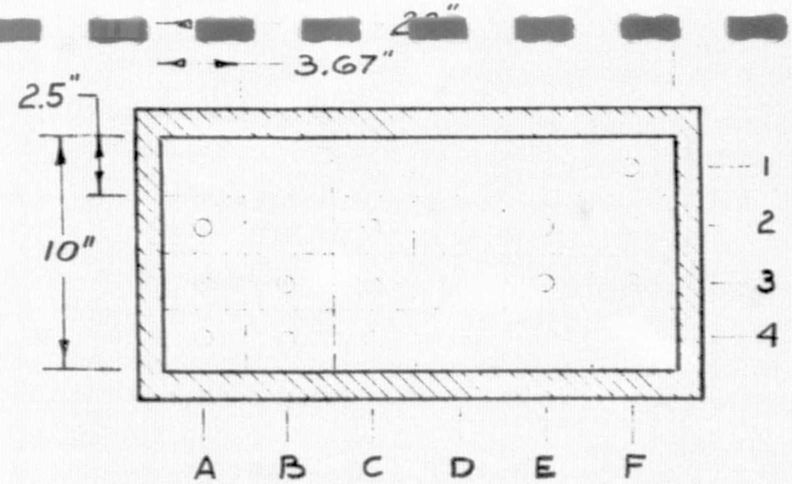

SECTION A-A

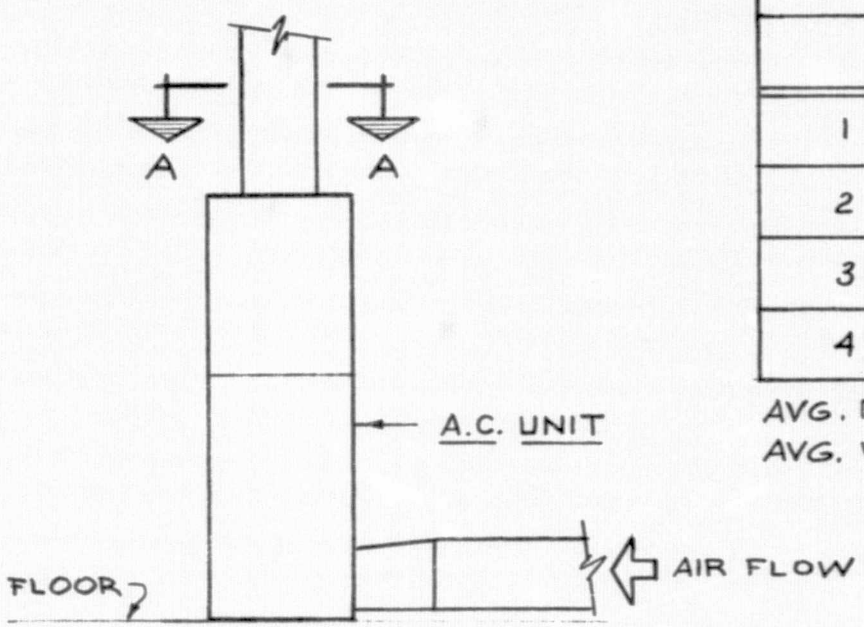

LEAVING DRY BULB TEMP.

	A °C/°F	B °C/°F	C °C/°F	D °C/°F	E °C/°F	F °C/°F
1	17.6 / 63.7	15.9 / 60.6	15.7 / 60.3	15.5 / 59.9	15.6 / 60.1	15.5 / 59.9
2	18.2 / 64.8	15.7 / 60.3	15.5 / 59.9	15.6 / 60.1	16.0 / 60.8	15.8 / 60.4
3	19.7 / 67.5	17.5 / 63.5	18.0 / 64.4	17.9 / 64.2	18.0 / 64.4	16.8 / 62.2
4	22.0 / 71.6	21.0 / 69.8	21.3 / 70.3	21.0 / 69.8	21.0 / 69.8	18.2 / 64.8

LEAVING WET BULB TEMP.

	A °C/°F	B °C/°F	C °C/°F	D °C/°F	E °C/°F	F °C/°F
1	15.5 / 59.9	14.6 / 58.3	14.2 / 57.6	14.0 / 57.2	13.9 / 57.0	14.1 / 57.4
2	15.0 / 59.0	14.2 / 57.6	14.0 / 57.2	14.1 / 57.4	14.3 / 57.7	14.5 / 58.1
3	15.8 / 60.4	14.3 / 57.7	15.0 / 59.0	15.4 / 59.7	16.3 / 61.3	14.7 / 58.5
4	17.5 / 63.5	17.2 / 62.9	17.2 / 62.9	16.7 / 62.1	16.6 / 61.9	15.4 / 59.7

AVG. DRY BULB TEMP. = 17.7 °C, 63.86 °F
AVG. WET BULB TEMP. = 15.18 °C, 59.32 °F

FIGURE B-4 THERMAL STRATIFICATION NO SPILLING
(DATA AT EVAPORATOR EXIT)

FIGURE B-5 COEFFICIENT OF PERFORMANCE
VS
HOT WATER INLET TEMPERATURE

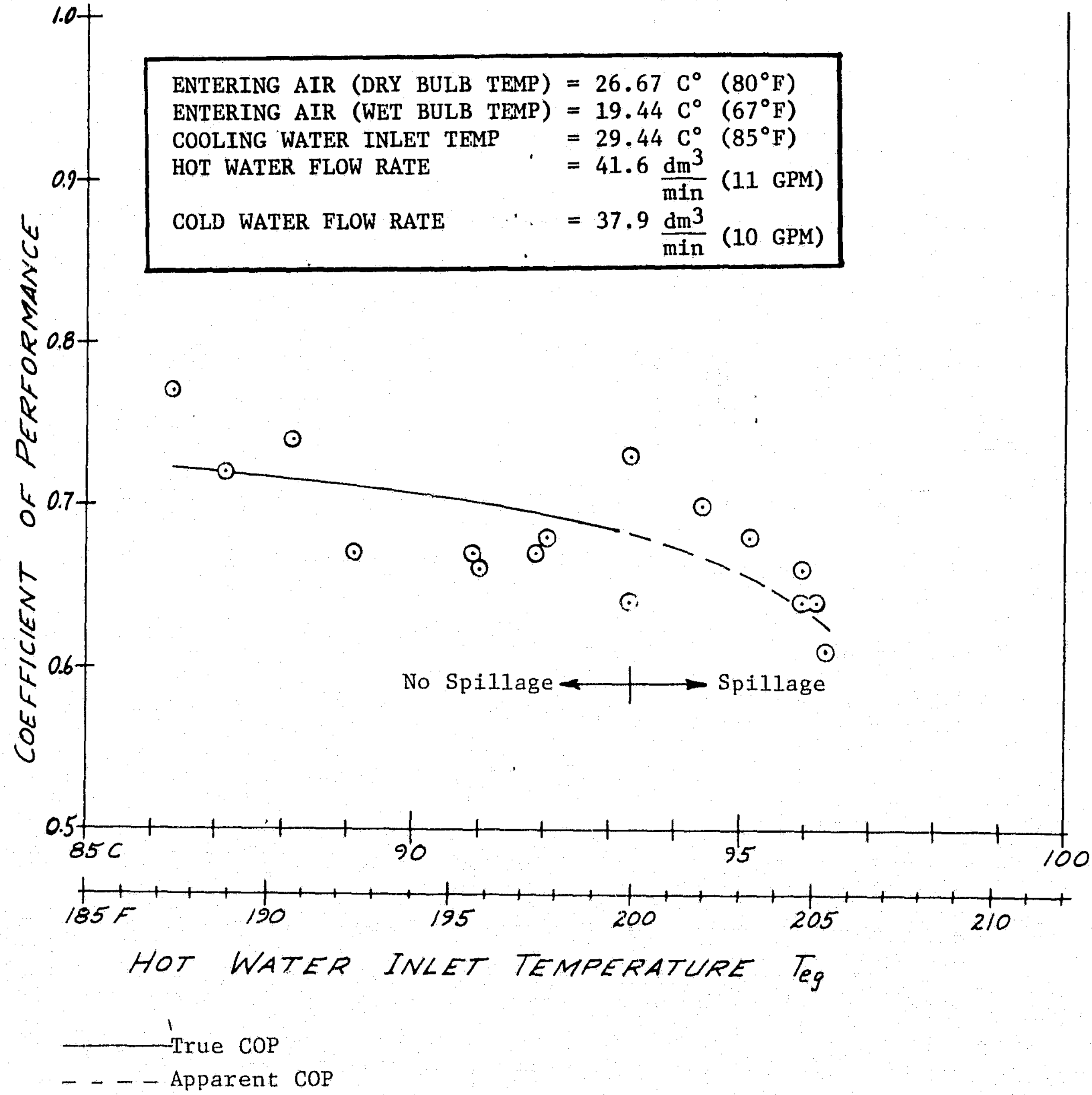

FIGURE B-6 EVAPORATOR HEAT LOAD
VS
HOT WATER INLET TEMPERATURE

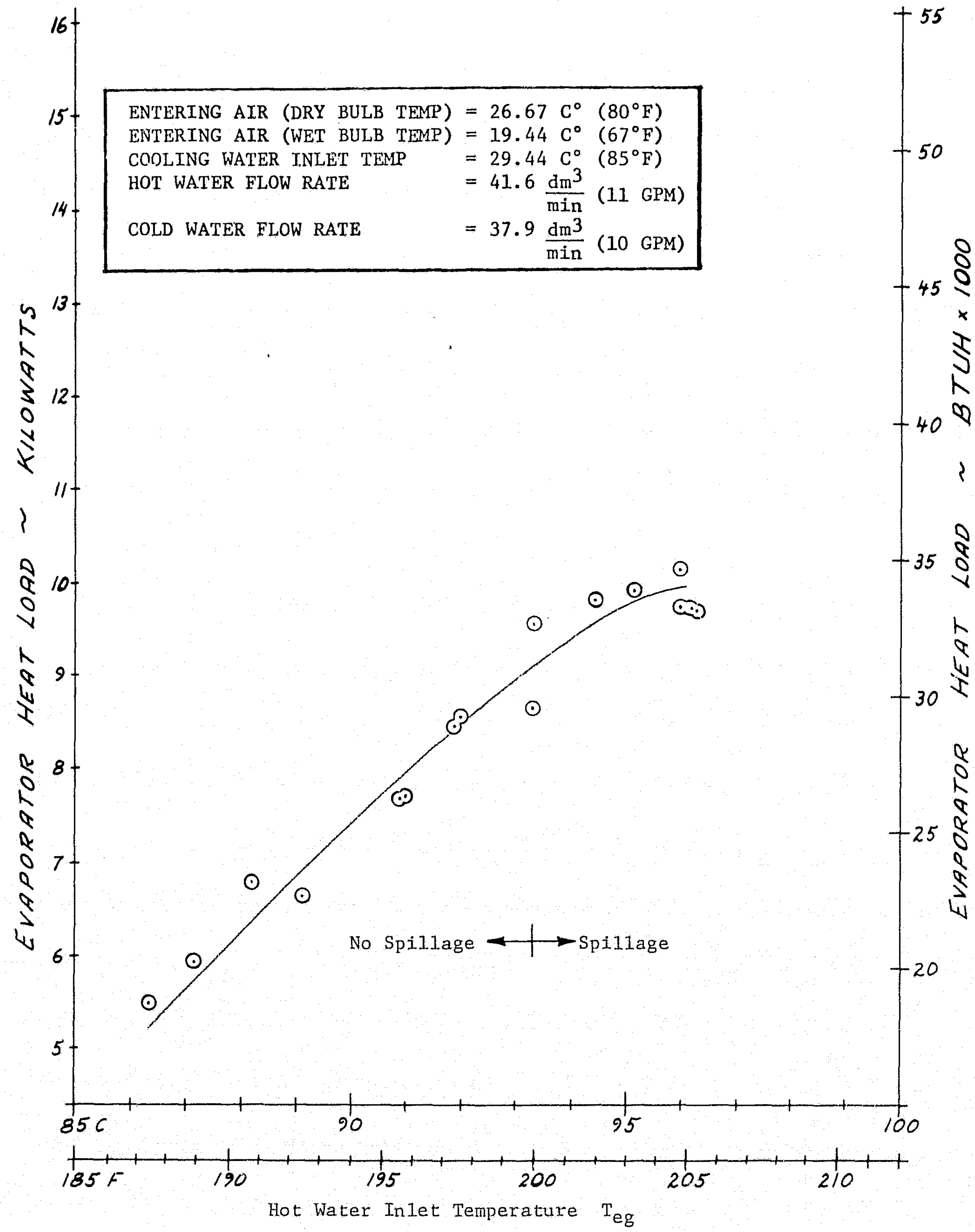

FIGURE B-7 GENERATOR HEAT LOAD VS HOT WATER INLET TEMPERATURE

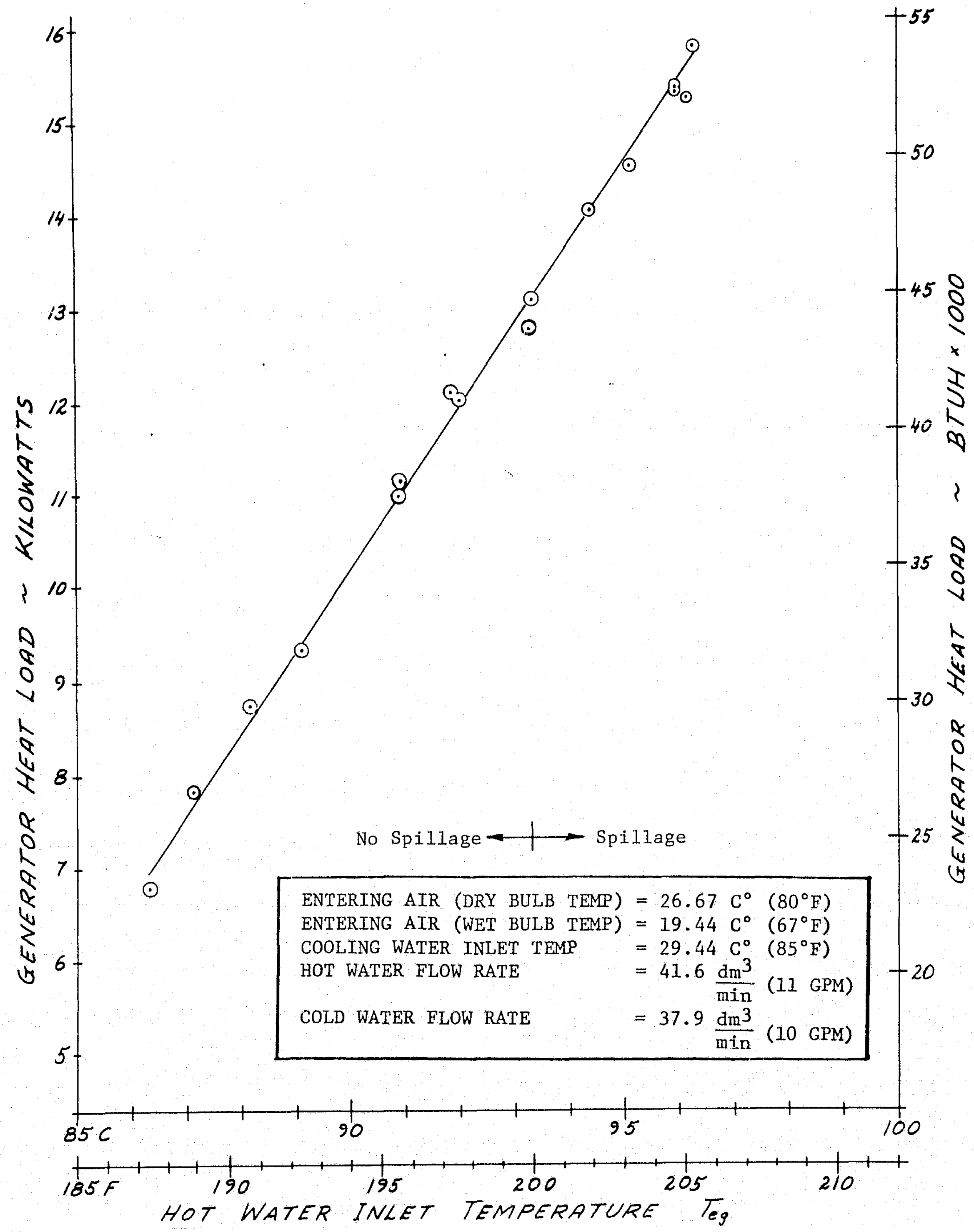

Two discrepancies are observed in the test data. In Runs I-27 and I-31, the condenser heat ratios (QCOND/QEVAP) equal 1.040; they should exceed 1.05. In addition, the COPs for these runs are high. They are on the verge of changing from a condition of "spilling" to one of "no spilling" of liquid refrigerant from evaporator to absorber. This could have lead to undetected thermal stratification in the airstream leaving the evaporator. The calculated evaporator heat load (QEVAP) would then exceed the actual evaporator heat load and the calculated condenser ratio would be lower than the actual value. In addition, the difference between 1.05 and 1.04 is 1% which is within the accuracy of the instrumentation. If thermal stratification did occur in these two cases, the QEVAP can be calculated from -

QEVAP = QCOND/1.05

Then the results of runs 27 and 31 would be:

RUN	QCOND/1.05 Watts/BTUH	COP	HT BAL
I-27	9728./33213	0.69	0.960
I-31	9455./32280	0.72	0.984

The second test data discrepancy is that runs 35, 36 and 37 show the generator heat input (QGEN) is less than the heat rejected by the absorber (QABS), and that the heat balances and COPs are significantly higher than those values in previous runs.

It should be noted that as the cutoff hot water temperature was approached (Run 37) steady state operation became more difficult to achieve. This decreased stability is reflected in the data in spite of the technique of averaging the readings which were recorded at regular intervals.

B.2 Generator and Separator

The generator and separator were examined nondestructively by X-ray. Figures B-8 and B-9 are drawn from these X-rays. The generator is a vessel with three coaxial helical coils connected in parallel. Each coil has seven turns. The hot water is inside the coils. The lithium-bromide solution is on the shell side of the coils, in the annulus formed by the outer shell and inner cylinder. The tubes are 3/4 inch O.D. stainless steel with 0.025 wall thickness, and a total of 24.7 m (81 feet) length.

The separator contains two inverted-vee shaped baffles for impingement of the solution as it exits from the delivery tube from the generator.

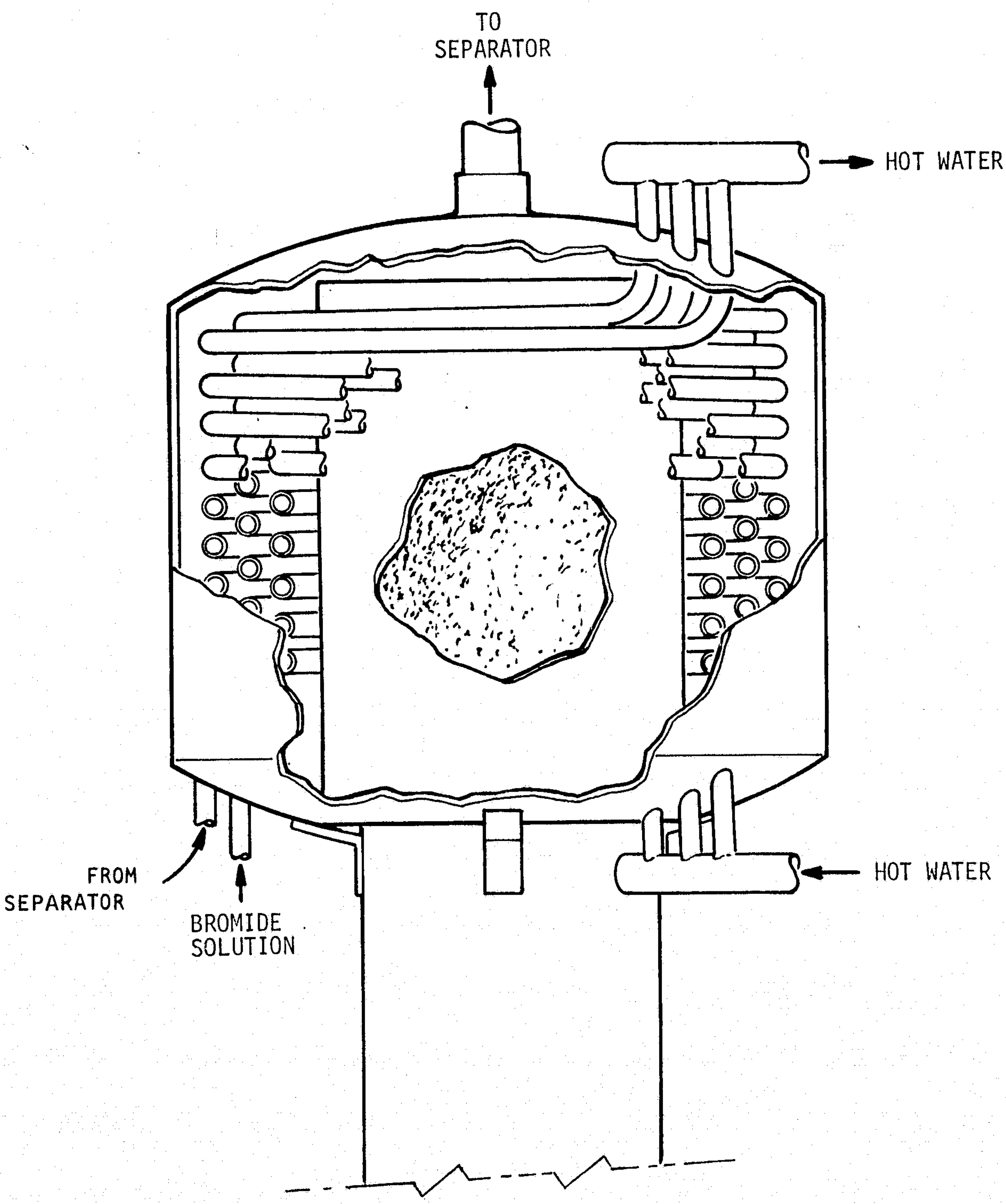

FIGURE B-8- Generator Cutaway

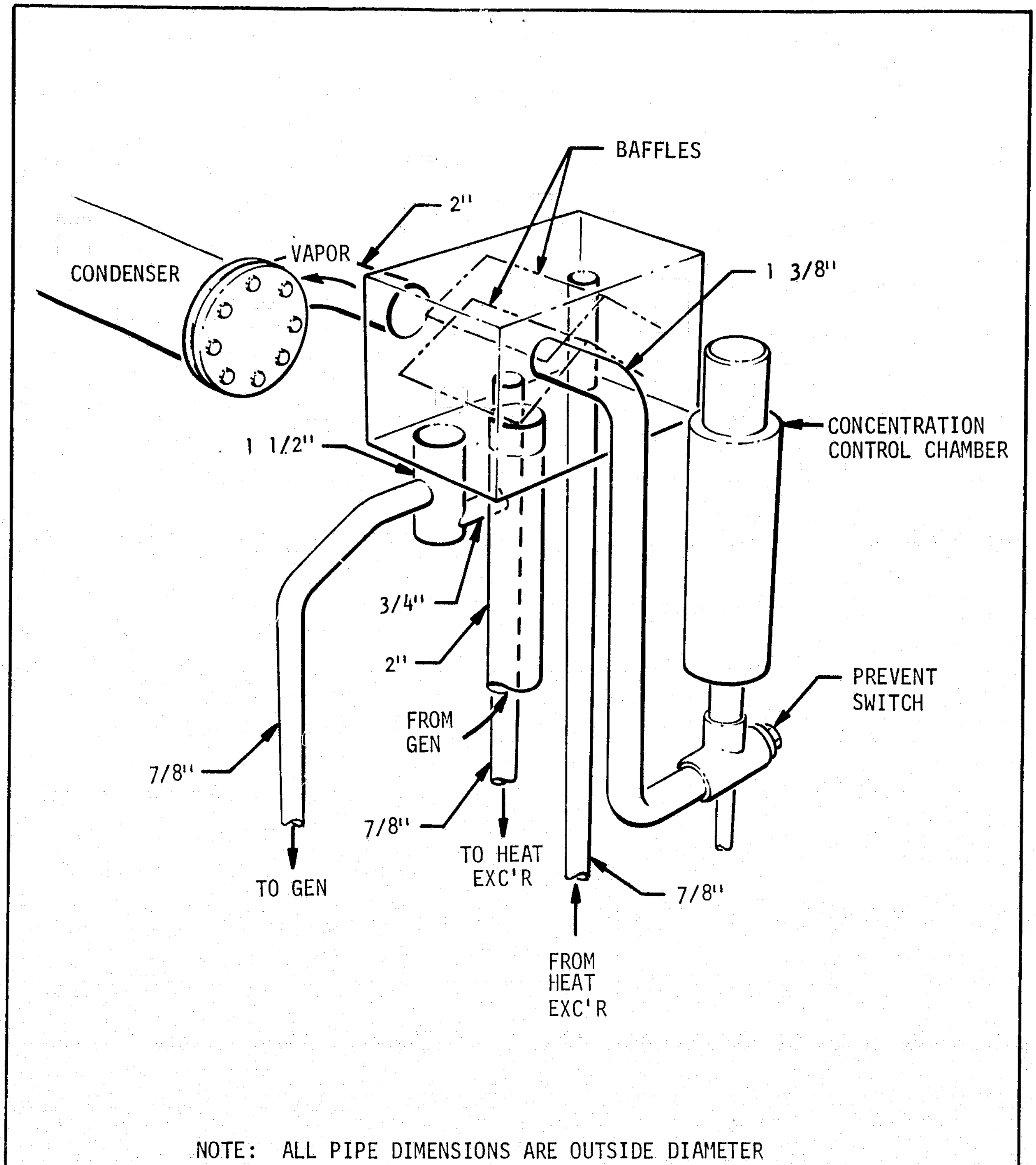

FIGURE B-9 - Separator Cutaway

C. SYSTEM MODIFICATION

Modification of the system includes the selection of a suitable off-the-shelf pump; removal of the original generator, separator, control chamber, and liquid trap; design and fabrication of the new generator; installation of the pump, new generator, and lines, and recharging the system.

The pump and generator are discussed in Sections C.1 and C.2, respectively, including functional requirements and design of the component. Section C.3 discusses the complete system modification.

C.1 Pump

The pump has several functional requirements to satisfy. They are listed below, along with estimates of fluid properties.

Volumetric Flow	3.8 to 7.6 dm^3/M	(1 to 2 GPM)
Pressure Differential	1.73×10^4 N/m^2	(130 mm Hg)
Fluid Temperature (Max)	50. C	(122°F)
Specific Gravity	1.60 to 1.70	
Viscosity Will be Less Than:	$6. \times 10^{-3}$ Ns/m^2	(6 cp.)

The volumetric flow requirement was estimated based on the system manufacturer's data for evaporator heat load, and weak and strong absorbent concentrations; and on lithium-bromide properties (Ref. 1, pages 247 & 248). The concentrations were known only at 96 C (205 F), but the new operating point is 85 C (185 F) so that the flow could be estimated only. The volumetric flow is overestimated to allow for flow regulation with a pump discharge valve.

The valve is selected for vacuum-tight service and compatibility with lithium-bromide solution. A diaphragm valve has no shaft seals or packing and offers excellent vacuum integrity. It is selected with the diaphragm made of Viton.

The pressure differential estimate is based on the height differential and friction loss requirements of the planned installation.

In order to eliminate shaft seals and leakage, the pump is magnetically coupled. The only seal required is an O-ring between the stator assembly and the pump casing.

The pump has no plastic parts, including the impeller, to preclude any outgassing which could contaminate the system, particularly the evaporator where cleanliness of the heat transfer surface is critical.

The pump Net Positive Suction Head (NPSH) requirement is low to prevent cavitation. The pump is located at the lowest level (See Figure A-2), i.e., at the base of the machine below the absorber exit to flood the pump inlet and maximize the static head. It is upstream of the liquid heat exchanger to minimize the solution temperature and the solution saturation pressure.

The selected pump, whose performance curve is shown in Figure C-1, is a Crane Dyna Pump, Model 383E, rated at 60 Hertz, 3450 RPM, 115 Volts AC, single-phase, capacitor start, 3.6 ampere draw at full load. It has "H" insulation for pumping temperatures up to 176 C (350 F). All wetted parts are stainless steel except for carbon graphite bearings and the O-ring seal.

C.2 Generator

Functionally, the generator must provide for

- Heat transfer
- Vapor/liquid separation
- Overflow of solution
- Low pressure drop for vapor outlet
- Structural integrity (leakage and stress)
- Mounting of generator and connecting lines.

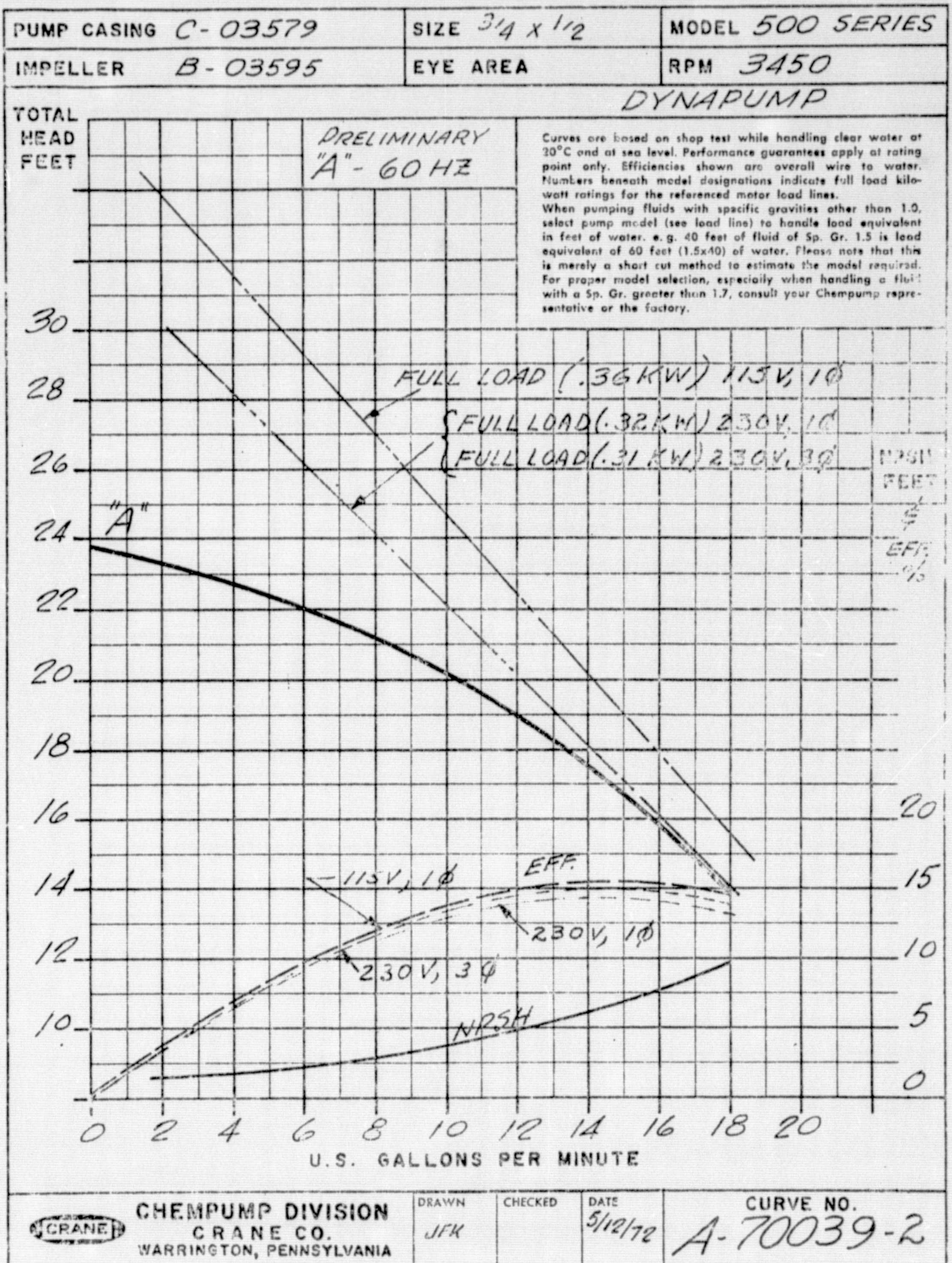

FIGURE C-1 PUMP PERFORMANCE CURVE

The design for the generator requires that conditions for both generator and absorber be specified or known in order to calculate the solution flow rate through the generator. These conditions are shown below:

Generator design heat load = 16.1 kw (55,000 BTUH)

Evaporator design heat load = 10.5 kw (36,000 BTUH)

Absorber Conditions:

Pressure = Evap. Pres. = P_{SAT} (@ 45°F) = 1.02 kN/m^2 (7.63 mm Hg)
(from Ref. 6, page 28)

Temperature = Entering tower water temperature + 5.6 C° (10 F°)

= 29.4 + 5.6 = 35 C (95 F)

Weak Absorbent Concentration (@ 7.63 mm Hg, 95 F), X_W = 52.75%

Generator Conditions:

Hot Water Flow = 41.6 dm^3 /M (11 GPM)

Hot Water (Entering/Leaving) = 85/79.4 C (185/175 F)

Pressure = Condenser Pressure = P_{SAT} (@ 105 F) = 7.60 kN/m^2 (57 mm Hg)

Solution Exit Temperature = 76.7 C (170 F)

Strong Absorbent Concentration (@ 57. mm Hg, 170 F), X_S = 55.8%

Average Concentration, X_{Avg} = 54.3%

The temperature of the solution entering the generator depends on the weak and strong solution flow rates and on the performance of the liquid heat exchanger. This temperature was selected conservatively for a low logarithmic mean temperature difference (LMTD) since the heat load is known. The value selected is 65.6 C (150 F). For counter flow configuration, the LMTD is:

$$\text{LMTD} = \frac{(85 - 76.7) - (79.4 - 65.6)}{l_n \left(\frac{85 - 76.7}{79.4-65.6}\right)}$$

LMTD = 10.8 C° (19.6 F°)

The solution flow rates are calculated by determining the refrigerant flow rate and by writing LiBr and water steady-state mass balances for the generator. The evaporator heat load QEVAP, and the saturation properties of the refrigerant at the condenser and evaporator conditions are known.

$$Wr = \frac{QEVAP}{h_{gEVAP} - h_{fCOND}}$$

$$Wr = 16.2 \text{ kg/hr } (35.7 \text{ lbm/hr})$$

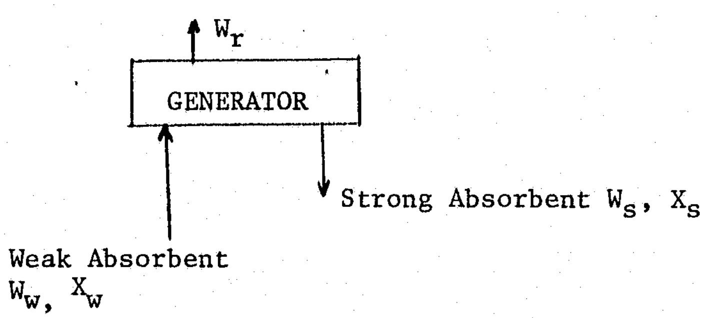

LiBr Balance: $X_w \; W_w - X_s \; W_s = 0$

Water Balance: $(1-X_w) \; W_w - (1-X_s) \; W_s - W_r = 0$

From which:

$$W_w = W_r \left(\frac{X_s}{X_s - X_w}\right) = 298.7 \text{ kg/hr} \quad (658.6 \text{ lbm/hr})$$

$$W_s = W_r \left(\frac{X_w}{X_s - X_w}\right) = 282.4 \text{ kg/hr} \quad (622.6 \text{ lbm/hr})$$

The volumetric flow F, is:

$$F = W/\rho H_2O \quad SG$$

Where the specific gravity (SG) data for lithium-bromide solutions is from reference 1, page 247 and water density ρH20 is from reference 3, page A-7.

The volumetric flows are:

$$F_w = 3.10 \text{ dm}^3\text{/M } (0.82 \text{ GPM})$$

$$F_s = 2.95 \text{ dm}^3\text{/M } (0.78 \text{ GPM})$$

The heat transfer-related properties including the Prandtl Number, of the hot water and of the lithium-bromide solution at the generator design point, are shown in Table C-1.

The following concepts for the generator design were evaluated on the basis of preliminary design calculations:

Shallow tray

Pool

Preheater

Falling Flim (Spray Feed)

Falling Film (Dripper Feed)

The shallow tray is depicted in Figure C-2. It consists of a single tray with the hot water filled single tube serpentined in the solution-filled tray. Due to the shallow depth, it will afford low static head, but packaging is difficult due to the large overall area required.

The pool type of generator is shown in Figure C-3. It has three or four concentric helical tube coils oriented vertically and submerged in the solution. Hot water is tube side; solution is shell side.

The preheater concept is to warm the entering solution in a separate heat exchanger in which only the sensible heat is added, and the solution, under pump pressure, has a higher velocity than is possible in the generator. The generator must provide for the vapor which is released from solution, and the solution velocity is therefore very slow.

The spray-fed falling film generator is shown in Figure C-4. This type of generator offers negligible static head and good heat transfer. The dripper-fed falling film generator is similar, but substitutes a dripper tray for the spray

TABLE C-1

DESIGN POINT PROPERTIES

HOT WATER	Average Temperature	=	82.2C (180 F)
	Viscosity, μ	=	0.3478 m Ns/m^2 (0.3478 cp, 0.8417 lbm/ft-hr)
	Specific Heat, Cp	=	4197. J/kg C (1.003 BTU/lbm F°)
	Conductivity, K	=	0.675 W/mC (0.390 BTU/Hr-Ft F°)
	Prandtl Number	=	μ Cp/K = 2.165
	Density, ρ	=	970.3 kg/m^3 (60.57 lbm/ft^3)

LITHIUM BROMIDE SOLUTION

Average Temperature	=	71.1C (160 F)
Average Concentration	=	54.3%
Viscosity μ	=	1.94 m Ns/m^2 (1.94 cp, 4.695 lbm/ft-hr)
Specific Heat, Cp	=	2.008 J/gC (0.48 BTU/lbm F)
Conductivity, K	=	0.469 W/mC (0.271 BTU/Hr-ft-F)
Prandtl Number	=	μ Cp/K = 8.3
Coefficient of Expansion	=	$\beta = \frac{1}{V}\left(\frac{\partial V}{\partial T}\right)_P$

For close approximation, the finite difference formulation may be used (Ref. 3, page 3-213).

$$\beta = \frac{\rho_1^2 - \rho_2^2}{2(t_2 - t_1)\rho_1 \rho_2}$$

$$\beta = \frac{SG_1^2 - SG_2^2}{2(t_2 - t_1)SG_1 SG_2}$$

$$\beta = 5.44 \times 10^{-4} C^{-1} \quad (3.02 \times 10^{-4} F^{-1})$$

Where t = temperature

SG = Specific Gravity

ρ = Density

Pressure vessel dimensions are maximum envelope size.

Dome is 3/16" thick low carbon steel.

Bottom is 1/8" thick with external rib stiffeners.

Coils are 1" O.D. with .065" wall thickness, 19 fins/inch, cupro-nickel.
(fins not shown for clarity)

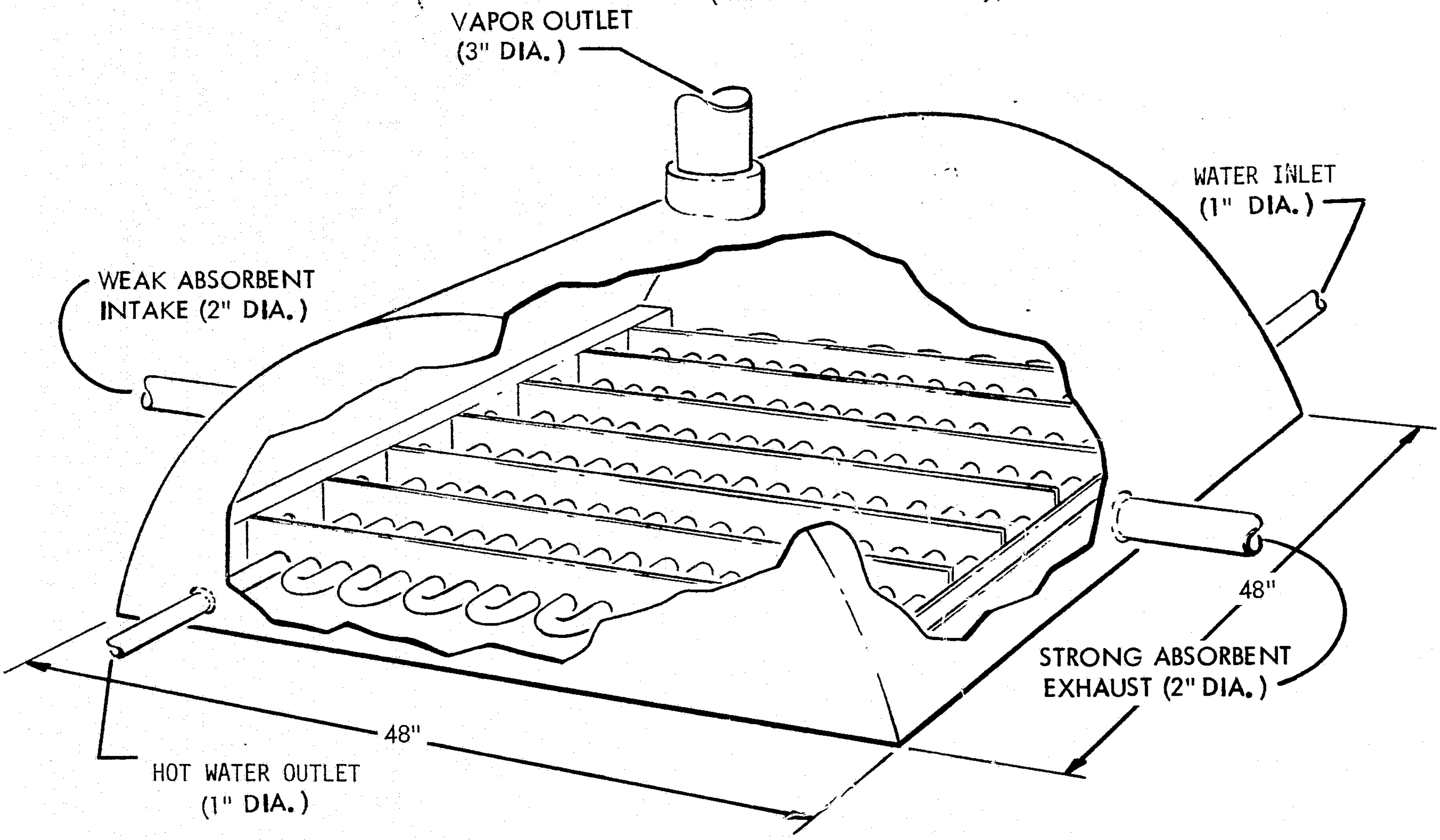

FIGURE C-2 SHALLOW TRAY GENERATOR

Pressure vessel dimensions are maximum envelope size.

Ellipsoidal heads are 3/16" thick low carbon steel.

Coils are 1" O.D. with .065" wall thickness, 19 fins/inch, cupro-nickel. (fins not shown for clarity)

Optional diameter for vapor outlet is 2" dia.
Optional diameter for strong absorbent line is 1" dia.

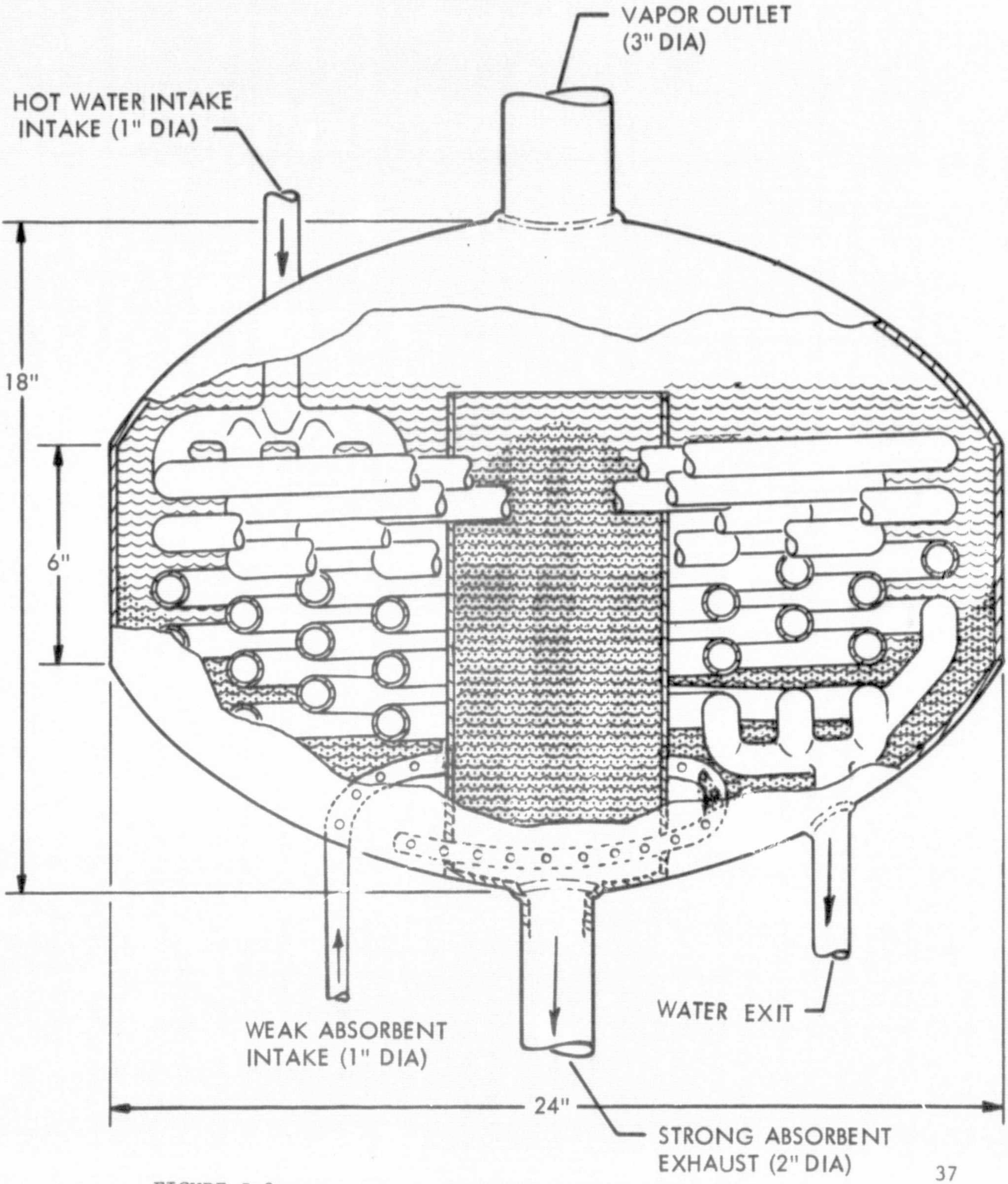

FIGURE C-3 POOL GENERATOR

Pressure vessel dimensions are maximum envelope size.

Ellipsoidal heads are 3/16" thick low carbon steel.

Coils are 3/4" O.D. with .065" wall thickness, etched plain tubing.

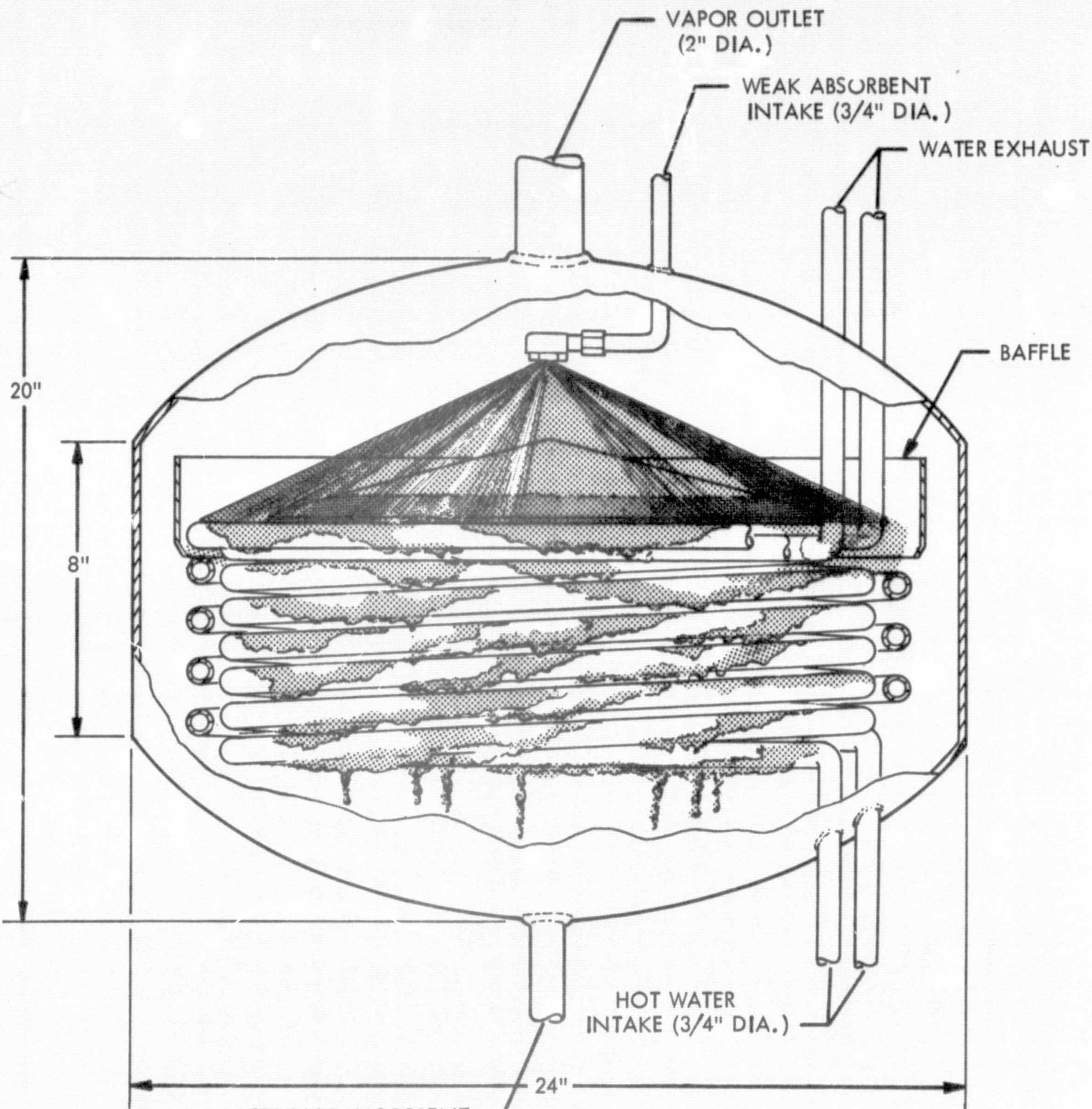

FIGURE C-4 FALLING FILM SPRAY-FED GENERATOR

nozzle. The vapor path is radially outward between coil turns, and then upward to the gènerator dome.

The preliminary design and evaluation for the various concepts is based on standard engineering methods. Standard equations and available heat transfer data are utilized. First, the heat transfer film coefficients inside the tubes (water side)h_i, and outside the tubes (solution side)h_o are calculated. These parameters are calculated from empirical relations that depend on fluid properties, velocity, and mode of heat transfer. The tube wall conductance is calculated and depends only on dimensions (inside and outside diameter) and thermal conductivity of the wall. These three parameters are combined into the overall heat conductance U, which is based on the outside heat transfer area A_o.

$$\frac{1}{U} = \frac{1}{h_o} + \frac{A_o}{h_i A_i} + \frac{A_o}{h_w A_m}$$

The tube length drops out of the area ratios which depend on tube diameters. The tube length, L, required is calculated by:

$$A_o = \frac{QGEN}{U \text{ X } LMTD}$$

$$L = \frac{A_o}{\pi D_o} \text{ for plain tubes}$$

$$L = \frac{A_o}{(A/L)} \text{ for finned tubes where (A/L) is manufacturer's catalog data.}$$

If the concept has acceptable heat transfer characteristics, then the design is extended to include structural and packaging dimensions and to determine any inherent problems.

The conceptual generators were examined with the following parametric values:

Tube Outer Diameter	0.75, 1.00 inch
Tube Material	Stainless Steel (316), Cupro Nickel (70/30)
Tube Outer Surface	Plain, Finned
Number of Tubes	1, 2, 3, 4

The inside heat transfer film coefficient is calculated for turbulent flow. Two equations are available to determine the heat transfer coefficient for this type of flow configuration. The McAdams equation (ref. 7, page 168, 169), which requires only bulk properties, is compared to the Colburn equation which requires film properties. The result, as shown below, is that the McAdams equation is adequate, and the simplicity offered by using bulk properties makes this equation the better choice for evaluation of the design concepts.

For turbulent flow inside tubes:

McAdams: $$\frac{h_{im}\, D_i}{K} = 0.023\, (\mathrm{Rey})_B^{0.8}\, (\mathrm{Pr})_B^{0.4}$$

Colburn: $$\frac{h_{ic}}{C_{PB} G}\, (\mathrm{Pr})_F^{2/3} = \frac{0.023}{(D_i\, G/\mu F)^{0.2}}$$

Where:
- B - Bulk Properties
- F - Film Properties
- G - Mass Velocity
- Pr - Prandtl Number
- Rey - Reynolds Number

The film temperature is used for evaluating properties of the fluid. The film temperature is:

$$T_F = 1/2\, (T_{B\ Avg} + T_{W\ Avg})$$

Where $T_{B\ Avg}$ = 82.2 C (180 F)

$T_{W\ Avg}$ = Average wall temperature

Worst Case for $T_{W\ Avg} = T_{soln\ avg}$ = 71.1C (160 F)

then T_F = 76.7C (170 F).

The Colburn equation is rewritten as:

$$\frac{h_{ic}\ D_i}{K_B} = 0.023\ (Rey)_B^{0.8}\ (Pr)_B^{0.4}\ \left(\frac{\mu F}{\mu B}\right)^{0.2}\ \frac{(Pr)_B^{\ 0.6}}{(Pr)_F^{\ 2/3}}$$

and the McAdams equation is substituted:

$$\frac{h_{ic}\ D_i}{K_B} = \frac{h_{im}\ D_i}{K_B}\ \left(\frac{\mu F}{\mu B}\right)^{0.2}\ \frac{(Pr)_B^{0.6}}{(Pr)_F^{2/3}}$$

$$h_{ic} = h_{im} \times C_1$$

$$\text{Where } C_1 = \left(\frac{\mu F}{\mu B}\right)^{0.2}\ \frac{(Pr)_B^{0.6}}{(Pr)_F^{2/3}}$$

The data for C_1 are

	Bulk 180°F	Film 170°F	
μ	0.8390	0.8998	LBM/FT-HR
C_p	1.00336	1.00236	BTU/LBM °F
K	0.3964	0.3916	BTU/HR FT °F

$C_1 = 0.914$

Therefore, the McAdams equation gives a higher estimate for h_i by no more than 9 1/2%. This will affect overall conductance U by less than 4% because $h_i \gg h_o$, as shown when h_o is evaluated, and worst case $T_{W\ Avg} = 160°F$ is conservative.

The McAdams equation is adequate and is used to calculate h_i.

The effect of coiled tubes on h_i is neglected as shown below. From reference 5, page 4-100, the heat transfer film coefficient for straight pipe is multiplied by $(1 + 3.5\ \frac{Di}{Dc})$ where Di is the inside diameter of the pipe and Dc is that of the coil.

This factor always exceeds unity. When the factor is neglected, the film coefficient is underestimated. The factor is readily evaluated for a typical case.

Di = 0.5 in. (approximate I.D. for 0.75 finned tube)

Dc = 24 in. (a maximum value).

Then the minimum value of this term is 1.073.
The results of the calculation for h_i are shown in Table C-2.

The outside heat transfer film coefficient is evaluated for three conditions:

1. Free surface evaporation (for tray or pool generators)
2. Falling film
3. Preheater annular section.

Free surface evaporation, according to reference 1, page 45, occurs "where the surface temperature exceeds the liquid saturation temperature by less than a few degrees, no bubbles are formed. Evaporation takes place at the free surface by convection of superheated liquid from the heated surface. The correlations of heat transfer coefficients for this region are similar to those for fluids under ordinary natural convection." This type of mechanism is correlated by (reference 1, page 46):

$$N_u = 0.16\ (Gr)^{1/3}\ (Pr)^{1/3}$$

Where Nu = Nusselt Number = $h_o D_o / K$

Gr = Grashof Number = $\dfrac{\beta\, g\, \rho^2 D_o^3\ \Delta T}{\mu^2}$

Pr = Prandtl Number = $\mu C_p / K$

ΔT = (Surface Temp - Bulk Temp)

Assume ΔT = 8.3 C° (15F°)

For finned tubing an equivalent diameter is found from the manufacturer's catalog data* and ho is multiplied by a weighted fin efficiency which is also catalog data*.

*Wolverine Trufin Engineering Data Book, 1968, Decatur, AL, p. 12, 86.

TABLE C-2

INSIDE HEAT TRANSFER

FILM COEFFICIENTS

No. Tubes	D_o (In)	h_i STAINLESS STEEL (Plain)		h_i CUPRO-NICKEL (Plain)		h_i Cupro-Nickel (Plain)	
		kW/m^2C	$BTU/HrFt^2 \cdot F$	kW/m^2C	$BTU/HrFt^2 \, ^oF$	kW/m^2C	$BTU/HrFt^2 \, ^oF$
1.	0.75	16.26	2865.	19.20	3383.	31.94	5629.
	1.00	9.254	1631.	10.43	1839.	15.37	2708.
2.	0.75	9.334	1645.	11.02	1943.	18.34	3233.
	1.00	5.316	937.	5.992	1056.	8.817	1554.
3.	0.75	6.746	1189.	7.972	1405.	13.26	2337.
	1.00	3.841	677.	4.329	763.	6.376	1124.
4.	0.75	5.362	945.	6.332	1116.	10.54	1857.
	1.00	3.053	538.	3.438	606.	5.050	890.

The results of the calculation for h_o for free surface evaporation are:

Do Inch	De Inch	Surface	Material	h_o W/m^2C	h_o $BTU/Hr\ Ft^2F$
0.75	--	Plain		455	80.2
	0.660	Finned	Cu/Ni	455.	80.2
	0.665	Finned	SS	461.	81.3
1.00	--	Plain		456.	80.3
	0.910	Finned	Cu/Ni	479.	84.4
	0.917	Finned	SS	456.	80.4

The heat transfer coefficient for falling film applied to the outside of horizontal tubes is found from the following relation (ref. 2, page 10-24).

For falling film Reynolds Number < 2100.

$$h_{a.m.} = 55 \left(\frac{K^2 \rho^{4/3} C}{L \mu^{1/3}}\right)^{1/3} \left(\frac{\mu}{\mu_w}\right)^{1/4} \left(\frac{4\Gamma}{\mu}\right)^{1/9}$$

for $0.4 < L < 6.0$ feet.

Where $h_{a.m.}$ = Film coef. based on arithmetic mean temperature difference BTU/Hr. Ft^2 °F

C = Specific Heat at constant pressure - BTU/LBM °F

K = Thermal conductivity - BTU/Hr Ft °F

L = Length of heat transfer surface - Feet

$L = \frac{\pi Do}{2}$ for horizontal tubes

μ = Viscosity - LBM/Hr-Ft, W ~ Wall Temp.

ρ = Density ~ LBM/Ft^3

$\Gamma = \frac{W}{2L_H} = \frac{W}{2\pi D_C}$ for horiz. coil

The falling film Reynolds Number for horizontal tube (with the weak absorbent as the falling film) is:

$$REY_{FF} = \frac{4W}{\mu\, 2L_H}$$

Where L_H = Length of horizontal tube - Feet

μ = Viscosity - LBM/Hr-Ft

w = Flow Rate - LBM/Hr

$L_H = \pi D_C$ D_C = Coil Diameter (center line)

If the falling film flow is distributed equally among N tube coils,

$$REY_{FF} = \frac{2 \times 658.6}{4.695\ \pi D_C\ N}$$

Let D_C = 2 feet

$$REY_{FF} = \frac{44.65}{N} < 2100$$ and the falling film is laminar.

If $\mu_w = \mu\, 180°F = 1.564\ c_p$, then

$$\left(\frac{\mu}{\mu_w}\right)^{1/4} = \left(\frac{1.94}{1.564}\right)^{1/4} = 1.055$$

As a conservative approximation, this term is reduced to unity due to the uncertainty of μ_W then,

$$h_{a.m.} = 55 \left(\frac{0.271^2\ (1.58 \times 62.4)^{4/3} \times 0.48}{\frac{\pi Do}{2 \times 12\ In/Ft} \times 4.695^{1/3}}\right)^{1/3} \left(\frac{44.65}{N}\right)^{1/9}$$

$$h_{a.m.} = \frac{350}{Do^{1/3}\ N^{1/9}}$$ Where Do - Inch
$h_{a.m.}$ - BTU/Hr Ft^2 °F

N	Do	Falling Film $h_{a.m.}$ kW/m2C	BTU/HrFt^2°F
1	0.75	2.173	383. BTU/Hr Ft^2 °F
	1.00	1.975	348.
2	0.75	2.009	354.
	1.00	1.827	322.
3	0.75	1.923	339.
	1.00	1.742	307.
4	0.75	1.861	328.
	1.00	1.685	297.

The preheater is shown as a tube within a tube.

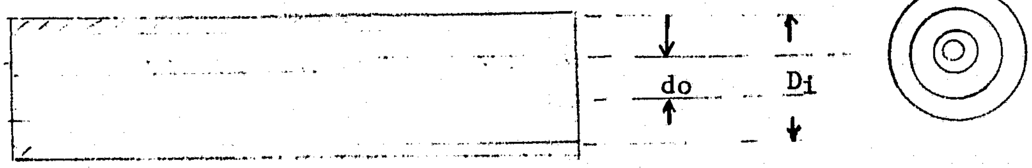

The solution is in the inner tube to have turbulent flow; the hot water is in the annulus. The McAdams equation for turbulent flow in pipes is used in both the shell side and tube side. The diameter assigned to the annular region is the equivalent hydraulic diameter D_H defined by -

$$D_H = \frac{4A_F}{P_W}$$

A_F = Flow area
P_W = Wetted perimeter

$$D_H = \frac{4\left(\frac{\pi}{4}\right)\left(D_i^2 - d_o^2\right)}{\pi\left(D_i + d_o\right)}$$

$$D_H = Di - do$$

The following coefficients are calculated with the McAdams equation.

do Inch	Di Inch	h_o kW/m^{2}C	h_o BTU/Hr Ft^2 F
0.50	1.50	6.037	1064.
0.84	1.77	6.321	1114.

The tube wall conductance based on the tube outside heat transfer area, $\frac{A_o}{A_m h_w}$ for the overall heat conductance U, is found by calculating an equivalent heat transfer coefficient for tube wall conductance (ref. 7, p. 40, 41, 52).

$$h_w = K_w / (r_o - r_i)$$

Where h_w = Equivalent heat transfer coefficient

K_w = Tube wall conductivity

r_i = Inside radius

r_o = Outer radius

The logarithmic mean area A_m is

$$A_m = \frac{Ao - Ai}{l_n \left(\frac{Ao}{Ai}\right)}$$

Where Ai = Inside heat transfer area

Ao = Outer heat transfer area

$$\frac{Ao}{A_m} = \frac{(\pi \, Do \quad L) \; l_n \left(\frac{\pi \, Do \; L}{\pi \, Di \; L}\right)}{\pi \, L \quad (Do - Di)}$$

Where Di = Inside diameter
Do* = Outer diameter
L = Length

*For externally finned tubing, Do = De, an equivalent diameter found in the tubing manufacturer's catalog data.

Combining the relations for h_w and Ao/Am, and since D = $2r$:

$$\frac{Ao}{Am \; h_w} = \frac{Do \; l_n \left(\frac{Do}{Di}\right)}{2 \; K_w}$$

The thermal conductivities for stainless steel and cupro-nickel (70/30) are K_{SS} = 9.4 and $K_{C/N}$ = 17.0 BTU/Hr Ft. F, respectively.

The tube wall conductances, based on outside area, are shown below:

	Plain Tube				Finned	
	Stainless Steel		Cupro Nickel		Cupro Nickel	
Do, Inch	0.75	1.00	0.75	1.00	0.75	1.00
De, Inch					0.660	0.910
Di, Inch	0.68	0.93	0.62	0.87	0.495	0.745
$\frac{Ao}{A_m h_w}$, $\frac{m^2C}{kW}$ X 10^5	5.740	5.670	6.167	6.015	8.202	7.864
$\frac{Ao}{A_m h_w}$, $\frac{HrFt^2F}{BTU}$ X 10^4	3.257	3.217	3.499	3.413	4.654	4.462

The total lengths of tubing required for the various generator concepts are shown in Table C-3. The preheater concept is shown to offer no advantage and is not considered further. It is also evident that the choice between stainless steel or cupro-nickel for the tubing material has negligible effect on the heat transfer or total length of tubing. Comparison of the results for finned and plain tubing shows that the former is approximately twice as effective for heat transfer via free convection.

The effect of coils in parallel paths on required pressure drop is analyzed in Appendix B. The results show that one coil of 0.75 tubing requires excessive pressure for the desired flow rate of hot water and should be avoided. Other factors that affect the selection of number of coils are generator packaging requirements, flow distribution of solution over the tubes, and the availability or delivery time of 0.75 versus 1.00 tubing.

The spray-fed falling film generator is examined further by examining the commercially available hollow-cone spray nozzle. The pump and spray nozzle will operate at the intersection of the pump performance curve and of the pressure/flow characteristic of the nozzle and associated lines. If the pump discharge valve is considered to be part of the nozzle-associated lines, the characteristic curve of the valve-nozzle-lines system will shift as the valve position is changed, and the operating or intersection point will change.

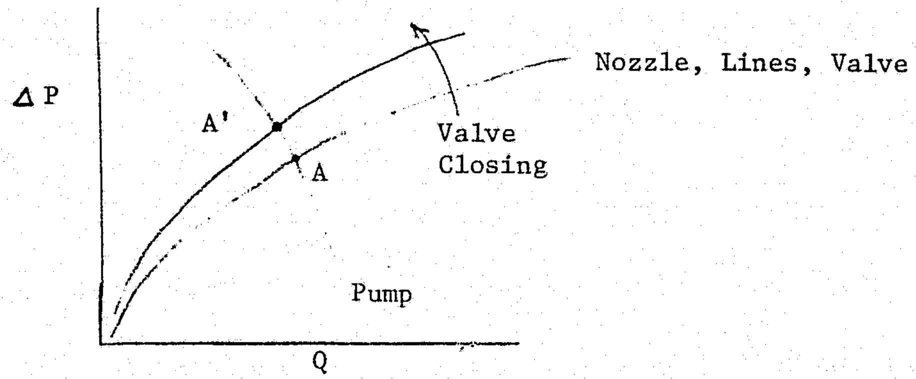

TABLE C-3

TOTAL LENGTH OF GENERATOR TUBING

Do Inch	COILS	TUBE SURFACE	PRHTR* + GEN		TRAY, POOL				FALLING FILM			
			Feet	Meters	SS Feet	SS Meters	CU/NI Feet	CU/NI Meters	SS Feet	SS Meters	CU/NI Feet	CU/NI Meters
0.75	1	Plain							47.5	14.5	47.4	14.4
	2								54.6	16.6	54.3	16.6
	3		10.2+164	3.11+50.0					60.3	18.4	59.5	18.1
	4				196	59.7	197	60.0	65.0	19.8	64.1	19.5
1.0	1								41.3	12.6	41.1	12.5
	2								49.0	14.9	48.6	14.8
	3		10.2+174	3.11+53.0					55.6	16.9	54.7	16.7
	4		10.2+180	3.11+54.9	157	47.9	154	46.9	61.3	18.7	60.1	18.3
0.75	1	Finned					83.5	25.5				
	2						86.4	26.3				
	3		8.6+99	2.62+30.2			88.9	27.1				
	4		8.6+102	2.62+31.1	102	31.1	90.0	27.4				
1.0	1						60.4	18.4				
	2						64.3	19.6				
	3						67.9	20.7				
	4				84	25.6	71.0	21.6				

*Preheater tubing not finned.

Preheater Length 10.2 Ft. - 0.84/0.71 OD/ID, 1.77 ID
8.6 Ft. - 0.50/0.43 OD/ID, 1.50 ID

The head or pressure available to the nozzle is estimated in Appendix C which includes spray nozzle manufacturer's data for spray angle and pressure/capacity for the nozzles of interest. With the pump and weak absorbent flow rate as previously specified, the maximum pressure drop available (i.e. with the pump discharge valve 100% open) for the spray nozzle is 145. kN/m^2 (21 psid). A spray nozzle that will deliver 3.10 dm^3/M (0.82 GPM) at this pressure differential is required. Due to the difficulty of obtaining an exact match, a variable nozzle or one that is designed and tested for the specific system, is required.

Spray angle of the nozzle (see manufacturer's data sheet in Appendix C) is a parameter which also must be considered. The spray nozzle/coil geometry is analyzed in Appendix D for a coil whose top turn is flat. The nozzle should be located such that most of the solution spray impinges on the top coil. Otherwise, baffles and other devices are necessary to funnel or feed the solution to the coil. The geometric relationships are developed in Appendix D for a single and double coil configuration and representative heights and dimensions are calculated.

The required tubing lengths are put into preliminary envelope dimensions to estimate vessel sizes for mounting and accessibility requirements. These data are shown below.

Envelope Dimensions

Falling Film	Centimeters	(Inches)
Spray	35.6 dia X 35.6 high	14 dia x 14 high
Dripper	35.6 dia X 61.0 long	14 dia x 24 long
Tray	96.5 X 111.8	38 x 44 for single serpentine coil
Pool	30.5 dia X 61.0 long	12 dia x 24 high

The effect of system parameters such as viscosity, specific gravity, generator pressure on the spray angle and hollow cone width, are best determined empirically. The effect of the vapor generation with its high specific volume on the hollow cone spray is also unknown. Due to the high degree of uncertainty of the operation of spray nozzles in a system such as the lithium bromide generator, and since a suitable test and development program is beyond the scope of this project, the spray-fed falling film generator concept was not pursued further.

Similarly, the dripper-fed falling-film generator was not retained as a candidate because of the test and development required to prove the reliability of a dripper design. Potential problems are streaming of solution through the dripper, clogging of the dripper due to precipitation of LiBr crystals which could occur during shutdown when the generator temperature decreases to ambient, and non-uniform flow distribution.

Therefore, in spite of the excellent heat transfer characteristics of the falling film generator, its development for a residential absorption air conditioner does not lend itself to the expediency required in the present program.

The shallow tray generator is designed structurally in Appendix E. Due to the large surface area, the pressure differential stresses require that the vessel be heavily reinforced and stiffened.

The relative advantages and disadvantages of the generator concepts are shown in Figure C-5. The selection of the pool type of generator for final design, fabrication, and installation into the LiBr air conditioner is based on three

FIGURE C-5

GENERATOR CONCEPT COMPARISON

CONCEPT	ADVANTAGES	DISADVANTAGES
Falling Film	Most efficient heat transfer Compact package Negligible submergence	Spray angle uncertainties Solution distribution per coil Dripper Uncertainties
Tray	Large solution/vapor interface Low submergence	Heavy pressure vessel
Pool	Compact package	Small solution/vapor interface High submergence
Preheater	None	

criteria. These criteria are sufficient heat transfer capability; no requirement for empirical data, test and development; and moderate packaging, mounting and accessibility requirements.

The sketches for the final design and fabrication are in Appendix F. Three thermometer wells are included for entering weak absorbent, leaving strong absorbent, and vapor temperatures. Two sight glasses, 90° apart, are shown. One is for viewing, the other is for the illumination source, and vice versa. A perforated plate is provided at the inlet at the generator base to distribute the weak absorbent uniformly around the circumference. The gaps between each coil, between the inner coil and the standpipe, and between the outer coil and the shell wall, are as small and uniform as fabrication practices allow, to prevent streaming and to maintain uniform flow.

Several locations for the generator are considered in Appendix G, based on pressure drop required in the vapor line from generator to condenser. The results show that there is negligible difference among the candidates based on pressure alone. The choice of location B is therefore based on better accessibility in the planned installation of the modified air conditioner at the Solar Demonstration House at the Marshall Space Flight Center, Huntsville, Alabama.

C.3 System Modification

The first step in the modification process is the draining and storage of the lithium bromide solution. This is performed by pressurizing the system to ambient pressure with clean, oil-free nitrogen. Solution was drained from the sampling ports into clean glass containers and capped to prevent absorption of

water vapor from the atmosphere, and to maintain cleanliness. Holes were drilled at the low points to drain solution from the generator and both sides or chambers of the liquid heat exchanger. Approximately 23.4 cubic decimeters (6.2 gallons) were drained from the air conditioner.

The generator, vapor tube, and separator are removed along with the control chamber, liquid trap, and associated lines. The weak absorbent line is cut at the low point between the noncondensible gas separator and the liquid heat exchanger for connecting lines to the pump, and from the discharge valve. The solution pump and discharge valve are mounted on the base plate. The purge pump line and the noncondensible gas line from the noncondensible gas separator at the base, are pinched off to preclude introducing vapor to the pump suction line.

The Chrysler generator is located such that the vapor line outlet is level with the vapor inlet to the condenser. The structure is reinforced to support the generator. The weak absorbent line from the liquid heat exchanger to the original generator is capped and the equalizer line from the top or dome of the liquid heat exchanger is used for the weak absorbent flow to the generator. The lines connecting to the control chamber and the liquid trap are capped.

System integrity is verified with leak checks on all new connections, caps, and plugged drain holes on the pump and valve. Bubble leak checks are performed with an approximately 50/50 mixture of helium and nitrogen at 103 kN/m^2 gage (15 psig). No bubbles were observed. The air conditioner was evacuated and filled such that, with the pump running, the level of absorbent in the base of the absorber uncovered the absorber purge line, but covered the weak absorbent exit line to maintain maximum head on the pump suction line. When the pump

is turned off, the solution level in the absorber rises as the generator drains. The fluid equilibrium level in the absorber is above the absorber purge line connection. <u>This requires that the pump be ON whenever the absorber purge line is purged.</u> The initial fill is approximately 39.75 dm^3 (10.5 gls.) of solution which compares closely with the volume estimate in Appendix H, of 40.4 dm^3 (10.6 gls.). (Note that approximately 23.5 dm^3 (6.2 gls.) weighing 35.2 kg (77.5 lbm) of solution were drained from the unit at the completion of the Phase I tests.)

The valve was positioned for minimum flash point temperature at the refrigerant return line outlet at the evaporator. It was found that this position did not vary for different conditions. A valve was added temporarily to the condenser outlet to enable sampling of the condensate and adjustment of the refrigerant mass in the system. Weak and strong absorbent weight percent concentrations of lithium bromide X_w and X_s, respectively, were measured by drawing samples and recording the specific gravity with a hydrometer and the temperature. The concentrations are calculated according to the following equation*.

$$X = -96.85 + (116.3)(SG) - (4.422)(SG^2) + (0.01569)(T)$$
$$+ (4.015 \times 10^{-5})(T^2) - (1.107 \times 10^{-5})(SG^2)(T^2)$$
$$-6.123\ (SG^3)$$

Where SG = Specific Gravity
T = Temperature - Fahrenheit
X = Weight percent of LiBr

*Reference J. G. Murray, Airtemp Corporation, Absorption Test Data Analysis for 235 Prototype Computer Program.

These concentrations compare very closely with the samples measured at the end of Phase I Test as shown below. The Phase I data are at rated conditions (Teg = 96.1C, 205F; Tea = 29.4C, 85F; F_{hot} = 41.6 dm^3/M, 11 gal.; F_{twr} = 37.9 dm^3/M, 10 gal.). The conditions for the Phase II data are in Table D-1.

LITHIUM BROMIDE CONCENTRATION DATA

TEST	S.G.	T(F)	X_w(%)	X_s(%)
End of Ø I	1.503	84.02	48.60	--
	1.540	91.94	--	50.96
II-5	1.488	101.3	47.99	--
	1.538	90.5	--	50.82
II-18	1.480	81.68	47.13	--
	1.542	84.92	--	50.95
II-35	1.499	78.3	48.24	--
	1.566	86.7	--	52.37

The refrigerant level was adjusted for spillage to start in the 86.1 to 87.8C (187 to 190F) range. This is a compromise between COP and capacity since the optimum condition is just prior to the onset of spillage and spillage increases the generator thermal energy requirement.

D. PHASE II TEST

The Phase II Test Program objective is to duplicate the Phase I test input parameters and to measure system cooling capacity (QEVAP) and system thermal requirements (QGEN). The fixed input parameters are cooling tower flow rate (F_{twr}), tower water temperature entering the absorber (T_{ea}), hot water flow rate (F_{hot}), and the air side inlet parameters (velocity, dry bulb, wet bulb). Hot water inlet temperature (T_{eg}) is the test variable.

The boiling, as observed visually through the generator sight glasses, is extremely violent especially at the higher portion of the temperature range, 93 to 96 C (200 to 205 F). Spilling of solution over the edge of the inner standpipe seems to be random rather than continuous. This would account for the non-steady tower water temperature ($T_{a/c}$) observed between the absorber exit and condenser inlet. Non-steady $T_{a/c}$ does not affect the overall tower heat load calculation

$$QTWR = (F\ Cp\,\rho)_{twr}\ (T_{1c} - T_{ea})$$

but it does affect the distribution of QTWR between the absorber and condenser heat loads (QABS and QCOND).

$$QABS = (FCp\,\rho)_{twr}\ (T_{a/c} - T_{ea})$$

$$QCOND = (FCp\,\rho)_{twr}\ (T_{1c} - T_{a/c})$$

$$QTWR = QCOND + QABS$$

The calculation procedure for Phase II data is modified because of the non-steady $T_{a/c}$, see Appendix I, by taking the ratio QGEN/QABS to be 1.05. QGEN is calculated from the measured hot water flow rate, and inlet and outlet temperatures.

$$QGEN = (F\ Cp\rho)_{hot}\ (T_{eg} - T_{lg})$$

$$QABS = QGEN/1.05$$

$$QCOND = QTWR-QABS$$

The evaporator heat load is approximated by assuming low liquid spillage to the absorber, then (see Phase I calculation procedure):

$$QEVAP = QCOND/1.05$$

An overall heat balance QTWR/(QEVAP + QGEN) is calculated. By the steady state energy equation, $\Sigma Q=0$, the heat balance should equal unity. QTWR and QGEN are measured and calculated directly, whereas only QEVAP is calculated from the above approximations. Only one case (II-48) shows a heat balance error which exceeds 2%, and it is less than 3%.

The raw test data for Phase II are shown in Table D-1. The reduced data and calculation results are contained in Table D-2. Figure D-1A and D-1B show the heat loads (QEVAP and QGEN) and the COP for test runs II-4 through -8, 51, 53, and 59. QEVAP rises very slowly above 88 C (190 F) due to the extremely violent boiling which causes lithium-bromide solution to be carried past the integral separator baffle at the generator vapor outlet. This "carryover" passes through the condenser to the evaporator whose apparent performance is degraded. The low COP (Figure D-1B) above 88 C (190 F) which occurs in conjunction with evaporator spillage, is due to the "carryover" since refrigerant is produced by the generator, but not utilized by the evaporator. In addition, if the QEVAP data at 85 to 87.55 C (185 to 189.59 F) are extrapolated on a straight line basis, to eliminate the effect of carryover, to 96.1 C (205 F), the QEVAP becomes 10.5 kW (36,000 BTUH).

TABLE 1 TEST DATA XWF 501 UNITS: S.I.

RUN	FLOW		AIR				HOT WTR		SOLUTION					COND		EVAP			TOWER WATER		
	HOT dm^3/M	TWR dm^3/M	T_{edb} °C	T_{ewb} °C	T_{1db} °C	T_{1wb} °C	T_{eg} °C	T_{1g} °C	T_{eas} °C	T_{1aw} °C	T_{egw} °C	T_{1gv} °C	T_{1gs} °C	T_v °C	T_{rr} °C	T_{fp} °C	T_{out} °C	SPILL	T_{ea} °C	$T_{a/c}$ °C	T_{1c} °C
II-4	34.4	37.5	26.90	18.91	14.94	14.45	85.13	80.33	37.34		63.04	74.45	75.61	38.04		9.24	18.00	N	29.54	33.73	36.96
II-5	34.4	37.5	26.77	19.22	15.46	14.67	85.05	80.13	37.61		62.97	74.42	75.45	37.85	37.5	8.87	18.13	N	29.32	33.5	36.85
II-6	37.9	37.5	26.75	19.11	14.91	14.19	87.55	82.47	37.24		64.34	76.59	77.69	38.82	38.61	9.39	18.15	Y	29.37	34.00	37.51
II-7	40.5	37.5	26.76	19.31	14.99	14.31	87.55	82.89	37.06		64.33	76.64	77.95	38.99	38.82	9.49	18.03	Y	29.4	34.05	37.59
II-8	40.5	37.5	26.59	19.34	15.44	14.76	85.02	80.89	37.64	31.33	63.57	74.62	75.82	37.91	38.18	9.46	18.32	N	29.42	33.63	36.72
II-9	40.5	37.5	26.85	19.5	15.63	14.77	82.97	79.28	37.42	31.07	62.53	72.93	74.2	37.13	37.41	9.05	17.67	N	29.42	33.13	35.93
II-10	40.5	37.5	26.7	19.48	16.05	15.05	81.03	77.45	36.90	30.75	61.30	71.53	72.7	36.38	36.1[illegible]	8.65	16.98	N	29.25	32.75	35.43
II-11	40.5	37.5	26.65	19.23	15.88	14.73	80.95	77.55	37.20	30.97	61.30	71.60	72.75	36.33	35.86	8.73	17.00	N	29.38	32.83	35.30
II-12	40.5	37.5	26.8	19.50	17.17	15.60	79.10	76.10	37.10	30.83	60.47	69.83	71.08	35.43	35.02	8.38	17.32	N	29.48	32.43	34.53
II-13	40.5	37.5	26.8	19.20	17.95	15.85	77.20	74.48	36.75	36.39	58.40	68.33	70.15	34.45	34.39	7.65	17.48	N	29.40	31.95	33.65
II-14	40.5	37.5	26.55	19.30	18.0	16.15	76.95	74.35	37.35	30.69	59.25	68.18	69.90	34.50	34.44	7.85	17.55	N	29.45	31.95	33.65
II-15	40.5	37.5	26.47	19.37	19.17	16.63	75.0	72.90	37.37	30.74	58.00	66.70	70.25	33.50	33.21	7.57	17.30	N	29.45	31.52	32.85
II-16	36.0	37.5	26.80	19.47	16.08	15.20	84.98	80.47	37.88	31.33	63.47	74.13	75.40	37.85	37.46	10.07	17.98	N	29.48	33.62	36.70
II-17	37.9	37.5	26.61	19.35	15.55	14.81	87.49	82.56	37.84	31.67	64.63	76.21	77.34	38.55	38.52	10.24	18.80	Y	29.38	33.74	37.36
II-18	34.4	37.5	26.53	19.18	15.28	14.48	85.06	80.49	36.9	31.07	63.16	74.0	75.12	37.31	37.14	9.06	17.38	N	29.34	33.24	36.3
II-19	40.5	37.5	26.67	19.38	15.90	15.10	85.13	80.97	37.97	30.91	65.17	76.07	76.72	37.95	38.09	10.97	18.73	Y	29.42	33.53	36.97
II-20	40.5	37.5	26.75	19.35	15.83	14.95	85.25	81.15	38.60	31.61	65.50	76.30	76.80	38.00	38.03	10.95	18.85	Y	29.50	33.75	37.00
II-21	40.5	37.5	26.93	19.45	15.80	14.93	85.35	81.38	38.30	31.25	65.40	76.35	77.15	37.90		9.85	18.55	N	29.50	33.58	36.85
II-22	41.6	68.5	24.15	17.03	11.23	10.62	95.33	90.38	40.87	32.22	71.03	84.52	85.72	35.87	30.20	3.37	14.18	N	27.12	29.93	32.10
II-23	41.6	68.5	28.7	20.2	17.1	15.7	86.55	81.25	35.50	30.00	63.00	75.00	75.90	33.75	33.44	8.10	16.90	Y	27.7	29.9	32.5
II-24	41.6	37.5	26.55	19.24	15.85	14.86	85.13	81.41	38.04	31.69	65.70	76.18	77.03	37.41	37.22	10.44	17.95	N	29.60	33.46	36.30
II-25	41.6	37.5	26.87	19.50	15.77	14.98	87.67	83.40	38.43	32.22	67.30	78.57	79.57	38.35	38.37	10.72	18.73	Y	29.57	33.75	37.18
II-26	41.6	37.5	26.70	19.33	15.75	14.92	90.20	85.17	38.17	31.24	67.87	80.58	81.60	39.22	38.96	10.47	18.00	Y	29.47	33.63	37.80
II-27	41.6	37.5	26.78	19.47	15.88	14.90	92.97	87.25	39.80	32.22	69.50	83.02	84.05	40.35	38.96	10.08	18.92	Y	29.40	33.88	38.62
II-28	41.6	37.5	26.61	19.48	15.99	15.05	95.91	89.86	29.83	32.40	71.03	85.64	86.76	40.93	38.85	9.16	18.75	Y	29.38	33.78	38.83
II-29	34.4	37.5	25.9	19.0	14.9	14.1	95.9	88.1	39.6		69.0	84.3	85.5	41.4	41.11	7.2	18.4	Y	29.5	34.5	39.9
II-30	41.6	51.9	25.50	18.50	14.15	13.33	87.73	82.98	38.8	31.67	66.0	77.73	78.7	37.13	37.22	7.48	16.73	Y	29.43	33.10	35.95
II-31	41.6	48.5	26.2	18.95	14.65	13.7	87.55	82.95	39.1	31.78	65.55	77.4	78.85	37.3	37.22	7.4	17.3	N	29.40	33.25	36.35
II-32	41.6	49.6	26.72	19.42	15.35	14.47	87.67	82.97	39.57	31.94	66.23	77.6	78.58	37.43	37.22	7.90	17.63	INT	29.53	33.37	36.27
II-33	41.6	49.6	26.70	19.43	15.23	14.33	87.90	83.15	39.2	31.44	66.10	77.63	78.65	37.20	37.06	7.70	17.08	Y	29.03	32.98	36.03
II-34	41.6	45.4	27.8	20.0	15.7	14.7	87.75	83.1								8.0		Y	28.9	32.95	36.3
II-35	41.6	49.6	26.19	18.65	14.51	13.60	87.61	83.04	38.45	31.11	65.5	77.5	78.35* 76.1	37.05	36.7	7.46	17.2	INT	29.38	33.04	36.0
II-36	41.6	49.6	26.88	19.65	15.72	14.83	85.13	81.0								7.08		N	29.33	32.6	35.27
II-37	41.6	49.6	26.38	19.57	15.62	14.77	85.02	80.98	39.0	31.67	64.9	75.4	77.1	36.3	36.61	7.08	17.0	N	29.48	32.78	35.37
II-38	41.6	49.6	29.73	23.97	21.60	20.77	96.27	89.77								7.23		Y	29.37	32.55	37.05
II-39	41.6	49.6	27.05	19.63	15.48	14.65	87.75	83.40	39.20	31.97	65.25	76.65	78.20	36.78	36.75	7.06	17.05	N	29.39	33.00	35.78
II-40	41.6	53.8	26.78	19.69	15.70	14.85	87.93	83.30	39.5	31.67	64.5	76.0	77.45	36.3	36.11	6.86	17.1	N	29.13	32.60	35.35
II-41	41.6	53.8	26.70	19.37	15.25	14.33	87.92	83.43	39.5	31.67	65.0	76.3	78.0	36.3	36.0	6.73	17.1	INT	29.03	32.23	35.17
II-42	41.6	53.8	26.82	19.23	15.03	14.02	87.97	83.28	38.85	31.11	64.8	76.4	78.0	36.0	35.56	6.52	16.95	INT	28.47	32.03	34.77
II-43	41.6	37.5			(100%,	97.58)	84.80	81.23											29.4	33.1	35.85
II-44	41.6	37.5			(56%,	98.4)	85.7	81.75											29.5	33.2	36.15
II-45	41.6	37.5			(28%,	97.6)	90.80	86.25								7.73			30.9	35.15	38.80
II-46	40.1	37.5			(14%,	95.75)	93.7	88.13								8.0			31.3	35.58	39.55
II-47	39.4	37.5			(0%,	96.63)	97.5	91.5						42.8		8.13			32.13	36.6	41.35

* Indicates temperature decrease from top of generator to heat exchanger inlet.

NOTE: (A,B) Where A→Source bypass valve % open
B→Source temperature.

N=No Y=Yes INT=Intermittent

RUN	FLOW		AIR				HOT WTR		SOLUTION					COND		EVAP			TOWER WATER		
	HOT dm^3/M	TWR dm^3/M	T_{edb} °C	T_{ewb} °C	T_{ldb} °C	T_{lwb} °C	T_{eg} °C	T_{lg} °C	T_{eas} °C	T_{law} °C	T_{egw} °C	T_{lgv} °C	T_{lgs} °C	T_v °C	T_{rr} °C	T_{fp} °C	T_{out} °C	[illegible]	T_{ea} °C	$T_{a/c}$ °C	T_{lc} °C
II-48	41.6	53.8	28.0	20.5	21.7	19.4	96.3	89.45	37.8		67.0	81.7	83.85	37.85	41.1	10.7	18.5	Y	29.1	31.15	35.85
II-49	40.9	53.4	24.38	18.35	16.40	15.20	95.58	89.20	38.9		67.5	81.7	83.5	39.0	38.3	7.9	17.65	Y	29.55	32.30	36.38
II-50	40.9	53.4	32.23	24.83	23.55	22.00	95.98	89.20								9.6		Y	29.38	32.00	36.35
II-51	40.9	37.5	26.30	19.42	16.85	15.72	96.50	90.50								9.0		Y	29.38	33.78	39.1
II-52	40.9	33.3	25.9	18.85	16.2	15.0	96.6	91.0								9.0		Y	29.4	34.2	39.9
II-53	41.6	37.5	26.73	19.45	16.50	15.40	96.33	90.13	40.08	32.0	67.50	83.43	85.08	41.03	40.14	8.63	18.05	Y	29.42	34.00	39.40
II-54	41.6	33.3	26.55	19.28	15.95	14.93	96.18	90.47								9.27		Y	29.37	34.87	40.40
II-55	42.0	29.5	25.80	18.60	15.15	14.20	95.97	90.57								9.52		Y	29.47	35.53	41.28
II-56	41.6	25.7	26.17	18.83	15.45	14.45	96.20	91.14								10.06		Y	29.32	36.32	42.24
II-57	41.6	21.6	26.96	19.39	16.15	15.55	96.17	91.53								10.92		Y	29.32	37.32	43.34
II-58	41.6	17.8	29.71	21.40	18.34	17.10	96.38	92.11								11.86		N	29.34	38.58	44.85
II-59	41.6	37.5	26.47	18.95	15.52	14.37	96.07	90.22	38.89	31.11	67.0	83.1	84.8	40.6	38.89	7.5	17.9	Y	29.38	34.07	39.15
II-60	41.6	37.5	32.45	23.95	21.60	20.21	96.15	89.58	37.22	29.44	67.0	82.25	84.1	38.95	37.22	6.65	17.65	Y	26.69	31.04	36.94
II-61	41.6	33.3	26.63	19.17	15.60	14.50	96.22	90.03	37.22	29.44	68.0	83.25	85.0	40.4	39.0	6.43	17.9	Y	26.72	32.22	38.30
II-62	41.6	29.5	25.80	18.33	14.58	13.50	96.18	90.35	37.22	29.44	69.0	83.5	85.1	41.15	39.44	6.68	17.8	Y	26.70	32.88	39.20
II-63	41.6	25.7	24.36	17.02	13.12	12.07	96.24	90.73	38.33	29.83	70.0	84.1	85.6	42.4	40.56	7.16	17.75	Y	26.64	33.78	40.48
II-64	41.6	21.6	24.64	17.39	13.44	12.47	96.29	91.30	38.33	30.0	70.5	84.8	86.35	43.7	41.67	7.90	17.9	Y	26.70	34.89	41.72
II-65	41.6	17.8	24.20	17.16	13.09	12.23	96.11	91.33	36.1	28.06	72.0	85.25	86.6	44.2	42.78	7.14	17.3	Y	23.96	33.63	41.90
II-66	41.6	21.6	23.34	16.41	12.08	11.37	96.23	90.83	35.0	27.78	68.0	84.2	85.61	42.2	40.56	6.3	16.95	Y	23.98	32.19	40.1
II-67	41.6	25.7	25.69	18.36	14.60	13.65	96.23	90.49	34.72	27.61	69.0	83.7	85.3	41.1	39.22	5.84	18.0	Y	23.89	31.10	38.78
II-68	41.6	29.5	27.55	19.85	16.43	15.33	96.45	90.10	34.44	27.5	67.0	82.8	84.4	39.6	38.06	5.65	18.0	Y	24.00	29.95	37.35
II-69	41.6	29.5	28.18	20.47	16.92	15.90	95.95	89.78	33.89	27.2	67.0	82.7	84.4	39.3	37.22	6.13	17.5	Y	23.98	30.27	37.27
II-70	41.6	33.3	34.4	25.5	23.0	21.85	95.8	89.25	33.89	27.2	66.5	81.5	83.3	37.8	36.1	6.35	17.5	Y	24.0	28.9	35.5
II-71	41.6	37.5	28.53	20.71	17.31	16.27	96.15	91.1	39.4		71.4	84.7	86.15	42.6	41.1	10.99	20.4	Y	32.14	36.88	41.3
II-72	41.6	31.4	28.90	20.94	17.56	16.56	96.11	91.4	40.56		71.7	85.0	86.35	43.8	41.7	11.58	20.8	Y	32.16	37.74	42.53
II-73	41.6	25.7	31.62	22.80	19.67	18.52	96.27	92.0	40.56		73.0	86.0	87.4	45.55	43.89	12.43	21.9	N	32.12	38.80	44.27
II-74	41.6	19.9	36.05	26.05	23.25	21.8	96.25	92.53								12.98		N	32.15	39.93	45.7
II-75	41.6	43.5	28.98	20.90	17.54	16.51	96.15	90.73	39.4		70.0	84.0	85.5	41.6	40.56	10.79	20.6	Y	32.14	36.38	40.43
II-76	41.6	49.6	26.45	19.07	14.80	13.93	87.78	82.95	39.69		64.3	76.2	77.52	37.17		7.47	17.37	N	29.35	33.13	36.12
II-77	41.6	49.6	26.77	19.48	15.75	14.72	85.21	80.92	39.5		63.26	74.37	76.03	36.34		6.98	16.91	N	29.42	32.77	35.38

N=No Y=Yes INT=Intermittent

TABLE D TEST DATA XWF 501 *UNITS:* CONVENTIONAL

RUN	FLOW HOT GPM	FLOW TWR GPM	AIR T_{edb} °F	AIR T_{ewb} °F	AIR T_{ldb} °F	AIR T_{lwb} °F	HOT WTR T_{eg} °F	HOT WTR T_{lg} °F	SOLUTION T_{eas} °F	SOLUTION T_{law} °F	SOLUTION T_{egw} °F	SOLUTION T_{lgv} °F	SOLUTION T_{lgs} °F	COND T_v °F	COND T_{rr} °F	EVAP T_{fp} °F	EVAP T_{out} °F	SPILL	TOWER WATER T_{ea} °F	TOWER WATER $T_{a/c}$ °F	TOWER WATER T_{lc} °F
II-4	9.09	9.9	80.42	66.04	58.89	58.01	185.23	176.59	99.21		145.47	166.01	168.1	100.47		48.63	64.40	N	85.17	92.71	98.53
II-5	9.09	9.9	80.19	66.60	59.83	58.41	185.09	176.23	99.70		145.35	165.96	167.81	100.13	99.5	47.97	64.63	N	84.78	92.3	98.33
II-6	10.00	9.9	80.15	66.40	58.84	57.54	189.59	180.45	99.03		147.81	169.86	171.84	101.88	101.5	43.9	64.67	Y	84.87	93.2	99.52
II-7	10.7	9.9	80.17	66.76	58.98	57.76	189.59	181.20	98.71		147.79	169.95	172.31	102.18	101.88	49.08	64.45	Y	84.92	93.29	99.66
II-8	10.7	9.9	79.86	66.81	59.79	58.57	185.04	177.60	99.75	88.40	146.43	166.32	168.48	100.24	100.72	49.03	64.98	N	84.96	92.54	98.1
II-9	10.7	9.9	80.33	67.1	60.14	58.58	181.34	174.70	99.35	87.93	144.56	163.28	165.56	98.84	99.33	48.29	63.80	N	84.96	91.63	96.67
II-10	10.7	9.9	80.06	67.06	60.89	59.09	177.85	171.41	98.42	87.35	142.34	160.75	162.86	97.48	97.0	47.57	62.56	N	84.65	90.95	95.77
II-11	10.7	9.9	79.97	66.61	60.58	58.51	177.71	171.59	98.96	87.75	142.34	160.88	162.95	97.39	96.55	47.71	62.60	N	84.88	91.09	87.75
II-12	10.7	9.9	80.24	67.1	62.91	60.08	174.38	168.98	98.78	87.50	140.85	157.69	159.94	95.77	95.03	47.08	63.17	N	85.06	90.37	94.15
II-13	10.7	9.9	80.24	66.56	64.31	60.53	170.96	166.06	98.15	97.50	137.12	154.99	158.27	94.01	93.9	45.77	63.46	N	84.92	89.51	97.50
II-14	10.7	9.9	79.79	66.74	64.4	61.07	170.51	165.83	99.23	87.25	138.65	154.72	157.82	94.10	94.0	46.13	63.59	N	85.01	89.51	92.57
II-15	10.7	9.9	79.65	66.87	66.51	61.93	167.0	163.22	99.27	87.33	136.40	152.06	158.45	92.3	91.77	45.63	63.14	N	85.01	88.74	91.13
II-16	9.5	9.9	80.24	67.05	60.94	59.36	184.96	176.85	100.18	88.40	146.25	165.43	167.72	100.13	99.43	50.13	64.37	N	85.06	92.52	98.06
II-17	10.0	9.9	79.90	66.83	59.99	58.66	189.48	180.61	100.11	89.00	148.33	169.18	171.21	101.39	101.33	50.43	65.84	Y	84.88	92.73	99.25
II-18	9.1	9.9	79.75	66.52	59.50	58.06	185.12	176.87	98.42	87.93	145.68	165.20	167.22	99.15	98.86	48.30	63.28	N	84.82	91.84	97.34
II-19	10.7	9.9	80.0	66.89	60.62	59.0	185.23	177.74	100.34	87.63	149.31	168.93	170.09	100.31	100.57	51.74	65.72	Y	84.95	92.36	98.54
II-20	10.7	9.9	80.15	66.83	60.49	58.91	185.45	178.07	101.48	88.9	149.90	169.34	170.24	100.40	100.45	51.71	65.93	Y	85.10	92.75	98.6
II-21	10.7	9.9	80.47	67.01	60.44	58.87	185.63	178.48	100.94	88.25	149.72	169.43	170.87	100.22	--	49.73	65.39	N	85.10	92.44	98.33
II-22	11.0	18.1	75.47	62.66	52.22	51.11	203.60	194.69	105.56	90.0	159.86	184.13	186.29	96.56	86.37	38.06	57.53	N	80.81	85.88	89.78
II-23	11.0	18.1	83.66	68.36	62.78	60.26	187.79	178.25	95.9	86.0	145.40	167.0	168.62	92.75	92.2	46.58	62.42	Y	81.86	85.82	90.50
II-24	11.0	9.9	79.79	66.63	60.53	58.75	185.23	178.54	100.47	89.05	150.26	169.12	170.65	99.34	99.0	50.79	64.31	N	85.28	92.23	97.34
II-25	11.0	9.9	80.36	67.10	60.38	58.97	189.80	182.12	101.18	90.0	153.14	173.42	175.22	101.03	101.07	51.29	65.72	Y	85.22	92.75	98.93
II-26	11.0	9.9	80.06	66.80	60.35	58.85	194.36	185.30	100.70	88.23	154.16	177.05	178.88	102.59	102.13	50.84	64.40	Y	85.04	92.54	100.04
II-27	11.0	9.9	80.21	67.04	60.59	58.82	199.34	189.05	103.64	90.0	157.10	181.43	183.29	104.63	102.13	50.15	66.05	Y	84.92	92.99	101.51
II-28	11.0	9.9	79.90	67.06	60.78	59.09	204.64	193.75	103.69	90.33	159.85	186.15	188.17	105.67	101.93	48.49	65.75	Y	84.88	92.80	101.89
II-29	9.1	9.9	78.62	66.20	58.82	57.38	204.62	190.58	103.28		156.20	183.74	185.9	106.52	106.0	44.96	65.12	Y	85.1	94.1	103.82
II-30	11.0	13.7	77.90	65.30	57.47	55.99	189.91	181.36	101.84	89.0	150.8	171.91	173.66	98.83	99.0	45.46	62.11	Y	84.97	91.58	96.71
II-31	11.0	12.8	79.16	66.11	58.37	56.66	189.59	181.31	102.38	89.2	149.99	171.32	173.93	99.14	99.0	45.32	63.14	N	84.92	91.85	97.43
II-32	11.0	13.1	80.09	66.95	59.63	58.04	189.80	181.34	103.22	89.5	151.22	171.68	173.45	99.38	99.0	46.22	63.74	INT	85.16	92.06	97.28
II-33	11.0	13.1	80.06	66.97	59.41	57.79	190.22	181.67	102.56	88.6	150.98	171.73	173.57	98.96	98.7	45.86	62.74	Y	84.25	91.36	96.85
II-34	11.0	12.0	82.04	68.0	60.26	58.46	189.95	181.58								46.4		Y	84.02	91.31	97.34
II-35	11.0	13.1	79.14	65.57	58.12	56.48	189.7	181.47	101.21	88.0	149.9	171.5	(173.03* 169.0)	98.7	98.0	45.43	62.96	INT	84.88	91.47	96.82
II-36	11.0	13.1	80.39	67.37	60.29	58.70	185.24	177.8								44.75		N	84.80	90.68	95.48
II-37	11.0	13.1	79.48	67.23	60.12	58.59	185.03	177.77	102.2	89.0	148.82	167.72	170.78	97.34	97.4	44.75	62.6	N	85.06	91.0	95.67
II-38	11.0	13.1	85.52	75.14	70.88	69.38	205.28	193.58								45.02		Y	84.86	90.59	98.69
II-39	11.0	13.1	80.69	67.33	59.86	58.37	189.95	182.12	102.56	89.55	149.45	169.97	172.76	98.20	98.15	44.71	62.69	N	84.90	91.40	96.40
II-40	11.0	14.2	80.20	67.44	60.26	58.73	190.27	181.94	103.1	89.0	148.1	168.8	171.41	97.34	97.0	44.35	62.78	N	84.43	90.68	95.63
II-41	11.0	14.2	80.06	66.86	59.45	57.80	190.25	182.18	103.1	89.0	149.0	169.34	172.4	97.34	96.8	44.12	62.78	INT	84.26	90.20	95.30
II-42	11.0	14.2	80.27	66.62	59.06	57.23	190.34	181.91	101.93	88.0	148.64	169.52	172.4	96.8	96.0	43.73	62.51	INT	83.24	89.66	94.58
II-43	11.0	9.9			(100%,	207.64)	184.64	178.21											84.92	91.58	96.53
II-44	11.0	9.9			(56%,	209.12)	186.26	179.15											85.1	91.76	97.07
II-45	11.0	9.9			(28%,	207.7)	195.44	187.25								45.91			87.62	95.27	101.84
II-46	10.6	9.9			(14%,	204.35)	200.66	190.63								46.4			88.34	96.04	103.19
II-47	10.4	9.9			(0%,	205.93)	207.5	196.7						109.0		46.63			89.83	97.88	106.43

*Indicates temperature decrease from top of generator to heat exchanger inlet.

NOTE: (A,B) where A ~ Source Bypass Valve % Open
B - Source Temperature

N=No Y=Yes INT=Intermittent

TABLE D-I TEST DATA XWF 501 UNITS: CONVENTIONAL

RUN	FLOW		AIR				HOT WTR		SOLUTION					COND		EVAP			TOWER WATER		
	HOT GPM	TWR GPM	T_{edb} °F	T_{ewb} °F	T_{ldb} °F	T_{lwb} °F	T_{eg} °F	T_{lg} °F	T_{eas} °F	T_{law} °F	T_{egw} °F	T_{lgv} °F	T_{lgs} °F	T_v °F	T_{rr} °F	T_{fp} °F	T_{out} °F	SPILL	T_{ea} °F	$T_{a/c}$ °F	T_{lc} °F
II-48	11.0	14.2	82.4	68.9	71.1	66.9	205.34	193.01	100.0	96.53	152.6	179.1	182.9	100.1	106.0	51.3	65.3	Y	84.38	88.07	96.53
II-49	10.8	14.1	75.88	65.03	61.52	59.36	204.04	192.56	102.0	97.48	153.5	179.1	182.3	102.2	101.0	46.2	63.8	Y	85.19	90.14	97.48
II-50	10.8	14.1	90.01	76.69	74.39	71.60	204.76	192.56								49.28		Y	84.88	89.60	97.43
II-51	10.8	9.9	79.34	66.95	62.33	60.29	205.70	194.90								48.20		Y	84.88	92.81	102.38
II-52	10.8	8.8	78.62	65.93	61.16	59.00	205.88	195.80								48.20			84.92	93.56	103.82
II-53	11.0	9.9	80.12	67.01	61.7	59.72	205.40	194.24	104.15	89.6	153.5	182.17	185.14	105.85	104.25	47.54	64.49	Y	84.95	93.20	102.92
II-54	11.0	8.8	79.79	66.71	60.71	58.88	205.13	194.84								48.68		Y	84.86	94.76	104.72
II-55	11.1	7.8	78.44	65.48	59.27	57.56	204.74	195.02								49.13		Y	85.04	95.96	106.31
II-56	11.0	6.8	79.11	65.89	59.81	58.01	205.16	196.05								50.11		Y	84.78	97.38	108.03
II-57	11.0	5.7	80.53	66.90	61.07	59.99	205.11	196.75								51.66		Y	84.78	99.18	110.01
II-58	11.0	4.7	85.48	70.52	65.01	62.78	205.48	197.80								53.35		N	84.81	101.44	112.73
II-59	11.0	9.9	79.64	66.11	59.93	57.86	204.92	194.39	102.0	88.0	152.6	181.58	184.64	105.08	102.0	45.50	64.22	Y	84.89	93.32	102.47
II-60	11.0	9.9	90.41	75.11	70.88	68.38	205.07	193.24	99.0	85.0	152.6	180.05	183.38	102.11	99.0	43.97	63.77	Y	80.04	87.87	98.49
II-61	11.0	8.8	79.94	66.50	60.08	58.10	205.19	194.06	99.0	85.0	154.40	181.85	185.0	104.72	102.2	43.58	64.22	Y	80.09	89.99	100.94
II-62	11.0	7.8	78.44	64.99	58.24	56.30	205.12	194.63	99.0	85.0	156.2	182.30	185.18	106.07	103.0	44.02	64.04	Y	80.06	91.18	102.56
II-63	11.0	6.8	75.85	62.64	55.62	53.73	205.23	195.31	101.0	85.7	158.0	183.38	186.08	108.32	105.0	44.89	63.95	Y	79.95	92.80	104.86
II-64	11.0	5.7	76.35	63.30	56.19	54.45	205.32	196.34	101.0	86.0	158.9	184.64	187.43	110.66	107.0	46.22	64.22	Y	80.06	94.80	107.10
II-65	11.0	4.7	75.56	62.89	55.56	54.01	205.00	196.39	97.0	82.5	161.6	185.45	187.88	111.56	109.0	44.85	63.14	Y	75.13	92.53	107.42
II-66	11.0	5.7	74.01	61.54	53.74	52.47	205.21	195.49	95.0	82.0	154.4	183.56	186.08	107.96	105.0	43.34	62.51	Y	75.16	89.94	104.18
II-67	11.0	6.8	78.24	65.05	58.28	56.57	205.21	194.88	94.5	81.7	156.2	182.66	185.34	105.98	102.6	42.51	64.4	Y	75.00	87.98	101.80
II-68	11.0	7.8	81.59	67.73	61.57	59.59	205.61	194.18	94.0	81.5	152.6	181.04	183.92	103.28	100.5	42.17	64.4	Y	75.2	85.91	99.23
II-69	11.0	7.8	82.73	68.84	62.45	60.62	204.71	193.61	93.0	81.0	152.6	180.86	183.92	102.74	99.0	43.04	63.5	Y	75.17	86.48	99.08
II-70	11.0	8.8	93.92	77.9	73.4	71.33	204.44	192.65	93.0	81.0	151.7	178.7	181.9	100.0	97.0	43.4	63.5	Y	75.2	84.0	95.9
II-71	11.0	9.9	83.35	69.28	63.16	61.29	205.07	195.98	103.0		160.52	184.46	187.07	108.7	106.	51.78	68.72	Y	89.85	98.38	106.34
II-72	11.0	8.3	84.02	69.69	63.61	61.81	205.00	196.52	105.0		161.1	185.0	187.43	110.84	107.	52.84	69.44	Y	89.89	99.93	108.55
II-73	11.0	6.8	88.91	73.04	67.40	65.33	205.28	197.6	105.0		163.4	186.8	189.32	113.99	111.0	54.38	71.42	N	89.81	101.84	111.68
II-74	11.0	5.25	96.89	78.89	73.85	71.24	205.25	198.55								55.36		N	89.87	103.87	114.26
II-75	11.0	11.5	84.16	69.62	63.57	61.72	205.07	195.31	103.0		158.0	183.2	185.9	106.88	105.0	51.42	69.1	N	89.85	97.48	104.77
II-76	11.0	13.1	79.61	66.32	58.64	57.08	190.01	181.31	103.43		147.74	169.16	171.53	98.90		45.44	63.26	N	84.83	91.64	97.01
II-77	11.0	13.1	80.19	67.06	60.35	58.50	185.38	177.66	103.1		145.87	165.87	168.85	97.41		44.56	62.44	N	84.96	90.99	95.68

N=No Y=Yes INT=Intermittent

TABLE 2 TEST RESULTS

RUN	NOTES	T_{eg} C F	T_{ea} C F	$F_{\circ Hot}$ dm^3/M GPM	F_{twr} dm^3/M GPM	Q_{EVAP} Watt BTUH	Q_{GEN} Watt BTUH	Q_{ABS} Watt BTUH	Q_{COND} Watt BTUH	COP	HEAT BAL	$\frac{Q_{ABS}}{Q_{EVAP}}$	$\frac{Q_{GEN}}{Q_{EVAP}}$
II-4	Generator in counter-flow configuration. Vary T_{eg}, F_{hot}.	85.13 185.23	29.54 85.17	34.4 9.09	37.5 9.9	8181.6 27933.1	11210.4 38273.9	10676.6 36451.3	8590.7 29329.8	0.730	0.994	1.305	1.370
II-5	X_s = 50.82% X_w = 47.99%	85.05 185.09	29.32 84.78	34.4 9.09	37.5 9.9	8184.5 27943.1	11496.5 39250.7	10949.1 37381.6	8593.8 29340.3	0.712	0.993	1.338	1.405
II-6		87.55 189.59	29.37 84.87	37.9 10.0	37.5 9.9	8299.6 28336.0	13032.2 44493.8	12411.6 42375.0	8714.7 29753.0	0.637	0.990	1.495	1.570
II-7		87.55 189.59	29.40 84.92	40.5 10.7	37.5 9.9	8634.2 29478.4	12799.1 43698.0	12189.6 41617.1	9065.9 30952.3	0.675	0.992	1.379	1.448
II-8		85.02 185.04	29.42 84.96	40.5 10.7	37.5 9.9	7743.5 26437.3	11361.9 38790.9	10820.8 36943.7	8130.7 27759.2	0.682	0.992	1.397	1.467
II-9		82.97 181.34	29.42 84.96	40.5 10.7	37.5 9.9	6881.6 23494.8	10148.9 34649.6	9665.6 32999.6	7225.7 24669.5	0.678	0.992	1.405	1.475
II-10	Low T_{eg}	81.03 177.85	29.25 84.65	40.5 10.7	37.5 9.9	6342.4 21653.8	9851.8 33635.2	9382.6 32033.5	6659.5 22736.5	0.644	0.991	1.479	1.553
II-11		80.95 177.71	29.38 84.88	40.5 10.7	37.5 9.9	6154.4 21012.0	9362.2 31963.9	8916.4 30441.8	6462.1 22062.6	0.657	0.991	1.449	1.521
II-12		79.10 174.38	29.48 85.06	40.5 10.7	37.5 9.9	4991.9 17042.9	8267.1 28224.9	7873.4 26880.9	5241.4 17895.0	0.604	0.989	1.577	1.656
II-13		77.20 170.96	29.40 84.92	40.5 10.7	37.5 9.9	3703.6 12644.7	7507.7 25632.4	7150.2 24411.8	3888.8 13276.9	0.493	0.985	1.931	2.027
II-14		76.95 170.51	29.45 85.01	40.5 10.7	37.5 9.9	3885.1 13264.1	7171.3 24483.9	6829.8 23318.0	4079.3 13927.3	0.542	0.987	1.758	1.846
II-15		75.00 167.00	29.45 85.01	40.5 10.7	37.5 9.9	3154.2 10768.8	5796.5 19790.1	5520.5 18847.7	3311.9 11307.3	0.544	0.987	1.750	1.838
II-16	Vary F_{hot}	84.98 184.96	29.48 85.06	36.0 9.5	37.5 9.9	7881.6 26908.8	10997.4 37546.5	10473.7 35758.6	8275.7 28254.2	0.717	0.993	1.329	1.395
II-17		87.49 189.48	29.38 84.88	37.9 10.0	37.5 9.9	8264.7 28216.7	12647.4 43179.8	12045.1 41123.6	8677.9 29627.6	0.653	0.991	1.457	1.530
II-18	X_s = 50.95%, X_w=47.13% CHANGED TO PARALLEL FLOW IN GENERATOR.	85.06 185.12	29.34 84.82	34.4 9.1	37.5 9.9	7479.2 25535.1	10715.9 36585.5	10205.6 34843.3	7853.2 26811.9	0.698	0.993	1.365	1.433

TABLE D 2 TEST RESULTS

RUN	NOTES	T_{eg} C F	T_{ea} C F	F_{Hot} dm^3/M GPM	F_{twr} dm^3/M GPM	Q_{EVAP} Watt BTUH	Q_{GEN} Watt BTUH	Q_{ABS} Watt BTUH	Q_{COND} Watt BTUH	COP	HEAT BAL	$\frac{Q_{ABS}}{Q_{EVAP}}$	$\frac{Q_{GEN}}{Q_{EVAP}}$
II-19		85.13 185.23	29.42 84.95	40.5 10.7	37.5 9.9	8291.9 28309.6	11437.7 39049.9	10893.1 37190.4	8706.5 29725.1	0.725	0.993	1.314	1.379
	Removed 263 ml condensate, SG = 1.000												
II-20	Trim	85.25 185.45	29.50 85.10	40.5 10.7	37.5 9.9	8320.9 28408.7	11269.0 38473.8	10732.4 36641.7	8736.9 29829.1	0.738	0.994	1.290	1.354
	Removed 202 ml condensate, SG = 1.000												
II-21		85.35 185.63	29.50 85.10	40.5 10.7	37.5 9.9	8269.9 28234.7	10917.0 37272.1	10397.1 35497.2	8683.5 29646.5	0.758	0.994	1.257	1.320
II-22	High Tower Flow, Vary T_{eg}	95.33 203.60	27.12 80.81	41.6 11.0	68.5 18.1	9923.0 33878.3	13923.6 47537.0	13260.5 45273.3	10419.1 35572.2	0.713	0.993	1.336	1.403
II-23		86.55 187.79	27.70 81.86	41.6 11.0	68.5 18.1	8139.9 27790.6	14971.0 51113.0	14258.1 48679.0	8546.9 29180.2	0.544	0.987	1.752	1.839
II-24		85.13 185.23	29.60 85.28	41.6 11.0	37.5 9.9	7041.0 24039.0	10501.5 35853.4	10001.4 34146.1	7393.1 25240.9	0.670	0.992	1.420	1.491
II-25		87.67 189.80	29.57 85.22	41.6 11.0	37.5 9.9	7906.7 26994.7	12042.8 41115.8	11469.3 39157.9	8302.1 28344.4	0.657	0.991	1.451	1.523
	Vary T_{eg}												
II-26		90.20 194.36	29.47 85.04	41.6 11.0	37.5 9.9	7726.3 26378.7	14192.7 48455.7	13516.8 46148.3	8112.6 27697.6	0.544	0.987	1.749	1.837
II-27		92.97 199.34	29.40 84.92	41.6 11.0	37.5 9.9	8176.2 27914.7	16100.7 54970.1	15334.0 52352.5	8585.0 29310.4	0.508	0.985	1.875	1.969
II-28		95.91 204.64	29.38 84.88	41.6 11.0	37.5 9.9	7920.7 27042.5	17017.3 58099.3	16206.9 55332.7	8316.8 28394.6	0.465	0.983	2.046	2.148
II-29	Low hot water flow Air Flow increased to 35.0 m^3/M (1236 CFM).	95.90 204.62	29.50 85.1	34.4 9.1	37.5 9.9	9229.0 31509.0	18157.8 61993.1	17293.1 59041.0	9690.5 33084.5	0.508	0.985	1.874	1.967
II-30	Effect of increased air	87.73 189.91	29.43 84.97	41.6 11.0	51.9 13.7	10157.1 34677.8	13408.2 45777.3	12769.7 43597.4	10665.0 36411.7	0.758	0.994	1.257	1.320
II-31		87.55 189.59	29.40 84.92	41.6 11.0	48.5 12.8	10440.6 35645.5	12985.3 44333.5	12366.9 42222.4	10962.6 37427.8	0.804	0.996	1.185	1.244
II-32	Tower Test	87.67 189.80	29.53 85.16	41.6 11.0	49.6 13.1	9995.6 34129.1	13266.1 45296.1	12634.4 43139.1	10495.4 35835.6	0.753	0.994	1.264	1.327
II-33	Tower Test	87.90 190.22	29.03 84.25	41.6 11.0	49.6 13.1	10744.2 36685.3	13405.9 45773.4	12767.5 43593.7	11281.4 38519.6	0.801	0.996	1.188	1.248

TABLE 2 TEST RESULTS

RUN	NOTES	T_{eg} C F	T_{ea} C F	F_{Hot} dm^3/M GPM	F_{twr} dm^3/M GPM	Q_{EVAP} Watt BTUH	Q_{GEN} Watt BTUH	Q_{ABS} Watt BTUH	Q_{COND} Watt BTUH	COP	HEAT BAL	$\frac{Q_{ABS}}{Q_{EVAP}}$	$\frac{Q_{GEN}}{Q_{EVAP}}$
II-34	Tower Test	87.75 189.95	28.9 84.02	41.6 11.0	45.4 12.0	10274.8 35082.6	13124.3 44811.8	12499.3 42677.9	10788.5 36836.7	0.783	0.995	1.216	1.277
II-35	Xw = 48.24, Xs = 52.37	87.61 189.7	29.38 84.88	41.6 11.0	49.6 13.1	9997.3 34134.9	12905.3 44064.1	12290.7 41965.8	10497.1 35841.7	0.775	0.995	1.229	1.291
II-36	Tower Test	85.13 185.24	29.33 84.80	41.6 11.0	49.6 13.1	8822.3 30123.1	11678.8 39876.3	11122.6 37977.4	9263.4 31629.3	0.755	0.994	1.261	1.324
II-37		85.02 185.03	29.48 85.06	41.6 11.0	49.6 13.1	8802.8 30056.4	11396.7 38913.1	10854.0 37060.1	9242.9 31559.2	0.772	0.995	1.233	1.295
	RECONFIGURE TO COUNTER FLOW IN GENERATOR												
II-38	Hot start, refrig rtrn = 1.05 SG	96.27 205.28	29.37 84.86	41.6 11.0	49.6 13.1	8557.8 29202.8	18280.6 62417.8	17410.1 59445.5	8980.4 30663.0	0.468	0.983	2.036	2.137
II-39	Teg reduced.	87.75 189.95	29.39 84.90	41.6 11.0	49.6 13.1	9768.6 33354.0	12276.8 41918.2	11692.2 39922.1	10257.0' 35021.7	0.796	0.996	1.197	1.257
II-40	High Tower Flow	87.93 190.27	29.13 84.43	41.6 11.0	53.8 14.2	10224.5 34910.8	13060.6 44594.3	12438.6 42470.8	10735.7 36656.3	0.783	0.995	1.217	1.277
II-41		87.92 190.25	29.03 84.26	41.6 11.0	53.8 14.2	10280.2 35100.9	12652.4 43200.7	12049.9 41143.5	10794.2 36856.0	0.813	0.996	1.17[illegible]	1.231
II-42		87.97 190.34	28.47 83.24	41.6 11.0	53.8 14.2	10362.6 35382.3	13217.2 45129.1	12587.8 42980.1	10880.7 37151.4	0.784	0.995	1.215	1.275
II-43	Hot Wtr Bypass Test	84.80 184.64	29.4 84.92	41.6 11.0	37.5 9.9	6793.2 23194.8	10093.6 34463.9	9613.0 32822.8	7132.8 24354.5	0.673	0.992	1.415	1.486
II-44		85.7 186.26	29.5 85.1	41.6 11.0	37.5 9.9	6321.8 21585.2	11157.5 38096.3	10626.1 36282.2	6637.9 22664.5	0.567	0.988	1.681	1.765
II-45		90.8 195.44	30.9 87.62	41.6 11.0	37.5 9.9	7886.9 26929.3	12823.5 43784.9	12212.9 41699.9	8281.3 28275.8	0.615	0.990	1.548	1.626
II-46		93.7 200.66	31.3 88.34	40.1 10.6	37.5 9.9	6668.3 22768.3	15116.3 51613.6	14396.5 49155.8	7001.7 23906.7	0.441	0.982	2.159	2.267
II-47		97.5 207.5	32.13 89.83	39.4 10.4	37.5 9.9	8310.1 28374.1	15942.7 54435.3	15183.5 51843.1	8725.6 29792.9	0.521	0.986	1.827	1.918

TABLE TEST RESULTS

RUN	NOTES	T_{eg} C / F	T_{ea} C / F	F_{Hot} dm³/M / GPM	F_{twr} dm³/M / GPM	Q_{EVAP} Watt / BTUH	Q_{GEN} Watt / BTUH	Q_{ABS} Watt / BTUH	Q_{COND} Watt / BTUH	COP	HEAT BAL	$\frac{Q_{ABS}}{Q_{EVAP}}$	$\frac{Q_{GEN}}{Q_{EVAP}}$
II-48	Cond'r Bypass Test:	96.3	29.1	41.6	53.8	6465.9	19266.1	18348.7	6789.2				
	BYP Closed	205.34	84.38	11.0	14.2	22077.4	65782.7	62650.2	23181.3	0.336	0.977	2.838	2.980
II-49	Bypass Valve Open	95.58	29.55	40.9	53.4	8064.0	17615.8	16777.0	8467.3				
		204.04	85.19	10.8	14.1	27534.1	60148.0	57283.8	28910.8	0.458	0.983	2.080	2.184
II-50	Bypass Valve Closed	95.98	29.38	40.9	53.4	7573.1	18718.8	17827.4	7951.8				
		204.76	84.88	10.8	14.1	25857.9	63913.9	60870.4	27150.8	0.405	0.980	2.354	2.472
II-51		96.50	29.38	40.9	37.5	9001.7	16563.8	15775.1	9451.7				
		205.70	84.88	10.8	9.9	30735.5	56555.9	53862.8	32272.2	0.543	0.987	1.752	1.840
II-52	Variable Tower Flow,	96.6	29.4	40.9	33.3	9040.8	15457.5	14721.4	9492.8				
	Fixed Tower Temperature	205.88	84.92	10.8	8.8	30869.0	52778.5	50265.2	32412.5	0.585	0.988	1.628	1.710
II-53		96.33	29.42	41.6	37.5	8855.1	17435.1	16604.9	9297.9				
		205.40	84.95	11.0	9.9	30235.2	59531.0	56696.2	31746.9	0.508	0.985	1.875	1.969
II-54		96.18	29.37	41.6	33.3	9649.9	16075.1	15309.6	10132.4				
		205.13	84.86	11.0	8.8	32948.9	54887.2	52273.5	34596.4	0.600	0.989	1.587	1.666
II-55		95.97	29.47	42.0	29.5	9099.5	15323.3	14593.6	9554.5				
		204.74	85.04	11.1	7.8	31069.6	52320.2	49828.8	32623.0	0.594	0.989	1.604	1.684
II-56		96.20	29.32	41.6	25.7	9006.9	14229.4	13551.8	9457.3				
		205.16	84.78	11.0	6.8	30753.4	48585.3	46271.7	32291.1	0.633	0.990	1.505	1.580
II-57		96.17	29.32	41.6	21.6	8086.0	13057.0	12435.2	8490.3				
		205.11	84.78	11.0	5.7	27609.0	44582.0	42459.0	28989.5	0.619	0.990	1.538	1.615
II-58		96.38	29.34	41.6	17.8	7302.3	11992.5	11421.5	7667.5				
		205.48	84.81	11.0	4.7	24933.3	40947.6	38997.7	26180.0	0.609	0.989	1.564	1.642
II-59		96.07	29.38	41.6	37.5	9213.0	16451.6	15668.2	9673.6				
		204.92	84.89	11.0	9.9	31457.0	56172.8	53497.9	33029.9	0.560	0.987	1.701	1.786
II-60		96.15	26.69	41.6	37.5	8584.8	18485.1	17604.8	9014.0				
		205.07	80.04	11.0	9.9	29312.1	63115.9	60110.4	30777.7	0.464	0.983	2.051	2.153
II-61	Variable Tower Flow,	96.22	26.72	41.6	33.3	9687.6	17389.1	16561.0	10172.0				
	Fixed Tower Temp.	205.19	80.09	11.0	8.8	33077.6	59373.7	56546.4	34731.5	0.557	0.987	1.710	1.795
II-62		96.18	26.70	41.6	29.5	9484.3	16388.2	15607.8	9958.5				
		205.12	80.06	11.0	7.8	32383.5	55956.2	53291.6	34002.7	0.579	0.988	1.646	1.728

TABLE . TEST RESULTS

RUN	NOTES	T_{eg}	T_{ea}	$F°_{Hot}$	F_{twr}	Q_{EVAP}	Q_{GEN}	Q_{ABS}	Q_{COND}	COP	HEAT BAL	$\frac{Q_{ABS}}{Q_{EVAP}}$	$\frac{Q_{GEN}}{Q_{EVAP}}$
		C F	C F	dm^3/M GPM	dm^3/M GPM	Watt BTUH	Watt BTUH	Watt BTUH	Watt BTUH				
II-63	Variable Tower Flow,	96.24	26.64	41.6	25.7	9440.4	15496.1	14758.2	9912.4				
	Fixed Tower Temp.	205.23	79.95	11.0	6.8	32233.7	52910.3	50390.8	33845.3	0.609	0.989	1.563	1.641
II-64		96.29	26.70	41.6	21.6	8652.3	14025.7	13357.8	9084.9				
		205.32	80.06	11.0	5.7	29542.6	47889.7	45609.2	31019.8	0.617	0.990	1.544	1.621
II-65		96.11	23.96	41.6	17.8	8857.9	13448.2	12807.8	9300.9				
		205.00	75.13	11.0	4.7	30244.8	45917.9	43731.3	31757.1	0.659	0.991	1.446	1.518
II-66	Variable Tower Flow,	96.23	23.98	41.6	21.6	9184.9	15183.5	14460.4	9644.1				
	Fixed Tower Temp.	205.21	75.16	11.0	5.7	31361.1	51842.8	49374.1	32929.2	0.605	0.989	1.574	1.653
II-67		96.23	23.89	41.6	25.7	10660.4	16137.5	15369.1	11193.4				
		205.21	75.00	11.0	6.8	36399.1	55100.4	52476.6	38219.0	0.661	0.991	1.442	1.514
II-68		96.45	24.0	41.6	29.5	9828.1	17856.5	17006.2	10319.5				
		205.61	75.2	11.0	7.8	33557.3	60969.6	58066.3	35235.2	0.550	0.987	1.730	1.817
II-69		95.95	23.98	41.6	29.5	10162.9	17344.4	16518.5	10671.1				
		204.71	75.17	11.0	7.8	34700.5	59221.2	56401.1	36435.6	0.586	0.988	1.625	1.707
II-70		95.8	24.0	41.6	33.3	8587.3	18425.4	17548.0	9016.6				
		204.44	75.2	11.0	8.8	29320.6	62912.3	59916.5	30786.6	0.466	0.983	2.043	2.146
II-71	Variable Tower Flow,	96.15	32.14	41.6	37.5	9741.2	14198.6	13522.4	10228.3				
	Fixed Tower Temp.	205.07	89.85	11.0	9.9	33260.6	48479.9	46171.3	34923.7	0.686	0.992	1.388	1.458
II-72		96.11	32.16	41.6	31.4	9441.6	13245.0	12614.2	9913.6				
		205.00	89.89	11.0	8.3	32237.5	45223.9	43070.4	33849.4	0.713	0.993	1.336	1.403
II-73		96.27	32.12	41.6	25.7	9717.4	11993.3	11422.2	10203.3				
		205.28	89.81	11.0	6.8	33179.4	40950.3	39000.3	34838.4	0.810	0.996	1.175	1.234
II-74		96.25	32.15	41.6	19.9	8239.2	10461.6	9963.4	8651.2				
		205.25	89.87	11.0	5.25	28132.2	35720.4	34019.4	29538.8	0.788	0.995	1.209	1.270
II-75		96.15	32.14	41.6	43.5	9948.5	15246.4	14520.4	10445.9				
		205.07	89.85	11.0	11.5	33968.5	52057.8	49578.9	35666.9	0.653	0.991	1.460	1.533
II-76	Verification Test	87.78	29.35	41.6	49.6	9765.0	13642.1	12992.4	10253.2				
		190.01	84.83	11.0	13.1	33341.7	46579.8	44361.7	35008.8	0.716	0.993	1.331	1.397
II-77		85.21	29.42	41.6	49.6	8495.7	12118.3	11541.2	8920.4				
		185.38	84.96	11.0	13.1	29007.8	41377.0	39406.7	30458.2	0.701	0.993	1.358	1.426

NOMENCLATURE FOR TABULAR DATA

Parameters

BTUH	British Thermal Units per Hour
C	Celsius
CFM	Cubic Feet per Minute
COP	Coefficient of Performance
dm^3/M	$(Decimeter)^3$ per Minute = Liters per Minute
F	Fahrenheit
F_{hot}	Flowrate, hot water
F_{twr}	Flowrate, cooling tower
GPM	Gallons per Minute
INT	Intermittent Spilling
m^3/M	Cubic Meters per Minute
N	No Spillage
QABS	Absorber Heat Load
QCOND	Condenser Heat Load
QEVAP	Evaporator Heat Load
QGEN	Generator Heat Load
SG	Specific Gravity
T	Temperature
X	Concentration
Y	Yes

Subscripts

a	absorber
c	condenser
db	dry bulb
e	entering
fp	flash point
g	generator
l	leaving
ml	milliliter
s	strong
v	vapor or vapor tube
w	weak
wb	wet bulb
x	heat exchanger

PHASE II, VARIABLE HOT WATER TEMPERATURE (NORMAL RANGE) COUNTERFLOW GENERATOR

GENERATOR AND EVAPORATOR HEAT LOADS VS. HOT WATER INLET TEMPERATURE

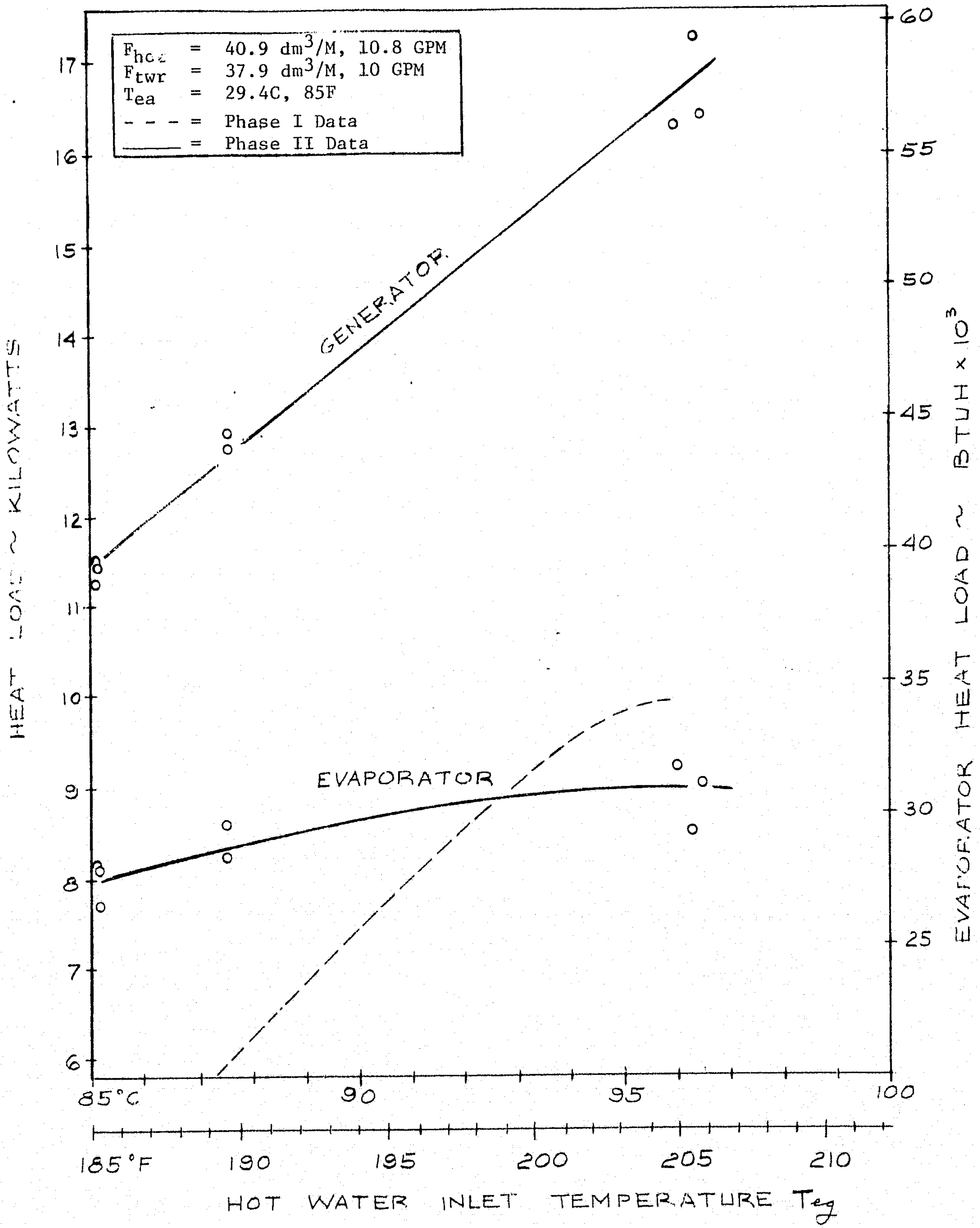

FIGURE D-1A

PHASE II, VARIABLE HOT WATER TEMPERATURE (NORMAL RANGE) COUNTERFLOW GENERATOR

COP VS. HOT WATER INLET TEMPERATURE

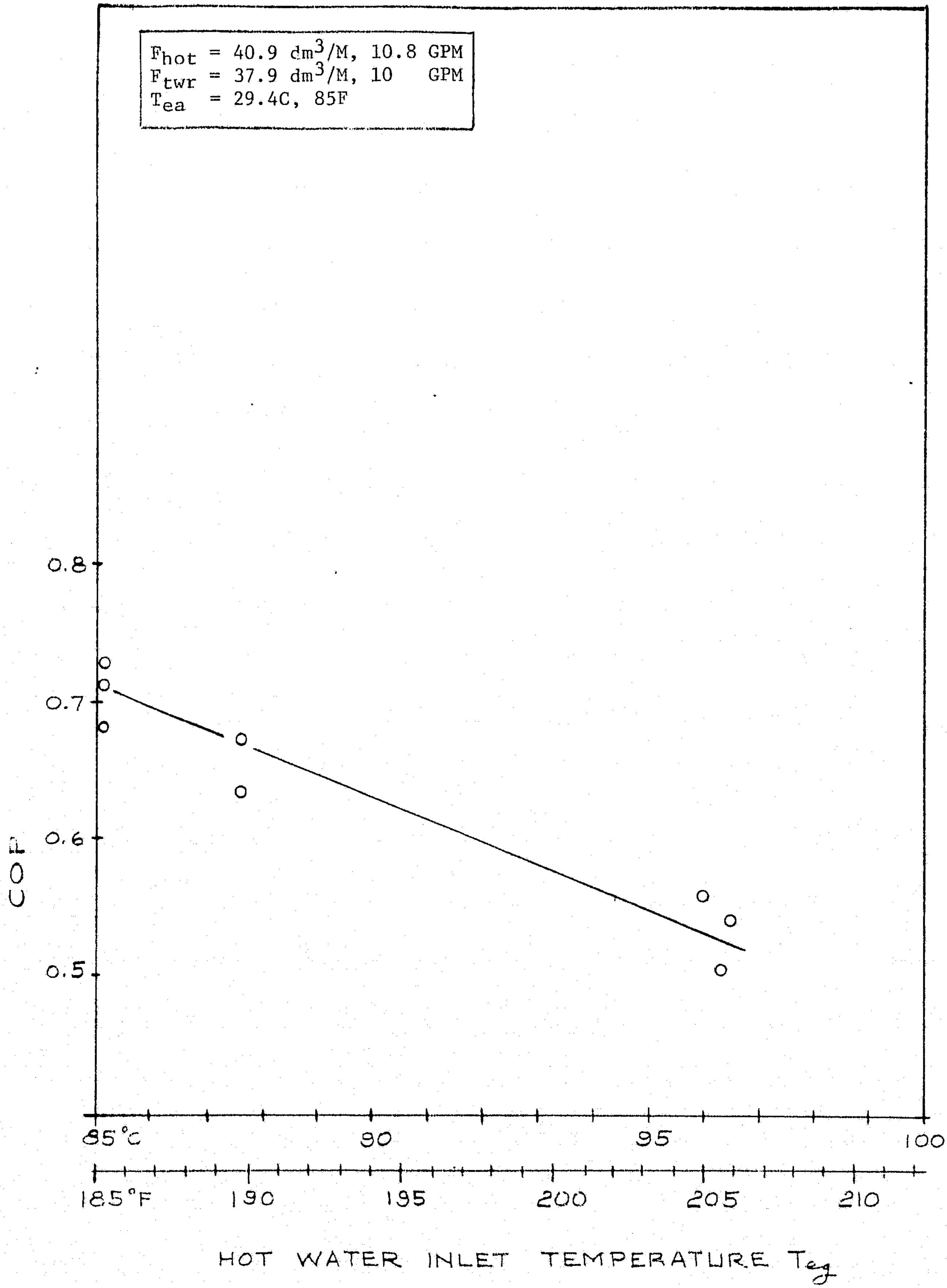

FIGURE D-1B

The performance of the Phase I unmodified machine and the Phase II system modified with the pump and the Chrysler-designed and built generator, are compared in Figure D-1A. The performance of the modified machine is better until the effects of "carryover" prevail at approximately 92.8 C (199 F).

It is expected that the capacity of the machine can be increased by eliminating the effects of static head (submergence) on the heat transfer and boiling in the generator. "Submergence" reduces the effective heat transfer area by retarding boiling which reduces the amount of refrigerant produced in the generator. Figure D-2 shows the existence of submergence. Thermocouple measurements are indicated vertically along the external surface of the generator shell. The measurements are taken in contact with the shell, under the insulation (2 inches of polyurethane). Submergence is evidenced by the cooling effect of the boiling on the solution. Without submergence, the solution temperature would be expected to rise slowly after the onset of boiling due to the increasing LiBr concentration and boiling point. The thermometer measurements of the leaving vapor and leaving solution temperatures, T_{1gv} and T_{1gs}, respectively, are more representative of the true temperatures because the thermometer wells extend 7.6 cm (3 inches) into the generator vessel.

The performance of the modified system at low temperatures is shown in Figures D-3A and D-3B, which contain data from runs II-7 through -15. The excellent low temperature performance of the generator is visible by observing QEVAP. Carryover is absent due to the less violent boiling. Reducing or eliminating submergence would raise the QEVAP data points.

The COP data (Figure D-3B) decrease with decreasing hot water inlet temperature; whereas the reverse is true for the Phase I data (see Figure B-5).

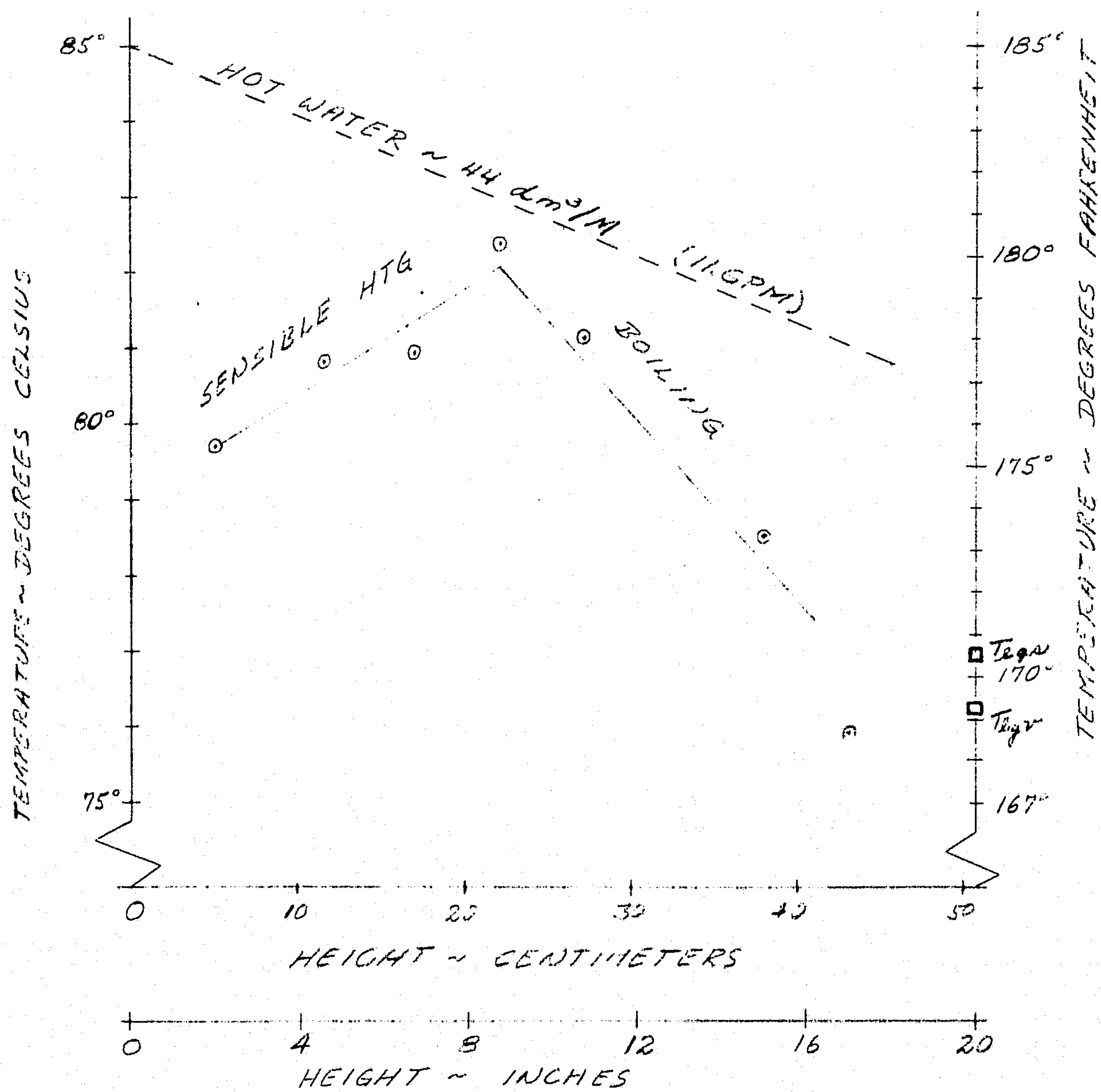

FIGURE D-2 SUBMERGENCE IN GENERATOR

NOTE: T_{1gv} = Vapor Temperature Leaving Generator
T_{1gs} = Solution Temperature Leaving Generator
⊙ = Thermocouple Measurement
☐ = Thermometer Measurement

PHASE II, VARIABLE HOT WATER TEMPERATURE (LOW RANGE) COUNTERFLOW GENERATOR

GENERATOR AND EVAPORATOR HEAT LOADS VS. HOT WATER INLET TEMPERATURE

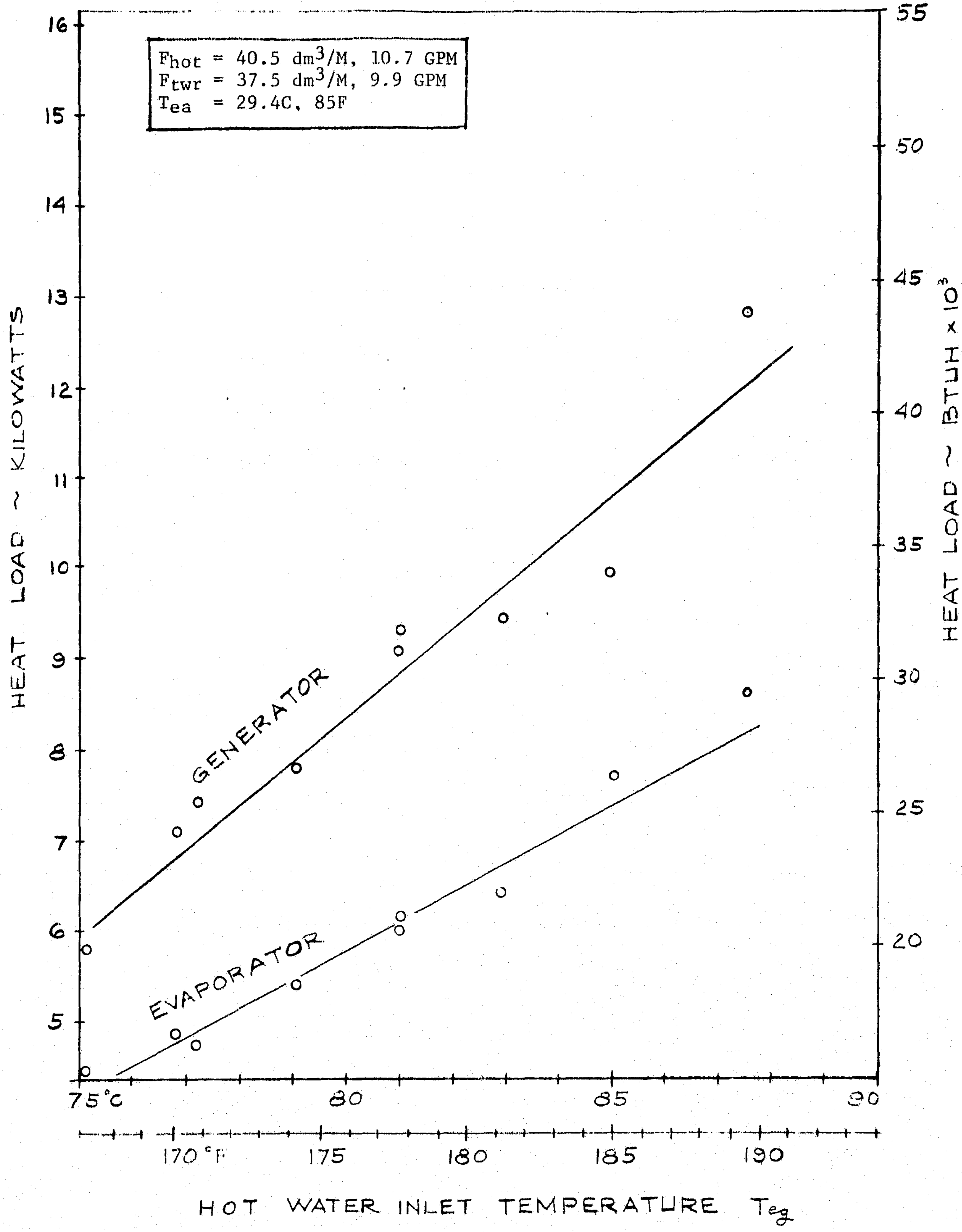

FIGURE D-3A

PHASE II, VARIABLE HOT WATER TEMPERATURE (LOW RANGE) COUNTERFLOW GENERATOR

COP VERSUS HOT WATER INLET TEMPERATURE

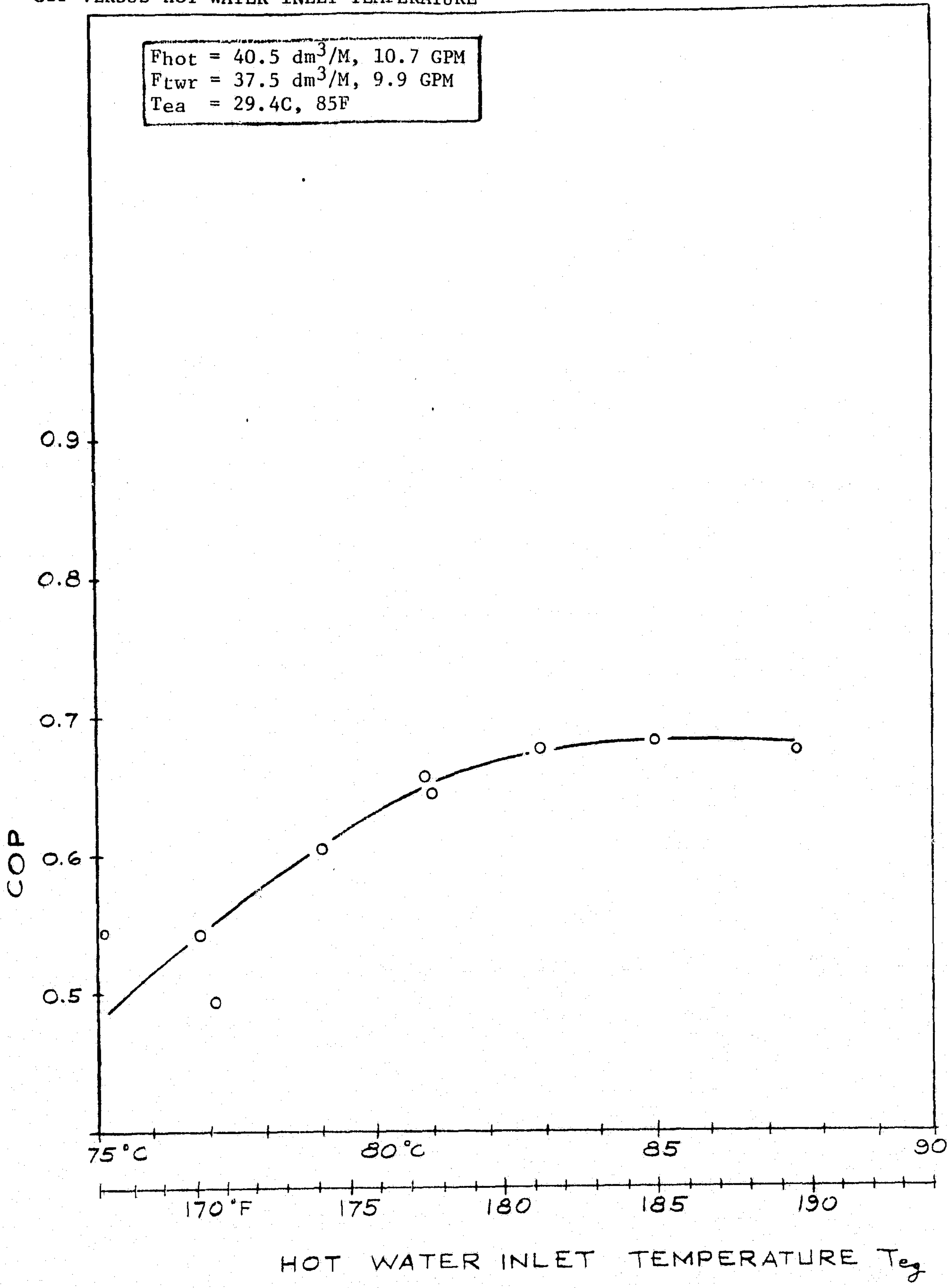

FIGURE D-3B

This effect is due to the pump and fixed weak absorbent flow rate in the modified air conditioner versus the variable, thermally pumped flow of the original system. The fixed flow requires more sensible heating due to a smaller concentration span at lower hot water temperatures. The sensible heating produces no refrigerant. The flow of the weak absorbent in the thermally pumped system depends on the generator heat load and hot water inlet temperature. It requires less sensible heating.

A refrigerant sampling valve was temporarily installed at the refrigerant sump at the base of the condenser, following run II-18. The presence of LiBr carryover in the refrigerant return was verified by taking hydrometer readings of the liquid refrigerant. The valve was at the end of a line which collected LiBr since it was dead-ended. This required removing the "residual" sample, and then taking a fresh sample for measurement because measurements of the residuals were abnormally high. Most readings of the samples indicated zero to 12% LiBr, although one reading showed 20% LiBr (transient data) and another indicated 17% (transient data). In both cases, subsequent readings indicated a return to a 3% to 4% level of LiBr weight concentration.

The flow direction of the hot water in the generator is changed for runs II-19 through -37, to a parallel configuration, i.e., inlet at the bottom and outlet at the top. Runs II-19, 20 and 21 show excellent results. These runs were used to trim the parallel configuration, but the data are not consistent with subsequent data.

Figure D-4A shows the generator and evaporator heat loads versus hot water inlet temperature for runs II-24 through -28. The COPs are shown in Figure D-4B.

PHASE II, VARIABLE HOT WATER TEMPERATURE (NORMAL RANGE) PARALLEL FLOW GENERATOR

GENERATOR AND EVAPORATOR HEAT LOADS VERSUS HOT WATER INLET TEMPERATURE

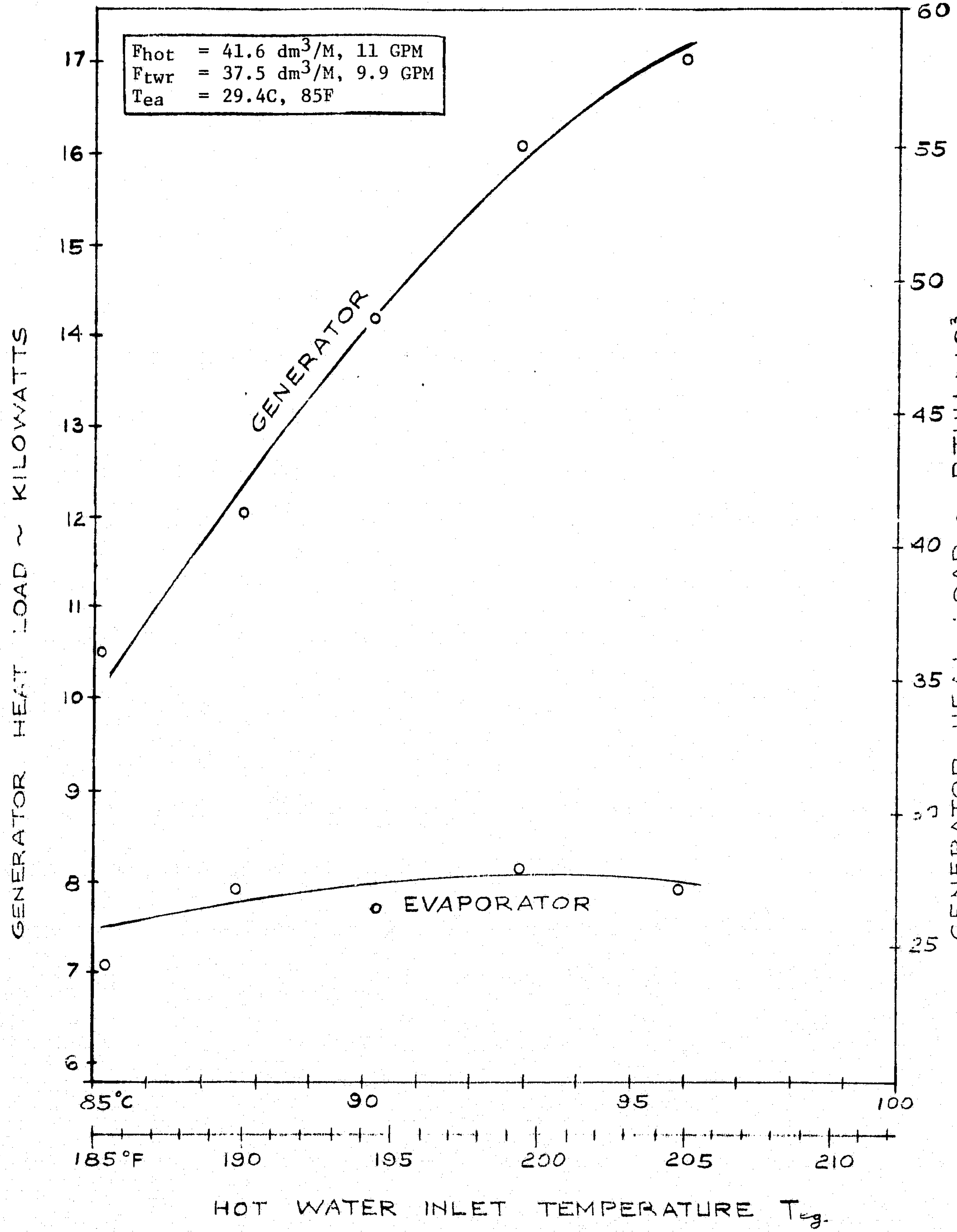

FIGURE D-4A

PHASE II, VARIABLE HOT WATER TEMPERATURE (NORMAL RANGE) PARALLEL FLOW GENERATOR

COP VERSUS HOT WATER INLET TEMPERATURE

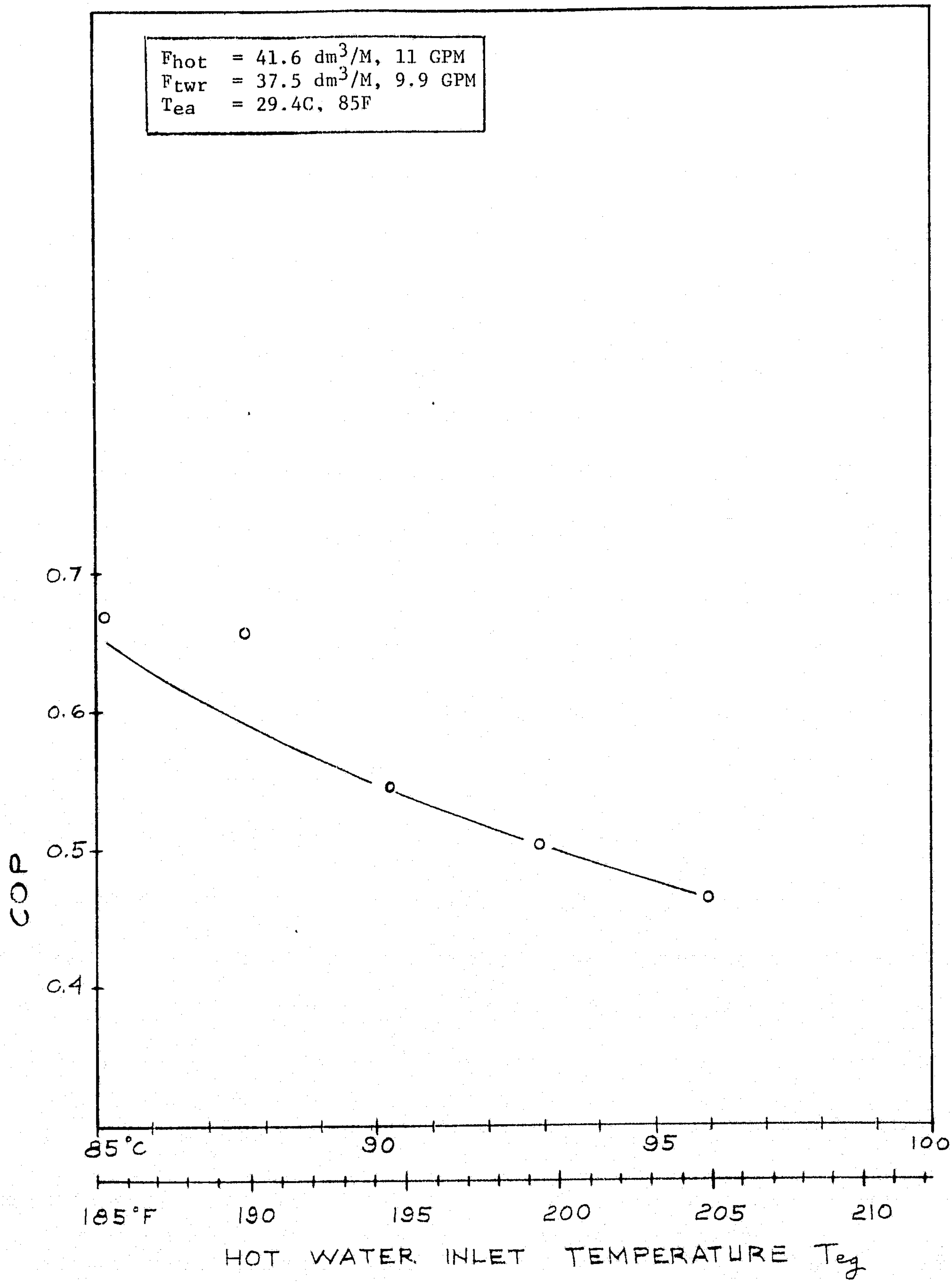

FIGURE D-4B

Comparison with Figures D-1A and D-1B shows that the counter flow configuration gives better performance, especially at the higher hot water inlet temperatures. Comparison of the results for Runs II-8, 24 and 43 illustrates how the two configurations yield almost similar results at T_{eg} = 85 C (185 F) due to the submergence reducing the effective heat transfer area. Comparison of Runs II-28, 51 and 53, shows that counterflow gives better performance at T_{eg} = 96 C (205 F). This is probably due to the effect of carryover as well as the tendency of counterflow to maintain a better local temperature difference between the hot water and the solution. Since the parallel flow tends to initiate boiling at a lower depth, the boiling is more violent due to greater bubble expansion and carryover is increased.

The air flow rate is increased slightly (3%) for Run II-29 and subsequent runs. It did not have a significant effect on the results because QEVAP is restricted more by carryover than by air flow or air side heat transfer.

Runs II-30 through 37, show the effect of varying tower conditions in the parallel configuration. The capacity of the modified system can be increased at rated conditions (Teg = 85C, 185F; F_{hot} = 41.6 dm^3/M, 11 GPM), to approximately 8.8 kW (2 1/2 tons) by increasing the tower flow to 49 dm^3/M at 29C (13 GPM at 84.2F). When Teg is increased to 87.8 C (190 F) with these tower conditions, the capacity rises to 10.5 kW (3 tons) as shown by Run II-33.

When the generator was returned to the counter flow configuration, it was subjected to a "hot start" (see the transient data below) to determine the effect of carryover under severe conditions. The hot water inlet temperature fell within a few minutes because the hot water heaters were not reset to a higher firing

rate. The normal practice is to approach the high temperature slowly to avoid overshoot and boiling. The data for Run II-38 show the steady state data which begin 39 minutes after the transient data.

Hot Start Data

Time (Minutes)	T_{eg} C	T_{eg} F	T_{fp} C	T_{fp} F	Spill
0	97.5	207.5	20.5	68.9	No
3	96.0	204.8	10.7	51.3	Yes
8	92.2	198.0	5.7	42.3	Yes

The effects of increasing the tower flow F_{twr} to 53.8 dm^3/M (14.2 GPM) are shown in Runs II-40, 41, and 42, with decreasing T_{ea}. The data show no improvement with the higher tower flow.

Runs 43 through 47 simulate having a hot water source bypass valve to control the generator inlet temperature. This valve allows a fraction of the generator exit flow to mix with sufficient flow from the high temperature source to maintain the desired flow at the desired temperature. Table D-1 includes the valve position data for these runs.

A condenser bypass valve was installed temporarily to reduce the tower water flow through the condenser while maintaining tower flow through the absorber. The objective is to reduce carryover by allowing the condenser temperature and pressure to rise. The pressure would then rise in the generator and reduce the violence of the boiling. Runs 48, 49 and 50 show the results. Time constraints did not allow the installing of instrumentation to measure either the condenser bypass or condenser through flow. The results show no significant improvement.

Runs II-51 through II-75, see Figures D-5A, 5B, 5C, show the results of varying tower flow rate F_{twr} and temperature of the cooling water entering the absorber T_{ea}. These tests vary the F_{twr} for T_{ea} = 23.9, 26.7, 29.4, 32.2 C (75, 80, 85, 90 F). Due to time constraints, these tests are with constant air reheat prower. The data in Table D-1 reflect this in the air temperatures. The runs for T_{ea} = 29.4 C (85 F) have approximately 10% lower reheat power than the other runs, which accounts for the T_{ea} = 29.4 C (85 F) curve being below the T_{ea} = 32.2 C (90 F) in Figure D-5A (QEVAP).

Most of the runs (II-51 through II-72) have spillage, and QEVAP and COP are relatively low which indicates the presence of LiBr carryover. The plateau in the QEVAP curve for T_{ea} = 29.4 C (85 F) is probably due to a greater amount of carryover, which indicates that this area of tower operation (F_{twr} = 34 to 38 dm^3/M, 9 to 10 GPM; T_{ea} = 29.4 C, 85 F) should be avoided.

PHASE II, VARIABLE TOWER CONDITIONS, COUNTERFLOW GENERATOR
EVAPORATOR HEAT LOAD VS. TOWER FLOW, TOWER TEMPERATURE

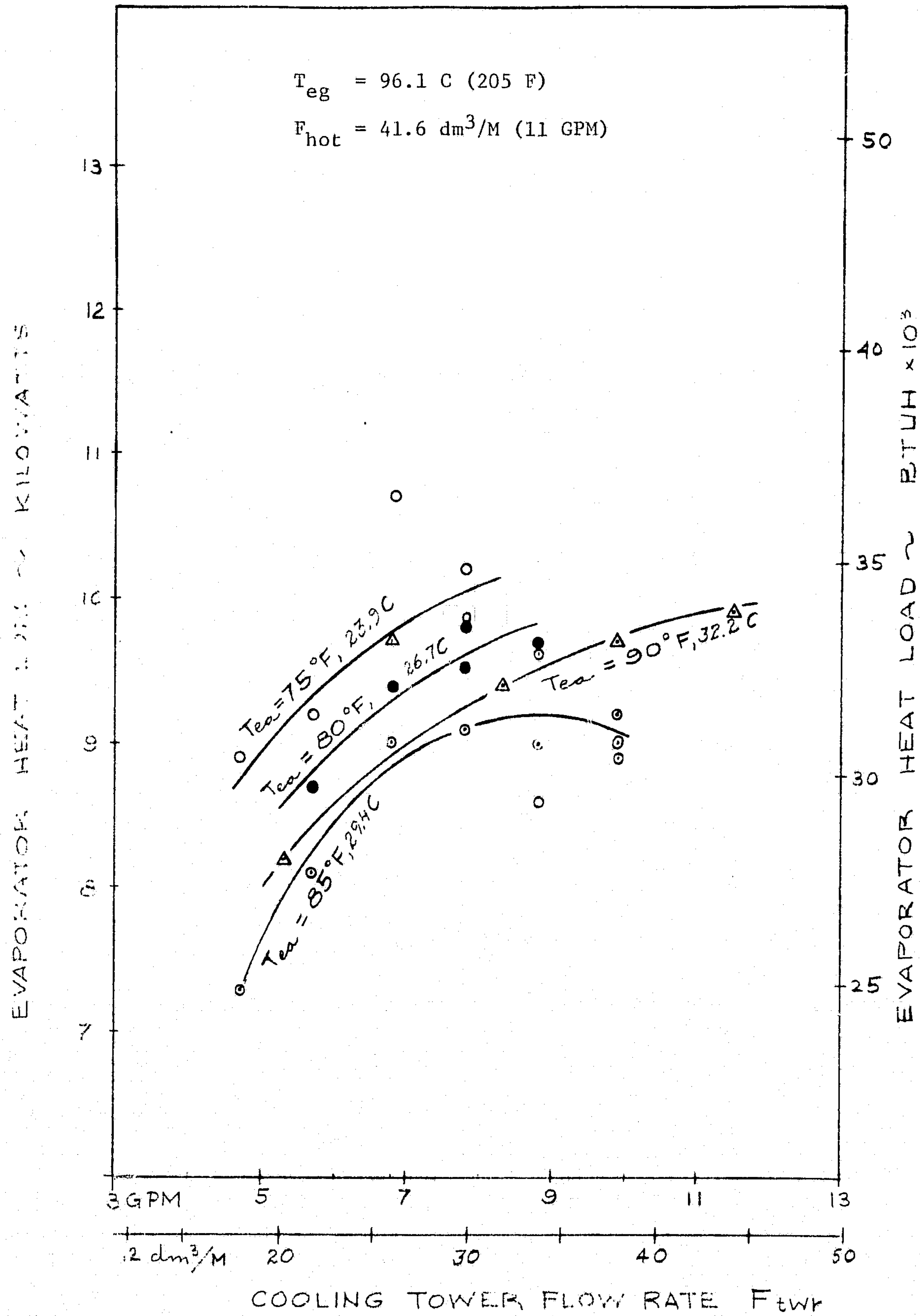

FIGURE D-5A

PHASE II. VARIABLE TOWER CONDITIONS, COUNTERFLOW GENERATOR

GENERATOR HEAT LOAD VS. TOWER FLOW, TOWER TEMPERATURE

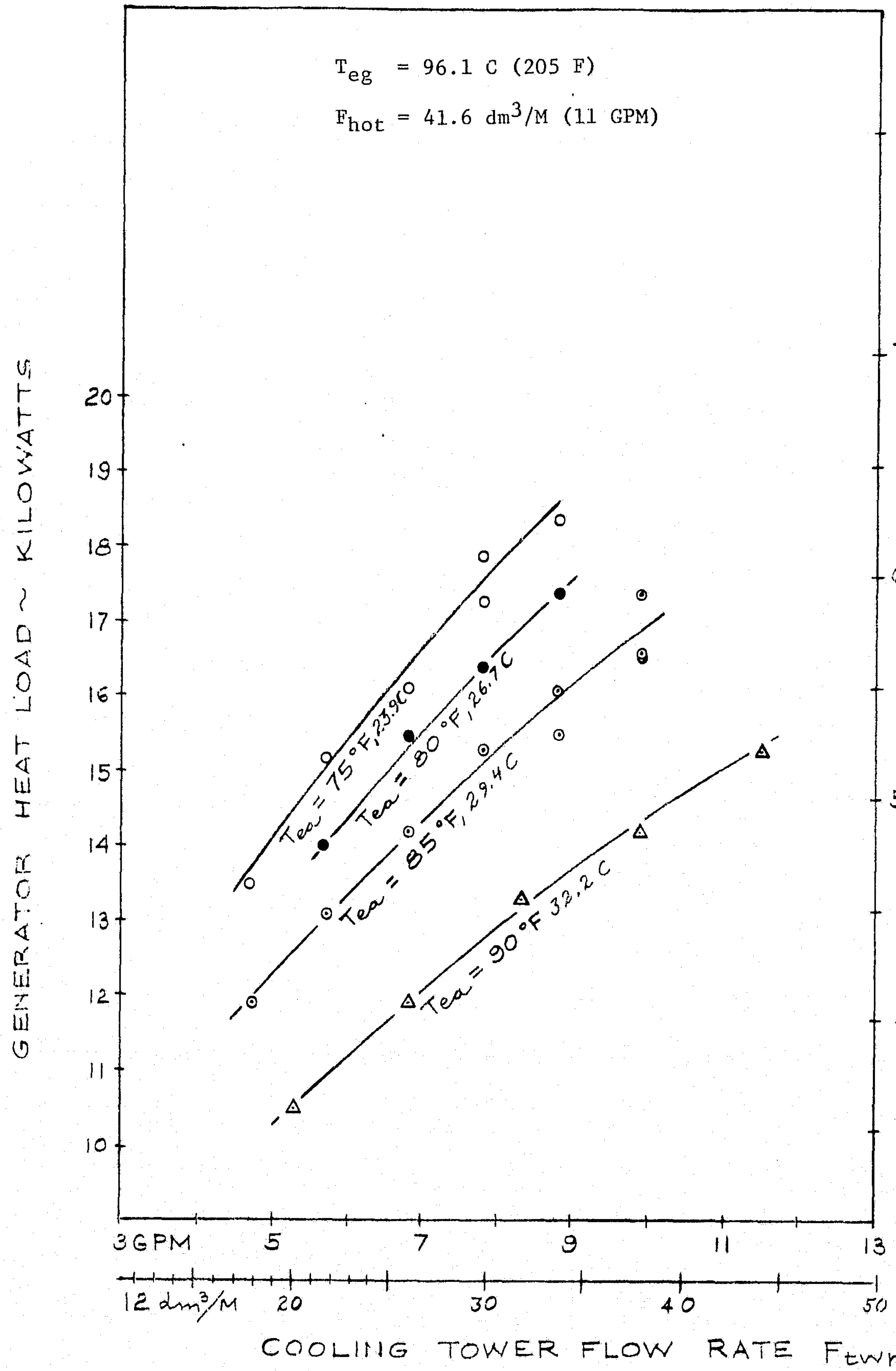

FIGURE D-5B

PHASE II, VARIABLE TOWER CONDITIONS, COUNTERFLOW GENERATOR

COP VS. TOWER FLOW, TOWER TEMPERATURE

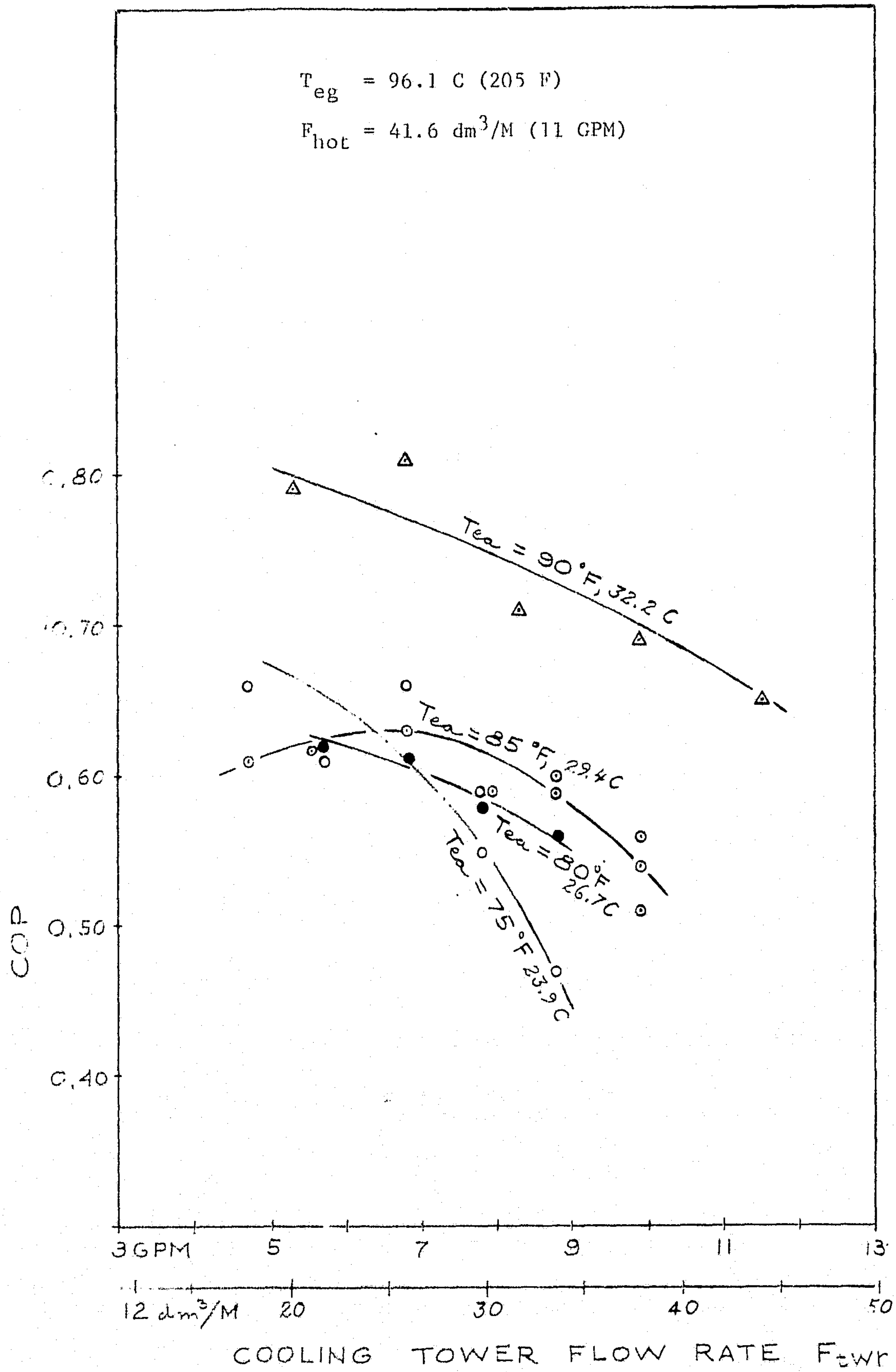

FIGURE D-5C

E. CONCLUSIONS

The conclusions of the test program are:

1. At rated conditions (T_{eg} = 85 C, 185 F; F_{hot} = 41.6 dm^3/M, 11 GPM; T_{ea} = 29.4 C, 85 F; F_{twr} = 37.9 dm^3/M, 10 GPM), the modified unit delivered 7 to 8 kW (2 to 2 1/3 tons) (refer to Runs II-8, 19, 20, 21 and 24 in Table D-2); whereas the as-received system ceased to cool at 86.1C (187F). The approximate 30 percent reduction from the original capacity (10.5 kW at 98.9C, 3 tons at 210F) is primarily due to the submergence effects and suppressed boiling in the generator as mentioned earlier.

2. The capacity of the modified system can be increased at rated conditions to approximately 8.8 kW (2-1/2 tons) by increasing the tower flow to 49 dm^3/M at 29°C (13 GPM at 84.2°F). When the hot water temperature is increased to 87.8°C (190°F) with these tower conditions, the capacity rises to 10.5 kW (3 ton). Reference Run II-33.

3. The carryover of LiBr to the condenser, which is encountered when the hot water temperature is elevated to 90.6 to 96.1°C (195 to 205°F), Runs II-26 to II-28, occurs in conjunction with spillage, and can be controlled by reducing the violence of the boiling in the generator. Runs II-51 through II-75 show the effect of reducing the tower flow rate at several absorber inlet temperatures which will increase condenser and generator pressures, hence suppressing the boiling in the generator; however, a reduction in cooling capacity will occur due to a decrease in the amount of refrigerant produced.

4. Counterflow gives better results than parallel flow (i.e., hot water inlet at top; outlet at the bottom) for high inlet hot water temperature (Runs II-28, 51, 53) and almost identical performance at lower inlet hot water temperature (Runs II-8, 24 and 43). This is due to the effects of submergence and carryover. Submergence reduced the heat transfer of

several of the middle-depth coils by retarding boiling which tends to equalize the heat transferred by the two configurations. Since the parallel flow will tend to initiate boiling at a lower depth, the boiling will be more violent due to greater bubble expansion. This will tend to increase carryover.

5. Submergence retards boiling and reduces the effective heat transfer area.

F. FUTURE WORK

1. An impingement type of separator module is designed which would remove droplets of LiBr solution from the vapor stream. The drawings are shown in Appendix J. Future work should include fabrication of the separator, installation in the vapor line between generator exit and condenser inlet, with the drain line connected to the strong absorbent line leaving the generator, and verification test.

2. Two types of heat exchangers are suggested to eliminate submergence effects. Future work should include evaluating the falling film (spray or dripper-fed) and the stacked tray concepts for use as a low temperature LiBr generator. Then the generator should be designed, fabricated, installed, and tested.

3. Modify the present submerged coil generator design to orient the coils horizontally as an expedient method to eliminate submergence and carryover. Submergence would be eliminated or reduced since the long dimension would be horizontal, and the depth reduced. Carryover would be eliminated by exposing the top section of the coils to act as a heated impingement separator and by installing an external separator.

NOMENCLATURE

A	Area
B	Barometer Reading
BTUH	British Thermal Units Per Hour
C	Celsius, Constant
CFM	Cubic Feet Per Minute
COP	Coefficient of Performance
Cp	Specific Heat at Constant Pressure
cp	Centipoise
D	Diameter
dm^3/M	Cubic Decimeter (liter) Per Minute
F	Volumetric Flow Rate, Fahrenheit
G	Mass Velocity
g	Gram
GPM	Gallons Per Minute
Gr	Grashof Number
h	Enthalpy, Film Coefficient of Heat Transfer
J	Joules
K	Thermal Conductivity
kg	Kilogram
kN/m^2	Kilo Newton Per Square Meter
kW	Kilowatt
L	Length
LiBr	Lithium Bromide
LMTD	Logarithmic Mean Temperature Difference
MW	Molecular Weight
mNs/m^2	Milli Newton-Second Per Square Meter

Nomenclature

m^3/M	Cubic Meter Per Minute
N	Number of moles, Number of coils, Number, No Spillage
Nu	Nusselt Number
P	Pressure
Pr	Prandtl Number
QABS	Absorber Heat Load
QCOND	Condenser Heat Load
QEVAP	Evaporator Heat Load
QGEN	Generator Heat Load
R	Universal Gas Constant
r	Radius
Rey	Reynolds Number
SG	Specific Gravity
T	Temperature
U	Overall Heat Conductance
V	Volume
W	Specific Humidity (weight moisture per unit weight of dry air); mass flow rate
W*	Specific Humidity at Saturation
X	Weight Concentration of Lithium Bromide
Y	Yes, spillage
β	Coefficient of Expansion
ρ	Density

SUBSCRIPTS

a	Air, Absorber
B	Bulk
c	Condenser
db	Dry Bulb
e	Entering
F	Film
f	Saturated Liquid
fp	Flash Point
g	Saturated Vapor, Generator
hot	Hot Water
i	Inside
l	Leaving
m	Mixture, Mean
o	Outside
r	Refrigerant
rr	Refrigerant Return
s	Strong
twr	Tower
v	Vapor, Vapor Tube
w	Weak, Wall
wb	Wet Bulb
x	Heat Exchanger

REFERENCES

1. ASHRAE Handbook of Fundamentals, American Society of Heating, Refrigerating, and Air Conditioning Engineers, Inc. 345 East 47th St., New York, N. Y. 10017, 1972

2. Chemical Engineers' Handbook, John H. Perry; R. H. Perry, C. H. Chilton, & S. D. Kirkpatrick, Editors, Fourth Edition, McGraw-Hill Book Co. 1963

3. Flow of Fluids, Crane, Technical Paper No. 410, 1969, 10th Printing Crane Co. 4100 S. Kedzie Ave., Chicago, Illinois 60632

4. Standard Handbook for Electrical Engineers, A. E. Knowlton, McGraw-Hill Book Company, Inc., 1957

5. Standard Handbook for Mechanical Engineers, Marks and Baumeister, Editor, 1967, Seventh Edition, McGraw-Hill Book Company.

6. Thermodynamic Properties of Steam, J. H. Keenan and F. G. Keyes, John Wiley & Sons, Inc., New York, N. Y., 1936

7. Principles of Engineering Heat Transfer, W. H. Giedt, D. Van Nostrand Co., Inc. 1957.

APPENDIX A - ERROR ANALYSIS

The generator, condenser, and absorber heat loads are calculated by measuring the inlet and outlet water temperatures and the water flow rate, and then by evaluating.

$$Q = WCp\,(T_{in} - T_{out})$$

Where Q = Heat Load

Cp = Specific Heat of Water at the Average Temperature

T_{in} = Inlet Temperature

T_{out} = Outlet Temperature

The evaporator heat load is calculated from the air side wet and dry bulb temperatures when spillage occurs. When spillage does not occur the condenser heat ratio QCOND/QEVAP can be taken as -1.05 so that the evaporator heat load can also be evaluated from the equation shown above.

For steady state operation, there is no accumulation of thermal energy within the system and the sum of the heat loads is zero.

$$\Sigma Q = (Q_A + Q_C) + (Q_E + Q_G)$$
$$\Sigma Q = 0$$

Where Q_A = Heat rejected by the absorber

Q_C = Heat rejected by the condenser

Q_E = Heat added to the evaporator

Q_G = Heat added to the generator

In general, due to instrumentation errors, ΣQ will be nonZero and can be taken as the system error ΔQ. Thus, during periods of No Spillage,

$$\Delta Q = -/Q_A/ - /Q_C/ + \frac{Q_C}{1.05} + Q_G$$

Where heat added to the system is positive. Then the test error

(1) $$\Delta Q = -/Q_A/ - 0.047619/Q_C/ + Q_G$$

The expected error is calculated from the root-mean-square error which is the most probable value of the resultant effect of the separate effects (Ref. Standard Handbook for Electrical Engineers, A. E. Knowlton, Ninth Edition, McGraw-Hill, 1957, page 212, Section 3-396). Thus the expected error is

$$QRMS = \left[\left(\frac{\partial Q}{\partial Q_A} \Delta Q_A\right)^2 + \left(\frac{\partial Q}{\partial Q_C} \Delta Q_C\right)^2 + \left(\frac{\partial Q}{\partial Q_G} \Delta Q_G\right)^2 \right]^{1/2}$$

(2) $$QRMS = \left[(\Delta Q_A)^2 + (0.047619\Delta Q_C)^2 + (\Delta Q_G)^2 \right]^{1/2}$$

Since $Q_i = W_i\, C_{pi} (T_{1i} - T_{2i})$, where i = A, C, G and

C_{pi} = Specific Heat of water through component i at the average temperature of T_{1i} and T_{2i}.

T_{1i} = Temperature of water entering component i

T_{2i} = Temperature of water entering component i

W_i = Water flow rate through component i

Then

$$\Delta Q_i^2 = \left(\frac{\partial Q_i}{\partial W_i} \Delta W_i\right)^2 + \left(\frac{\partial Q_i}{\partial C_{pi}} \Delta C_{pi}\right)^2 + \left(\frac{\partial Q_i}{\partial T_{1i}} \Delta T_{1i}\right)^2 + \left(\frac{\partial Q_i}{\partial T_{2i}} \Delta T_{2i}\right)^2$$

Since $\Delta T_{1i} = \Delta T_{2i}$

(3) $$\Delta Q_i^2 = (C_{pi}[T_1 - T_2] \Delta W_i) + (W_i [T_{1i} - T_{2i}] \Delta C_{pi})^2 + 2(W_i C_{pi} \Delta T_{1i})^2$$

QRMS will be evaluated for Run 37 using the test data.

For the generator error ΔQ_G :

Flowmeter reads 0.0450 $\frac{m^3}{Min}$ (11.9 Gal. per min)

T_{1G} = 86.35° C. (187.43° F.)

T_{2G} = 84.13° C. (183.43° F.)

T_{AVG} = 85.24° C. (185.43° F.)

C_{PG} = 4.20061 j/gm°C (1.00397 BTU/lbm°F)

Density ρ_G = 968.26 kg/m^3 (8.0805 lbm/Gal)

W_G = 43.617 kg/Min (96.1580 lbm/Min)

The flowmeter accuracy is stated as ± 1.% of full scale (F.S.) when the meter is calibrated. Full scale for the hot water flowmeter is 0.08744 m^3/min (23.10 GPM).

ΔW_G = ± 0.01 x (F.S.) x ρ_G

= ± 0.8467 kg/Min (1.8666 lbm/Min)

The extended range thermometers have an accuracy of $\pm$ 0.1C°. Then

ΔT_{1G} = $\pm$ 0.1 C° ($\pm$0.18F°).

The specific heat is known to within

$$\Delta C_{PG} = \pm 0.00004 \text{ J/gmC°} \quad (\pm 0.00001 \text{ BTU/lbmF°})$$

From Equation 3,

$$(4) \qquad \Delta Q_G^2 = 1.9993 \times 10^5 \text{ watts}^2 \quad \left(647.63 \ \frac{\text{BTU}^2}{\text{Min}^2}\right)$$

Similarly, for the absorber error ΔQ_A:

Flowmeter reads 0.0375 m^3/ min (9.9 GPM)

T_{1A} = 29.35°C (84.83°F)

T_{2A} = 32.03°C (89.66°F)

T_{AVG} = 30.69°C (87.245°F)

C_{PA} = 4.17835 J/gmC°(0.99865 BTU/lbmF°)

γ_A = 995.46 kg/m^3 (8.30753 lbm/Gal)

W_A = 37.305 kg/Min (82.2445 lbm/min)

The flowmeter accuracy is $\pm$ 1.% of full scale (F.S.) which is 0.1018 m^3/ min. (26.9 GPM) for the condensing water flow meter.

ΔW_A = $\pm$0.01 x (F.S.) x γ_A

= $\pm$ 1.0136kg/min (2.2347 lbm/min)

ΔT_{1A} = $\pm$ 0.1C° ($\pm$0.18 F°)

ΔC_{PA} = $\pm$0.00004 J/gm C° ($\pm$0.00001 BTU/lbmF°)

From Equation 3,

(5) $\Delta Q_A^2 = 1.7081 \times 10^5 \text{ watts}^2 \ (553.32 \ \frac{BTU}{min}^2 \ 2)$

The condenser flowrate equals the absorber flowrate:

$W_C = 37.305$ kg/min (82.2445 lbm/min)

$\Delta W_C = \pm 1.0136$ kg/min (± 2.2347 lbm/min)

The condenser water temperatures are

T_{1C} = 32.03°C (89.66°F)

T_{2C} = 34.25°C (93.65°F)

T_{AVG} = 33.14°C (91.655°F)

C_{PC} = 4.17818 J/gmC° (0.99861 BTU/lbm F°)

The thermometer and specific heat accuracies are:

ΔT_{1C} = 0.1C° (± 0.18F°)

ΔC_{PC} = ± 0.00004 J/gm C° (± 0.00001 BTU/lbmF°)

From Equation 3,

(6) $\Delta Q_C^2 = 1.5937 \times 10^5 \text{ watts}^2 \ (516.26 \ \frac{BTU^2}{min^2})$

Combining (4), (5), and (6) into (2) gives

$$(QRMS) = 609.2 \text{ watts } (34.67 \frac{BTU}{Min}, 2080 \text{ BTUH})$$

The test error as measured during Run 37 and evaluated from Equation (1) is

$$\Delta Q = -460 \text{ watts } (-1570 \text{ BTUH})$$

(7) and $/\Delta Q/ < /QRMS/$

Relation (7) gives confidence in the test instrumentation, calibration, and in the data.

APPENDIX B

ANALYSIS OF PRESSURE DROP

IN A SET OF PARALLEL COILS

L = Length of coiled tube
N = Number of turns per coil
R = Coil radius (to tube centerline)

Subscripts refer to individual coils beginning with "1" for the inner coil.

Assume equal coil height and gap

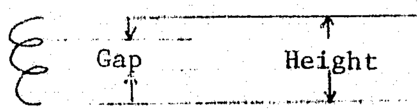

Then $N_1 = N_2 = \cdots N_j$ for j number of coils

$L_1 = 2\pi R_1 N_1 \quad L_2 = 2\pi R_2 N_2 \quad --- \quad L_j = 2\pi R_2 N_j$

Total Length $L_T = \sum_{1}^{j} L_j$

(1) $$L_T = N\, 2\pi \sum_{1}^{j} R_j$$

For multiple coils in parallel:

ΔPs are equal (neglecting manifold losses).

Flow rates and Reynolds Numbers will vary.

$$\Delta P_1 = \Delta P_2 = ---- \Delta P_j$$

$$\frac{\rho f_1 L_1 V_1^2}{144\, D_1 2g} = \frac{\rho f_2 L_2 V_2^2}{144\, D_2\, 2g} = \cdots \frac{\rho f_j L_j V_j^2}{144\, D_j\, 2g}$$

Since $D_1 = D_2 = \cdots = D_j$

$$f_1 L_1 V_1^2 = f_2 L_2 V_2^2 = ----- = f_j L_j V_j^2$$

For turbulent flow in a smooth conduit*

*Ref. 1, p. 87.

(For $2000 < Rey < 10^5$); $f = \frac{0.3164}{N_{RE}^{0.25}}$

or $f = C_f\ V^{-0.25}$

Where $C_f = 0.3164\ (\frac{\mu}{\rho D})^{0.25}$

Then $L_1 V_1^{1.75} = L_2\ V_2^{1.75} = - - - - = L_j\ V_j^{1.75}$

For Incoming Tube, I, feeding the coils,

$$Q_I = \sum_1^j Q_j$$

$$A_I V_I = A \sum_1^j V_j$$

If $A_I = A$ then $V_I = \sum_1^j V_j$

Since $V_2 = V_1\ (\frac{L_1}{L_2})^{1/1.75}$, $V_3 = V_1\ (\frac{L_1}{L_3})^{1/1.75}$, $V_j = V_1\ (\frac{L_1}{L_j})^{1/1.75}$

Then

$$V_I = V_1 + V_1\ (\frac{L_1}{L_2})^{1/1.75} + - - - - + V_1\ (\frac{L_1}{L_j})^{1/1.75}$$

$$V_I = V_1\ \left[1 + \sum_2^j (\frac{L_1}{L_j})^{1/1.75}\right]$$

$\frac{L_1}{L_2} = \frac{2\pi R_1\ N_1}{2\pi R_2\ N_2}$ and $N_1 = N_2\ \therefore\ \frac{L_1}{L_2} = \frac{R_1}{R_2}$, $\frac{L_1}{L_j} = \frac{R_1}{R_j}$

$$V_I = V_1 \left[1 + \sum_2^j (\frac{R_1}{R_j})^{1/1.75}\right]$$

(2) and $f_1 = C_f\ \left(V_I \Big/ \left[1 + \sum_2^j (\frac{R_1}{R_j})^{1/1.75}\right]\right)^{-0.25}$

from Reference 3, page A-27, for ΔP in a coiled tube:

(3) $(\frac{L}{D}) = R_t + (n - 1)\ (R_\ell + \frac{R_b}{2})$

n = number of 90° bends in coil

R_t = resistance of one 90° bend ~ L/D

R_ℓ = resistance due to length of one 90° bend ~ L/D

R_b = bend resistance due to one 90° bend ~ L/D

Note: $n = 4N$

$$\Delta P = \frac{\rho f L V^2}{144\ D\ 2g}$$

(4) $P = 0.006531 \ f_1 \ V_1^{\ 2} \ (\frac{L}{D})_1$

Assume R_j's = 6", 7.25, 8.5, 9.75 for 0.75 tubing

6", 7.5, 9.0, 10.5 for 1.00 tubing

do (inch)	j	N	V_1		ΔP	
			m/s	(Ft/Sec)	kN/m^2	(psi)
0.75	1	16	2.962	9.718	93.6	13.57
	2	8	1.561	5.121	19.7	2.85
	3	6	1.090	3.577	7.86	1.14
	4	4	0.853	2.797	3.45	0.50
1.00	1	14	1.584	5.196	18.8	2.73
	2	7	0.842	2.763	4.07	0.59
	3	5	0.593	1.944	1.59	0.23
	4	4	0.466	1.528	0.83	0.12

Conclusion: One coil of 0.75 tubing requires high pressure drop and should be avoided.

Other Factors: Generator packaging
Tubing availability (0.75 vs. 1.00).
Flow distribution over tubes.

APPENDIX C

SPRAY NOZZLE

PRESSURE AVAILABLE

Must match pump and nozzle characteristics.

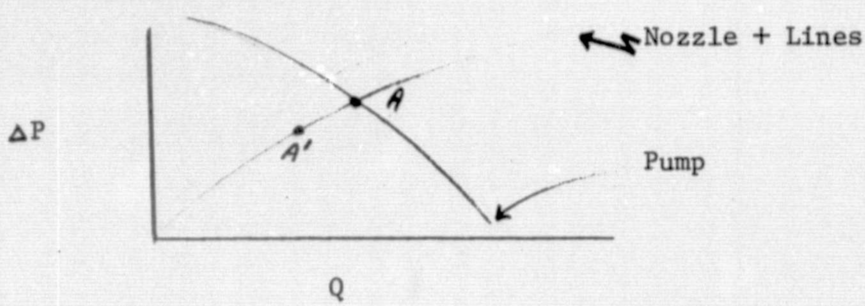

Use regulating valve to shift operating point.

First, calculate maximum pressure available at nozzle inlet with regulating valve 100% open, and LiBr = 0.82 GPM.

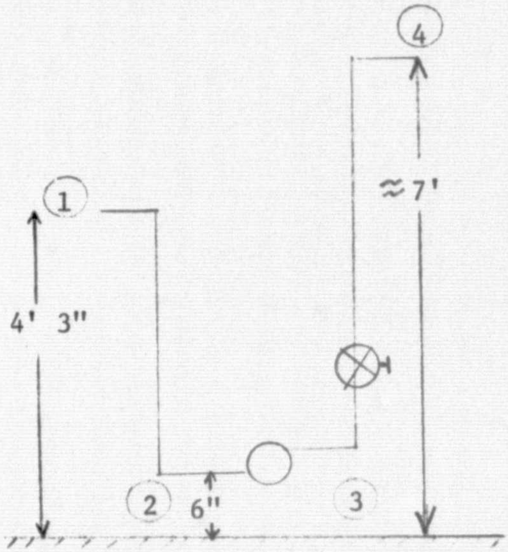

$$H_4 = H_1 + H_{2/3} - H_{LV} - H_{Lf}$$

H_{LV} = Head loss due to valve

H_{Lf} = Head loss due to friction

From Grinnell Catalog DV-73 for 1/2 inch diaphragm valve, screwed end, metal -

$C_V = 4.4$ (100% Open)

$$\Delta P = G \left[\frac{GPM}{C_V}\right]^2$$

ΔP - PSID

G - Specific Gravity

GPM - Gallons per minute

$$H_{LV} = \frac{\Delta P\ (144)}{\rho\ g}$$

$$H_{LV} = \frac{144}{(G\ \rho H20)} \times \frac{G}{1} \times \left[\frac{GPM}{C_V}\right]^2$$

$= 0.08015$ Ft.

For head loss due to friction:

$$H_{Lf} = \frac{fL}{D}\frac{V^2}{2\ g}$$

D - Internal Dia - Ft.
f - Friction factor
g - Accel of Gravity - 32.2 Ft/Sec^2
L - Length of tubing - Ft.
V - Velocity - Ft/Sec.

$$Rey = \frac{4\ W}{\pi\ D \mu}$$

$$f = \frac{0.3164}{(Rey)^{0.25}} = 0.04385 \quad \text{(Ref. 1, p. 87)}$$

Assume six 90° elbows:

One 90° El, Std. $\frac{L_{EQ}}{D} = 30$

Equivalent length of six elbows with

D = 0.06292 Ft. (.815 inch) is

$L_{EQ} = 180\ D \approx 11.5$ Ft.

Total tube length $L_T = L_{1-2} + L_{2-3} + L_{3-4} + L_{EQ}$

$= 3\ 1/2 + 2 + 5 + 11\ 1/2$

$L_T = 22$ ft.

$$V = \frac{Q\ 4}{\pi D^2}$$

$H_{Lf} = 0.082$ Ft.

$H_{2/3}$ = 35 feet from Crane Dynapump data (Figure C-1)

$$H_1 = \frac{144\ P_1}{\rho\ g} + \frac{V_1^2}{2\ g} + z_1 \qquad \text{Where } P_1 = 7 \text{ mmHg} \quad (0.1354 \text{ psi})$$

$$V_1 = 0$$

$$H_1 = 4.45 \text{ ft.} \qquad z = 4.25 \text{ ft.}$$

$$H_4 = H_1 + H_{2/3} - H_{LV} - H_{Lf}$$

$$= 4.45 + 35. - 0.080 - 0.082$$

$$H_4 = 39.3 \text{ ft.}$$

$$H_4 = \frac{144\ P_4}{\rho\ g} + \frac{V_4^{\ 2}}{2\ g} + z_4$$

$$P_4 = 22.11 \text{ psia}$$

Press Across Nozzle $\Delta P_N = P_4 - P_{GEN}$

$$= 22.11 - 1.12$$

$$\Delta P_N = 21. \text{ psid}$$

This is max ΔP_N available (with valve 100% open). Flow through nozzle must exceed required flow at 21 psid.

Nozzle equations:

$$Q_{LiBr} = Q_{Catalog} \times \frac{1}{\sqrt{SG}}$$

$$\frac{Q_1}{Q_2} = \sqrt{\frac{PSID_1}{PSID_2}}$$

Factors: Viscosity
Specific Gravity
Flow Distribution
Packaging - Spray Height, D_{COIL}
Angle vs. Pressure
Effect of vacuum on angle.

Options: Nozzle Orientation
First turn of coil to be flat
Depend on baffles
Larger pump with smaller nozzle orifice
Drippers.

SPRAY ANGLE INFORMATION

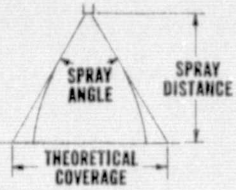

This table lists the theoretical coverage of spray patterns as calculated from the included spray angle of the spray and the distance from the nozzle orifice. These values are based on the assumption that the spray angle remains the same throughout entire spray distance. In actual practice, the tabulated spray angle does not hold for long spray distances. Write for Data Sheets on actual spray coverage.

Included Spray Angle	THEORETICAL COVERAGE AT VARIOUS DISTANCES (IN INCHES) FROM NOZZLE ORIFICE											
	2"	4"	6"	8"	10"	12"	15"	18"	24"	30"	36"	48"
5°	0.2"	0.4"	0.5"	0.7"	0.9"	1.1"	1.3"	1.6"	2.1"	2.6"	3.1"	4.2"
10°	0.4"	0.7"	1.1"	1.4"	1.8"	2.1"	2.6"	3.1"	4.2"	5.2"	6.3"	8.4"
15°	0.5"	1.1"	1.6"	2.1"	2.6"	3.2"	3.9"	4.7"	6.3"	7.9"	9.5"	12.6"
20°	0.7"	1.4"	2.1"	2.8"	3.5"	4.2"	5.3"	6.4"	8.5"	10.6"	12.7"	16.9"
25°	0.9"	1.8"	2.7"	3.5"	4.4"	5.3"	6.6"	8.0"	10.6"	13.3"	15.9"	21.2"
30°	1.1"	2.1"	3.2"	4.3"	5.4"	6.4"	8.1"	9.7"	12.8"	16.1"	19.3"	25.7"
35°	1.3"	2.5"	3.8"	5.0"	6.3"	7.6"	9.5"	11.3"	15.5"	18.9"	22.7"	30.3"
40°	1.5"	2.9"	4.4"	5.8"	7.3"	8.7"	10.9"	13.1"	17.5"	21.8"	26.2"	34.9"
45°	1.7"	3.3"	5.0"	6.6"	8.3"	9.9"	12.4"	14.9"	19.9"	24.8"	29.8"	39.7"
50°	1.9"	3.7"	5.6"	7.5"	9.3"	11.2"	14.0"	16.8"	22.4"	28.0"	33.6"	44.8"
55°	2.1"	4.2"	6.3"	8.3"	10.3"	12.5"	15.6"	18.7"	25.0"	31.2"	37.5"	50.0"
60°	2.3"	4.6"	6.9"	9.2"	11.5"	13.8"	17.3"	20.6"	27.7"	34.6"	41.6"	55.4"
65°	2.5"	5.1"	7.6"	10.2"	12.7"	15.3"	19.2"	22.9"	30.5"	38.2"	45.8"	61.2"
70°	2.8"	5.6"	8.4"	11.2"	14.0"	16.8"	21.0"	25.2"	33.6"	42.0"	50.4"	67.2"
75°	3.1"	6.1"	9.2"	12.3"	15.3"	18.4"	23.0"	27.6"	36.8"	46.0"	55.2"	73.6"
80°	3.4"	6.7"	10.1"	13.4"	16.8"	20.2"	25.2"	30.3"	40.3"	50.4"	60.4"	80.6"
85°	3.7"	7.3"	11.0"	14.7"	18.3"	22.0"	27.5"	33.0"	44.0"	55.0"	66.0"	88.0"
90°	4.0"	8.0"	12.0"	16.0"	20.0"	24.0"	30.0"	36.0"	48.0"	60.0"	72.0"	96.0"
95°	4.4"	8.7"	13.1"	17.5"	21.8"	26.2"	32.8"	39.3"	52.4"	65.5"	78.6"	105"
100°	4.8"	9.5"	14.3"	19.1"	23.8"	28.6"	35.8"	43.0"	57.2"	71.6"	85.9"	114"
110°	5.7"	11.4"	17.1"	22.8"	28.5"	34.3"	42.8"	51.4"	68.5"	85.6"	103"	
120°	6.9"	13.9"	20.8"	27.7"	34.6"	41.6"	52.0"	62.4"	83.2"	104"		
130°	8.6"	17.2"	25.7"	34.3"	42.9"	51.5"	64.4"	77.3"	103"			
140°	10.9"	21.9"	32.9"	43.8"	54.8"	65.7"	82.2"	98.6"				
150°	14.9"	29.8"	44.7"	59.6"	74.5"	89.5"	112"					
160°	22.7"	45.4"	68.0"	90.6"	113"							
170°	45.8"	91.6"										

FLOW OF WATER THROUGH SCHEDULE 40 STEEL PIPE

Recommended capacity range for each size is shown in blue.

Flow in G.P.M.	Pressure Drop in p.s.i. for Various Pipe Sizes (In 10 Ft. Length)							
	⅛"	¼"	⅜"	½"	¾"	1"	1¼"	1½"
0.3	.42							
0.4	.70	.16						
0.5	1.1	.24						
0.6	1.5	.33						
0.8	2.5	.54	.13					
1.0	3.7	.83	.19	.06				
1.5	8.0	1.8	.40	.12				
2.0	13.4	3.0	.66	.21	.05			
2.5		4.5	1.0	.32	.08			
3.0		6.4	1.4	.43	.11			
4.0		11.1	2.4	.74	.18	.06		
5.0			3.7	1.1	.28	.08		
6.0			5.2	1.6	.38	.12		
8.0			9.1	2.8	.66	.20	.05	
10				4.2	1.0	.30	.08	
15					2.2	.64	.16	.08
20					3.8	1.1	.28	.13
25						1.7	.42	.19
30						2.4	.59	.27

Flow in G.P.M.	Pressure Drop in p.s.i. for Various Pipe Sizes (In 10 Ft. Length)							
	2"	2½"	3"	3½"	4"	5"	6"	8"
35	.11	.04						
40	.14	.06						
45	.17	.07						
50	.20	.08						
60	.29	.12	.04					
70	.38	.16	.05					
80	.50	.20	.07					
90	.62	.25	.09	.04				
100	.76	.31	.11	.05				
125	1.2	.47	.16	.08	.04			
150	1.7	.67	.22	.11	.06			
200	2.9	1.2	.39	.19	.10			
250			.59	.28	.15	.05		
300			.84	.40	.21	.07		
400				.70	.37	.12	.05	
500					.57	.18	.07	
750						.39	.16	.04
1000						.68	.27	.07
2000							1.0	.26

APPROXIMATE FRICTION LOSS IN PIPE FITTINGS

in terms of equivalent feet of straight pipe.

Pipe Size Std. Wt.	Actual inside diam. in.	Gate Valve FULL OPEN	Globe Valve FULL OPEN	45 Elbow	Run of Std. tee	Std. elbow or run of tee reduced ½	Std. tee thru side outlet
⅛	.269	.15	8	.35	.40	.75	1.4
¼	.364	.20	11	.50	.65	1.1	2.2
½	.622	.35	18.6	.78	1.1	1.7	3.3
¾	.824	.44	23.1	.97	1.4	2.1	4.2
1	1.049	.56	29.4	1.2	1.8	2.6	5.3
1¼	1.380	.74	38.6	1.6	2.3	3.5	7.0
1½	1.610	.86	45.2	1.9	2.7	4.1	8.1
2	2.067	1.1	58	2.4	3.5	5.2	10.4
2½	2.469	1.3	69	2.9	4.2	6.2	12.4
3	3.068	1.6	86	3.6	5.2	7.7	15.5
4	4.026	2.1	113	4.7	6.8	10.2	20.3
5	5.047	2.7	142	5.9	8.5	12.7	25.4
6	6.065	3.2	170	7.1	10.2	15.3	31

MISCELLANEOUS EQUIVALENTS AND FORMULAS

UNIT	EQUIVALENT	UNIT	FORMULA
Ounce	28.35 Gr.	Fahrenheit (F°)	$= \frac{9}{5}$ C° + 32
Pound	0.4536 Kg	Centigrade (C°) (Celcius)	$= \frac{5}{9}$ (F°−32)
Horse Power	0.746 Kw.	Circumference of Circle	= 3.1416 x Diameter
British Thermal Unit	0.2520 Kg Cal.	Area of a Circle	= .7854 x Square of the Diameter
Square Inch	6.452 Sq. Cm.	Volume of a Sphere	= .5236 x Cube of the Diameter
Square Foot	0.09290 Sq. M.	Area of a Sphere	= 3.1416 x Square of the Diameter
Acre	0.4047 Hectare		
Acre	43,560 Sq. Ft.		

WhirlJet NOZZLES wide spray

Spray Characteristics—Hollow cone spray pattern with extra wide spray angle. Uniform spray distribution.

Construction—Two-piece design with interchangeable cap. Large diameter body inlet and cap orifice passages. Choice of types A and B with standard whirlchamber design . . . or types AX and BX with the exclusive, patented slope-bottom design for much less wear and longer life.

Materials—Nozzles supplied in choice of brass, steel and types 303 and 316 stainless steel . . . other materials upon order. See page 21 for PVC nozzle sizes.

Type A standard and **Type AX** slope-bottom designs female connection

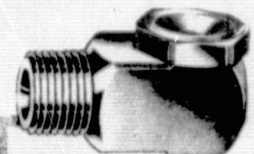

Type B standard and **Type BX** slope-bottom designs male connection

WIDE HOLLOW CONE SPRAY PATTERN

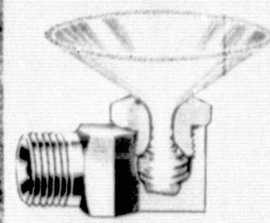

EXCLUSIVE PATENTED SLOPE-BOTTOM DESIGN for Types AX and BX

Prevents the "drilling" effect found in standard design whirlchambers, by diffusing the vortex forces that are present. Greatly increases nozzle life.

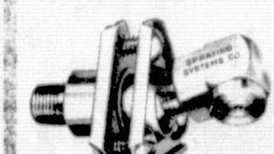

WhirlJet Nozzle held by Adjustable Joint . . . permits easy adjustment of spray direction for more effective spray coverage. See pages 54 through 61 for spray nozzle accessories.

Nozzle No. Type A, AX Female Conn.	Nozzle No. Type B, BX Male Conn.	Size	Pipe Conn. NPT	Body Inlet Diam. Nom.	Orifice Diam. Nom.	CAPACITY GPM (gallons per minute) at p.s.i. (pounds per square inch) 5 p.s.i.	7 p.s.i.	10 p.s.i.	15 p.s.i.	20 p.s.i.	30 p.s.i.	40 p.s.i.	60 p.s.i.	80 p.s.i.	SPRAY ANGLE* 10 p.s.i.
		0.5-0.5W	1/8"	1/32"	3/64"			.05	.06	.07	.09	.10	.12	.14	112°
		1-1W	1/8"	1/16"	1/16"			.10	.12	.14	.17	.20	.25	.28	114°
1/8A-	1/8B-	2-3W	1/8"	5/64"	7/64"		.21	.25	.31	.35	.43	.50	.61	.71	114°
		3-3W	1/8"	3/32"	7/64"		.25	.30	.37	.42	.52	.60	.73	.85	114°
		3-5W	1/8"	3/32"	1/8"		.29	.34	.42	.48	.59	.68	.83	.96	116°
1/8AX-	1/8BX-	2-10W	1/8"	5/64"	11/64"		.35	.41	.51	.59	.72	.82	1.0	1.2	130°
		5-5W	1/8"	1/8"	1/8"		.42	.50	.61	.71	.86	1.0	1.2	1.4	116°
		5-10W	1/8"	1/8"	11/64"	.46	.54	.65	.80	.92	1.1	1.3	1.6	1.8	126°
		8-10W	1/8"	5/32"	11/64"	.64	.75	.90	1.1	1.3	1.6	1.8	2.2	2.5	124°
		1-1W	1/4"	1/16"	1/16"			.10	.12	.14	.17	.20	.25	.28	110°
		1-5W	1/4"	1/16"	1/8"			.17	.21	.24	.29	.34	.42	.48	100°
		1-10W	1/4"	1/16"	11/64"			.21	.26	.30	.36	.42	.51	.60	112°
		1-15W	1/4"	1/16"	7/32"			.24	.29	.34	.42	.48	.59	.68	105°
1/4A-	1/4B-	2-5W	1/4"	5/64"	1/8"		.29	.34	.42	.49	.60	.68	.84	.89	118°
		2-10W	1/4"	5/64"	11/64"		.35	.41	.51	.59	.72	.82	1.0	1.2	138°
		5-5W	1/4"	9/64"	1/8"		.42	.50	.61	.71	.86	1.0	1.2	1.4	114°
		5-10W	1/4"	9/64"	11/64"	.46	.54	.65	.80	.92	1.1	1.3	1.6	1.8	130°
		5-15W	1/4"	9/64"	7/32"	.52	.64	.77	.94	1.1	1.3	1.5	1.8	2.2	130°
1/4AX-	1/4BX-	8-10W	1/4"	5/32"	11/64"	.64	.75	.90	1.1	1.3	1.6	1.8	2.2	2.5	129°
		10-10W	1/4"	3/16"	11/64"	.71	.84	1.0	1.2	1.4	1.7	2.0	2.5	2.8	120°
		8-15W	1/4"	5/32"	7/32"	.78	.92	1.1	1.4	1.6	1.9	2.2	2.7	3.1	129°
		10-15W	1/4"	3/16"	7/32"	.86	1.0	1.2	1.5	1.7	2.1	2.4	3.0	3.4	120°
		15-15W	1/4"	15/64"	7/32"	1.1	1.3	1.5	1.8	2.1	2.6	3.0	3.7	4.2	101°
		5-10W	3/8"	9/64"	11/64"	.46	.54	.65	.80	.92	1.1	1.3	1.6	1.8	130°
		5-15W	3/8"	9/64"	7/32"	.52	.64	.77	.94	1.1	1.3	1.5	1.8	2.2	138°
		8-10W	3/8"	11/64"	11/64"	.64	.75	.90	1.1	1.3	1.6	1.8	2.2	2.5	122°
		10-10W	3/8"	13/64"	11/64"	.71	.84	1.0	1.2	1.4	1.7	2.0	2.5	2.8	116°
3/8A-	3/8B-	8-15W	3/8"	11/64"	7/32"	.78	.92	1.1	1.4	1.6	1.9	2.2	2.7	3.1	133°
		10-15W	3/8"	13/64"	7/32"	.86	1.0	1.2	1.5	1.7	2.1	2.4	3.0	3.4	126°
		8-25W	3/8"	11/64"	19/64"	.92	1.1	1.3	1.6	1.9	2.3	2.6	3.2	3.7	122°
		10-20W	3/8"	13/64"	15/64"	.97	1.1	1.4	1.7	1.9	2.4	2.7	3.3	3.9	118°
		15-15W	3/8"	15/64"	7/32"	1.1	1.3	1.5	1.8	2.1	2.6	3.0	3.7	4.2	116°
3/8AX-	3/8BX-	15-20W	3/8"	15/64"	15/64"	1.2	1.5	1.7	2.1	2.5	3.0	3.5	4.3	4.9	113°
		20-20W	3/8"	9/32"	15/64"	1.4	1.7	2.0	2.4	2.8	3.5	4.0	4.9	5.6	106°
		15-30W	3/8"	15/64"	5/16"	1.6	1.8	2.2	2.7	3.1	3.8	4.4	5.4	6.2	116°
		25-25W	3/8"	19/64"	19/64"	1.8	2.1	2.5	3.1	3.5	4.3	5.0	6.1	7.1	105°
		25-30W	3/8"	19/64"	5/16"	2.0	2.3	2.8	3.4	4.0	4.9	5.6	6.9	7.9	105°
1/2A- 1/2AX-	1/2B- 1/2BX-	50-50W	1/2"	3/8"	7/16"	3.5	4.2	5.0	6.1	7.1	8.6	10.0	12.3	14.2	110°
3/4A- 3/4AX-	3/4B- 3/4BX-	80-80W	3/4"	1/2"	9/16"	5.7	6.7	8.0	9.8	11.3	13.8	16.0	19.6	23	115°

*See page 3 for spray angle data.

Patent Nos. 2,815,248, 3,326,473 and Foreign Patents.

WHEN ORDERING—Specify complete Nozzle No. and material. Example: 1/8AX2-3W WhirlJet Nozzle, stainless steel.

INTERMEDIATE CAPACITIES—Caps are interchangeable for in-between capacities within each pipe size group . . . write for Data Sheets 5412 and 5414.

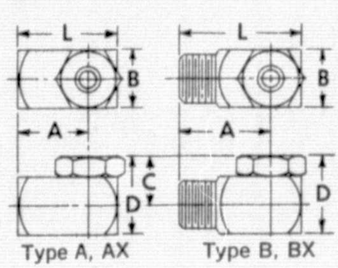

Type A, AX Female Conn.	Net Weight Max.	A Max.	B Max.	C Max.	D Max.	L Max.	Type B, BX Male Conn.	Net Weight Max.	A Max.	B Max.	C Max.	D Max.	L Max.
1/8A,AX	1 1/2 oz.	11/16"	5/8"	15/32"	25/32"	1"	1/8B,BX	1 1/2 oz.	7/8"	5/8"	15/32"	25/32"	1 3/16"
1/4A,AX	2 3/4 oz.	7/8"	3/4"	17/32"	29/32"	1 1/4"	1/4B,BX	2 1/2 oz.	1"	3/4"	17/32"	29/32"	1 3/8"
3/8A,AX	4 1/4 oz.	1 1/32"	7/8"	11/16"	1 1/8"	1 15/32"	3/8B,BX	4 oz.	1 1/8"	7/8"	11/16"	1 1/8"	1 9/16"
1/2A,AX	8 3/4 oz.	1 3/8"	1 1/8"	27/32"	1 13/32"	1 15/16"	1/2B,BX	7 oz.	1 3/8"	1 1/8"	27/32"	1 13/32"	1 15/16"
3/4A,AX	11 oz.	1 9/16"	1 1/4"	15/16"	1 9/16"	2 3/16"	3/4B,BX	10 3/4 oz.	1 5/8"	1 1/4"	15/16"	1 9/16"	2 1/4"

APPENDIX D

SPRAY NOZZLE/COIL GEOMETRY

CASE I - Consider single helical coil of 1" OD tubing, with top turn flat.

Consider two candidate hollow cone spray nozzles:

A) $\frac{3}{8}$ AX - 5 - 15W Spray Angle $\theta = 138°$

B) $\frac{3}{8}$ AX - 8 - 10W $\theta = 122°$

Assume spray angle θ increases by 5° due to vacuum.

$$\theta_A = 143°, \quad \theta_B = 127°$$

Subscripts refer to nozzles A, B.

Assume spray impingement is on 120° of arc (from "11 o'clock" position to "3 o'clock" position) and is centered as shown in the figure.

Assume width of hollow cone α is 7° (Based on data from Chrysler Airtemp Division A.M.&S. Laboratory Test Report No. 111701-3, File: AB 02-04-XX, Spray Nozzle Evaluation).

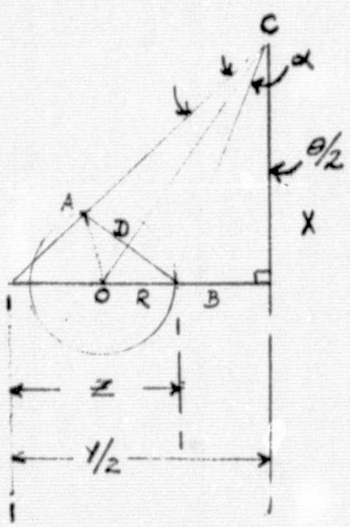

α = Spray width angle
θ = Spray angle (outer)
R = Tube radius
X = Height of nozzle exit above tube center
Y = Outer diameter of spray circle at height X
Z = Width of spray circle at height X

$$\overline{BC} = \sqrt{X^2 + \left[(Y/2) - z\right]^2}$$

$$\overline{DB} = \overline{BC} \sin \frac{\alpha}{2}$$

$$\overline{DB} = \frac{1}{2} \overline{AB}$$

Combining the three equations above, gives -

$$\overline{AB} = 2(\sin \frac{\alpha}{2}) \sqrt{X^2 + (\frac{Y}{2} - z)^2}$$

$$\frac{Y}{2} - z = X \, \mathrm{Tan} \, (\frac{\theta}{2} - \alpha)$$

$$\overline{AB} = 2 \, (\sin \frac{\alpha}{2}) \sqrt{X^2 + X^2 \, \mathrm{Tan}^2 \, (\frac{\theta}{2} - \alpha)}$$

$$= 2 \, X \, (\sin \frac{\alpha}{2}) \sqrt{1 + \mathrm{Tan}^2 \, (\frac{\theta}{2} - \alpha)}$$

$$\overline{AB} = 2X \, (\sin \frac{\alpha}{2}) \, (\sec [\frac{\theta}{2} - \alpha])$$

(1) $$X = \overline{AB} \, \frac{\cos \, (\frac{\theta}{2} - \alpha)}{2 \sin \frac{\alpha}{2}}$$

For Nozzle A: $X_A = 3.526 \, \overline{AB}$

B: $X_B = 4.520 \, \overline{AB}$

For 1" OD tube, and 120° coverage,

$$\frac{\overline{AB}}{2} = R \sin \frac{\measuredangle AOB}{2}$$

$$\overline{AB} = 1'' \sin 60$$

$$= 0.87 \text{ inch}$$

and $X_A = 3.07$

$X_B = 3.93$

Let R_C = Radius of helix to tube center

$R_C = (Y/2) - Z + R$

2) $R_C = X \tan\left(\frac{\theta}{2} - \alpha\right)$

R_{CA} = 6.44 inch

R_{CB} = 5.94 inch

Add 1.5" radially for vapor path between the tube and the shell. The shell internal diameter is:

$ID = 2\ (R_C + 1.5 + R)$

ID_A = 16.88 inch

ID_B = 15.88 inch

Calculate total height:

$H = ND + (N-1)\ h + X + 2.5$

D = Tube diameter
h = Gap between turns
H = Total height
N = Number of turns
X = Height of nozzle exit above tube center

2.5 is added for nozzle height and coil entrance and exit

$N = \frac{L}{2 \pi R_C}$ Rounded to next higher integer

N = 14 turns

Take h = 0.5 inch

H_A = 26.1 inch

H_B = 26.9 inch

CASE II

For Two 3/4" Coils

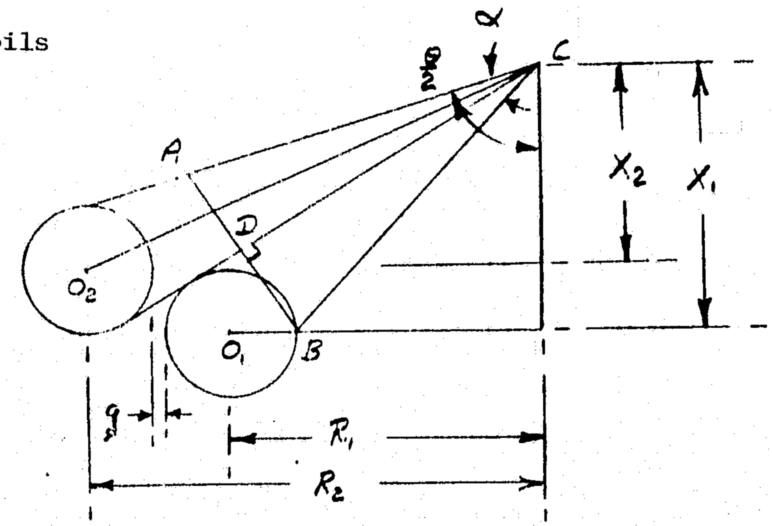

Assume spray is uniform and equally divided between the two tubes. Then

$$\angle ACD = \angle DCB = (1/2)\alpha$$

Assume $X_1 - X_2 = R_T$ tube radius

1 $$X_2 = \sqrt{\overline{O_2C}^2 - R_2^{\,2}}$$

2 $$\sin\left(\frac{\theta}{2} - \frac{\alpha}{4}\right) = \frac{R_2}{\overline{O_2C}}$$

3 $$\sin\frac{\alpha}{4} = \frac{R_T}{\overline{O_2C}}$$

From 2 and 3 : 4 $$R_2 = \frac{R_T}{\sin\frac{\alpha}{4}} \times \sin\left(\frac{\theta}{2} - \frac{\alpha}{4}\right)$$

and 1 becomes $$X_2 = \sqrt{\frac{R_T^2}{\sin^2\frac{\alpha}{4}} - \frac{R_T^2}{\sin^2\frac{\alpha}{4}}\sin^2\left(\frac{\theta}{2} - \frac{\alpha}{4}\right)}$$

$$X_2 = \frac{R_T}{\sin\frac{\alpha}{4}} \sqrt{1 - \sin^2\left(\frac{\theta}{2} - \frac{\alpha}{4}\right)}$$

5 $$X_2 = \frac{R_T \cos\left(\frac{\theta}{2} - \frac{\alpha}{4}\right)}{\sin\frac{\alpha}{4}}$$

6 Also $R_1 = R_T + X_1 \tan\left(\frac{\theta}{2} - \alpha\right)$

Gap between coils:

7 $g = R_2 - R_1 - 2\,R_T$

8 $X_1 = X_2 + R_T$ by assumption on page D-4.

Evaluate equations 5, 8, 4, 6, 7, to find X_2, X_1, R_2, R_1, g, respectively for nozzles A & B.

X_{2A} =	4.25 inch	X_{2B} =	5.81 inch
X_{1A} =	4.625	X_{1B} =	6.19
R_{2A} =	11.52	R_{2B} =	10.82
R_{1A} =	10.07	R_{1B} =	9.73
g_A =	+0.7	g_B =	+0.34

The internal diameter of the shell is

$ID = 2\,(R_2 + 1.5 + R_T)$ where 1.5 is allowed for vapor travel between tube and shell.

$ID_A = 2\,(11.52 + 1.5) + 0.75 = 26.8$ inch

$ID_B = 2\,(10.82 + 1.5) + 0.75 = 25.4$ inch

Total height is calculated as indicated:

Since vapor path is radially outward between coils and then upward between shell and coil, assume gap between turns -

$h_1 = 0.25$
$h_2 = 0.75$

$$H_1 = N_1\ 2\ R_T + (N_1 - 1)\ h_1$$

$$H_2 = N_2\ 2\ R_T + (N_2 - 1)\ h_2$$

Make $H_2 = H_1$

$$2\pi(N_1 R_1 + N_2 R_2) = L_T$$

$$= 55 \times 12 \text{ inches}$$

Solving for N_1 and N_2, and rounding to the next higher integral number of turns,

N_{1A} = 6 turns $\quad N_{1B}$ = 6 turns

N_{2A} = 5 turns $\quad N_{2B}$ = 5 turns

Total Height -

$H_T = H_1 + X_1 + 2.5$ where 2.5 is added for nozzle height and coil entrance and exit.

H_{TA} = 12.9 inch

H_{TB} = 14.5 inch

APPENDIX E

STRUCTURAL DESIGN OF

TRAY GENERATOR

Box design to hold ΔP of 14.7 psi

Dimensions = 30 inches X 30 inches X 6 inches

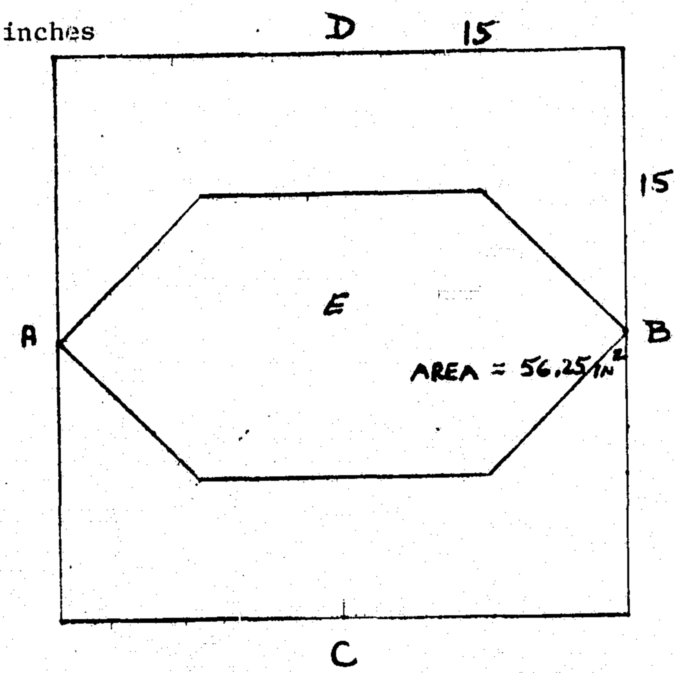

For Section EC Loading

$$W_{ToT} = 14.7 \times 1.5 \times 56.25 \times 2 = 2480 \text{ lbs.}$$

Idealized loading on AB is assumed to take part of span ADB which is shown in shaded area.

LOADING DIAGRAM FOR MEMBER AB

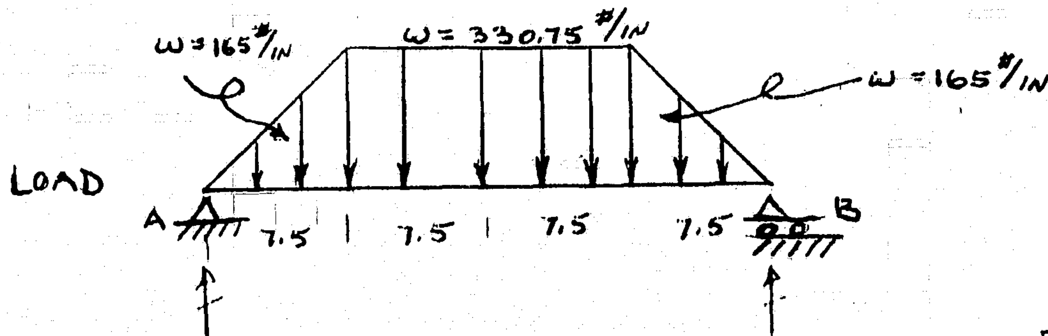

$R_A = R_B = \frac{1}{2}\left[2(165 \times 7.5) + 330(15)\right]$

$R_A = R_B = 3721$ LBS

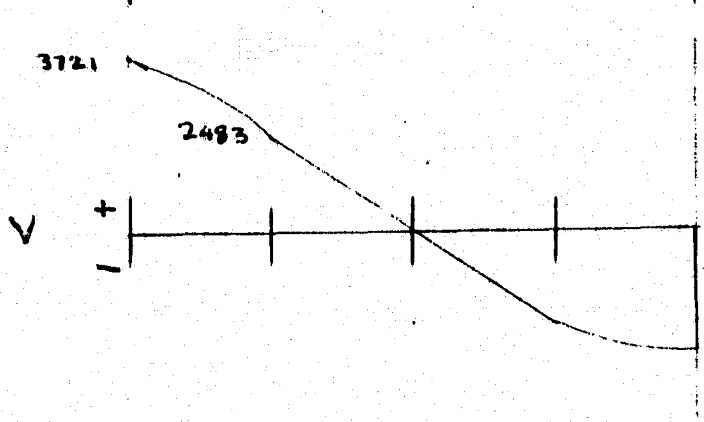

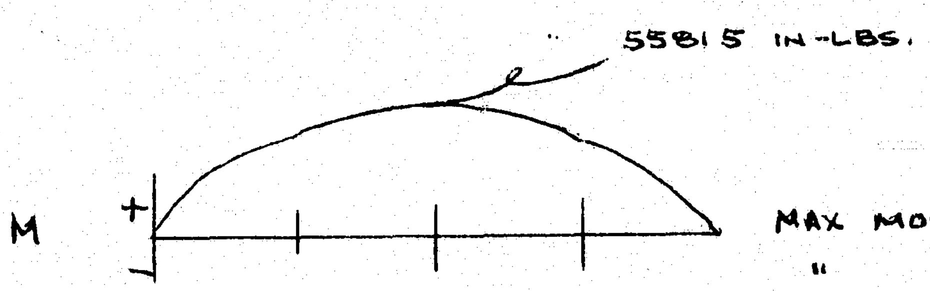

MAX MOMENT = 3721(15)

" " = 55815 IN-LBS

USING MATERIAL WITH $F_{ty} = 18$ KSI $= .5\,F_y$
FROM AISC HB FOR 36 KSI STEEL

$f_b = \frac{Mc}{I} = M\frac{1}{S}$ WHERE $S = I/c$

$f_b = 55815 \times \left(\frac{1}{.79}\right) =$ PSI

MUST USE
LARGER ANGLE
SAY $3\frac{1}{2} \times 3\frac{1}{2} \times \frac{3}{8}$

$f_b = 55815 \times \frac{1}{1.2} = 46{,}512$ PSI

SECTION GETTING TOO LARGE THEREFORE

THE USE OF A "T" SECTION IS RECOMMENDED

TRYING ANGLE TEE WITH SECTIONS

WELDED TOGETHER

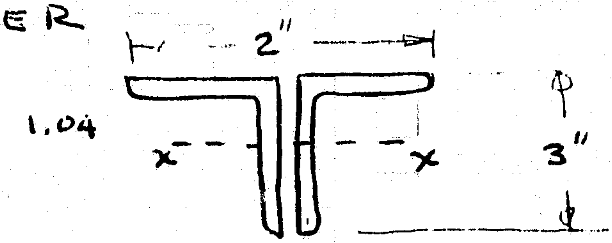

$I = 3.1 \ in^4$

$S = I/c = \frac{3.1}{1.96} = 1.6 \ in^3$

A of two angles = 3.46 in²
wt/ft of two ∡ = 11.8 lb/lin ft

$f_b = \frac{M}{S} = 55815/1.6 = 34{,}884 \text{ PSI}$

$\boxed{\text{USE } 3 \times 2 \times 3/8 \text{ PER AISC PG 1-69}}$

PANEL SIZING

CHECKING THE PANEL FOR MEMBRANE STRESSES,

$a/b = 1.0$

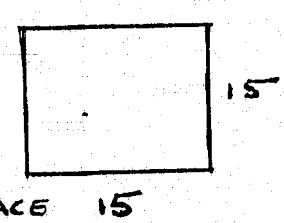

ALL EDGES SUPPORTED WITH
UNIFORM LOADING OVER ENTIRE SURFACE

$K = .044$
$K_1 = .29$ } REF STRESS NOTES,

$\text{STRESS @ CENTER} = K_1 \frac{W}{t^2}$

$W = 14.7 \times 15 \times (15)^2$
$W = 4961 \text{ LBS}$

$\text{"} = 16 \text{ KSI} = \frac{.29 \times 4961}{t^2}$

$t = \left(\frac{.29 \times 4961}{16000}\right)^{1/2} = .30$ inches

THIS THICKNESS IS NOT ACCEPTABLE

PANEL SIZING CONT'D

USING $a/b = 15/10 = 1.5$

$$K = .084$$
$$K_1 = .49$$

$$W = 14.7 \times 1.5 \times 10 \times 15 = 3262 \text{ LBS}$$

$$t = \left[\frac{.49 \times 3262}{16000}\right]^{1/2} = .316 \text{ in}$$

THIS THICKNESS IS STILL TOO LARGE
WILL USE 2' MAJOR FRAMES WITH LIGHT
INTERCOSTALS. THEREFORE TRY PANEL OF
10" x 10"

$$K = .044$$
$$K_1 = .29$$

$$t = \left[\frac{.29 \times 14.7 \times 1.5 \times 100}{16000}\right]^{\frac{1}{2}}$$

$$t = .199 \text{ in}$$

TRYING $10 \times 7.5 \Rightarrow a/b = 10/7.5 = 1.33$

$$K_1 = .42$$

$$t = \left[\frac{.42 \times 14.7 \times 1.5 \times 10 \times 7.5}{16000}\right]^{\frac{1}{2}}$$

$$t = .208 \text{ inches.}$$

TRYING $7.5 \times 7.5 \quad a/b = 1$

$$K_1 = .29$$

$$t = \left[\frac{.29 \times 14.7 \times 1.5 \times 7.5 \times 7.5}{16000}\right]^{\frac{1}{2}} = .1499 \text{ inches}$$

SIZING OF INTERCOSTALS

$$AREA = (7.5 \times 7.5)/2 = 28.125\ in^2$$

$$W = 14.7 \times 1.5 \times 28.125 = 620\ LBS$$

$$MOMENT = \frac{620}{2} \times \frac{7.5}{2} = 1163\ in\text{-}Lbs.$$

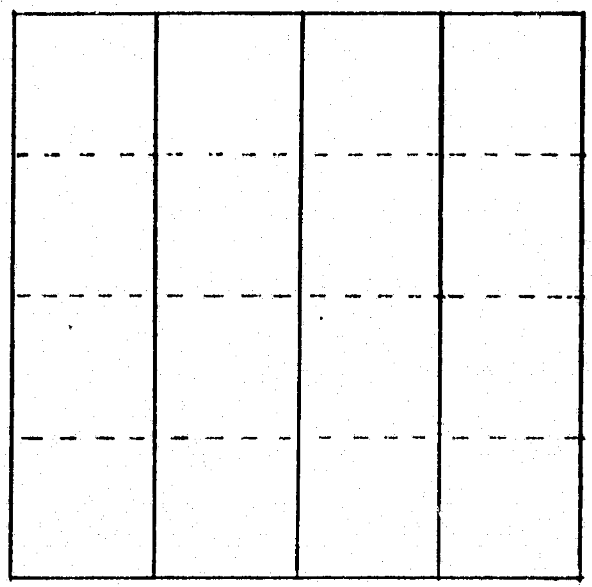

USING $1\frac{3}{4} \times 1\frac{1}{4} \times \frac{1}{8}$ ANGLE

$$f_b = \frac{M}{S} = 16000\ PSI = F_c$$

$$S = 1163/16000 = .073$$

S FOR ABOVE ANGLE IS .094

CHECKING FOR LATERAL STABILITY OF THE ANGLE

$$c = P_{cr}/P_e = 1 \ ; \ 1/\sqrt{c} = 1$$

$$\rho = \sqrt{I/A} \qquad I = \frac{.125(1.75)^3}{12}$$

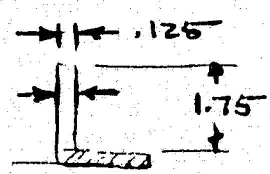

$$A = .125(1.75)$$

$$I/A = \frac{.056}{.219} = .255$$

$$\rho = .504$$

LATERAL STABILITY CHECK CONT'D

$$L' = L/\sqrt{c} = L$$

$$\frac{L'}{\rho} = \frac{L}{\rho} = \frac{1.75}{.504} = 3.47 \approx 3.5$$

$$F_c = \frac{\pi^2 E}{(L/\rho \times \sqrt{c})^2} = \frac{\pi^2 \times 29 \times 10^6}{(3.5)^2} = \underline{\underline{\text{LARGE}}}$$

FROM STRESS NOTES $F_c \approx F_{cy}$ MAT'L $= 60\text{KSI}$

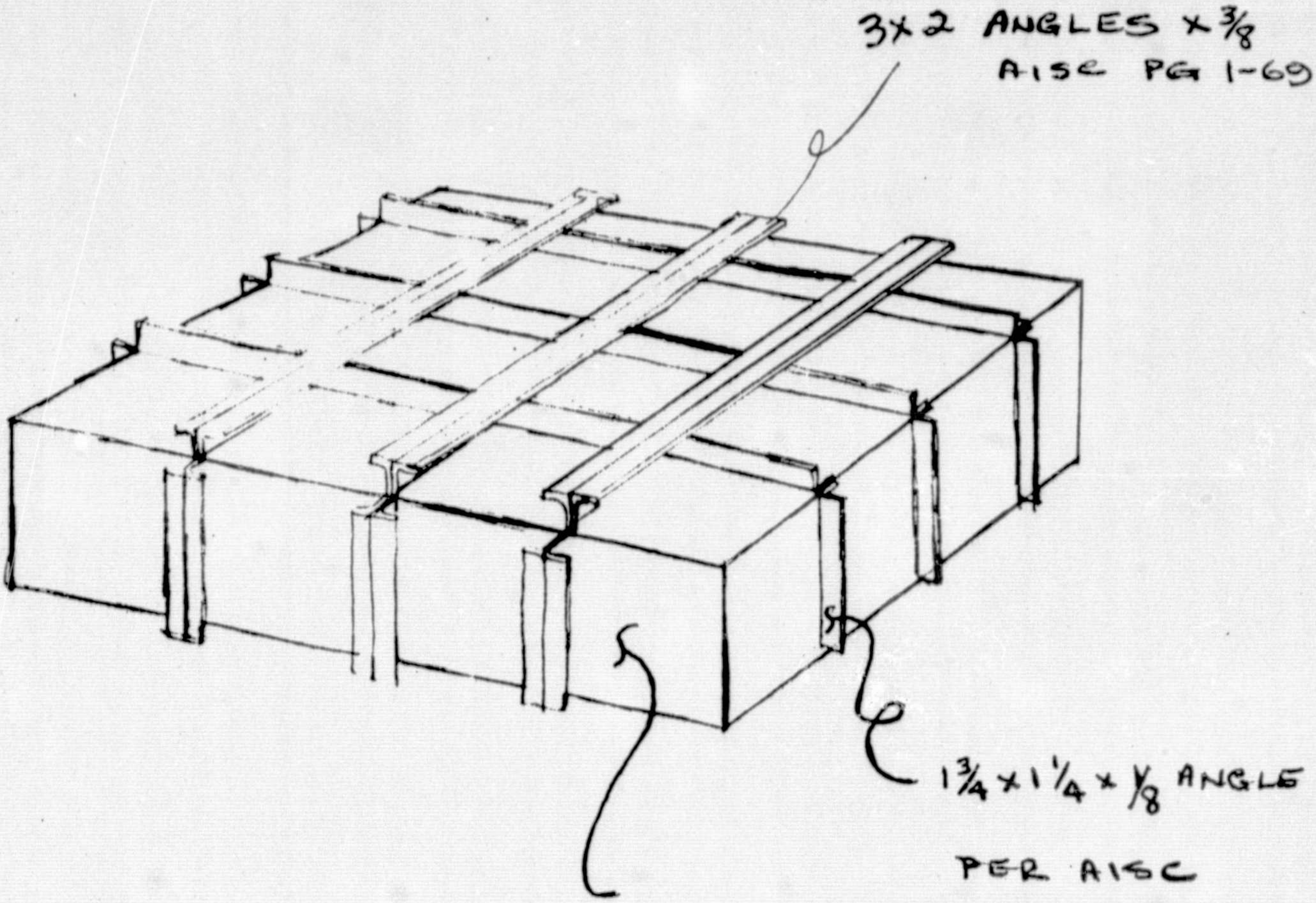

PLATE t = .15 INCHES

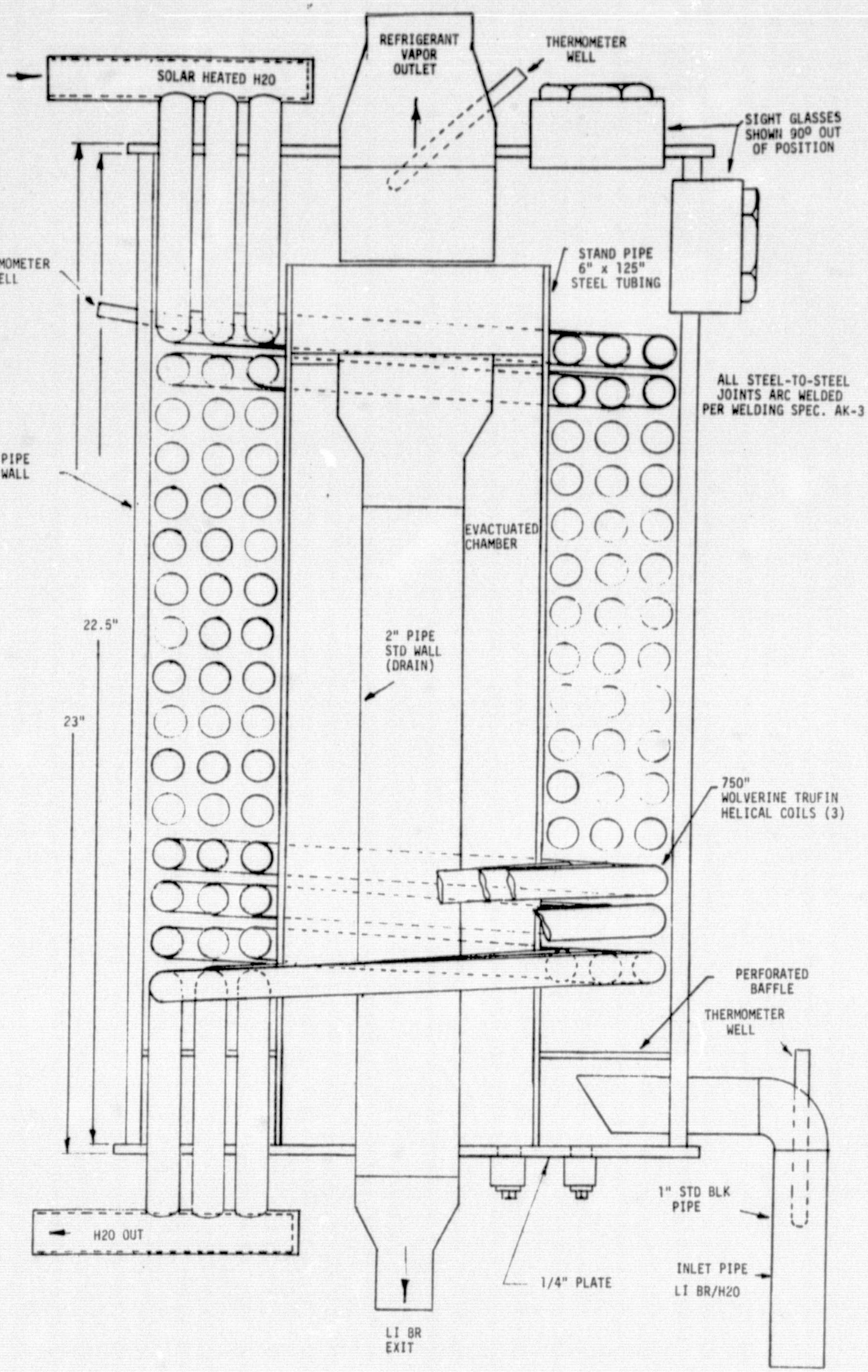

CHRYSLER LOW TEMPERATURE LITHIUM BROMIDE ABSORPTION GENERATOR

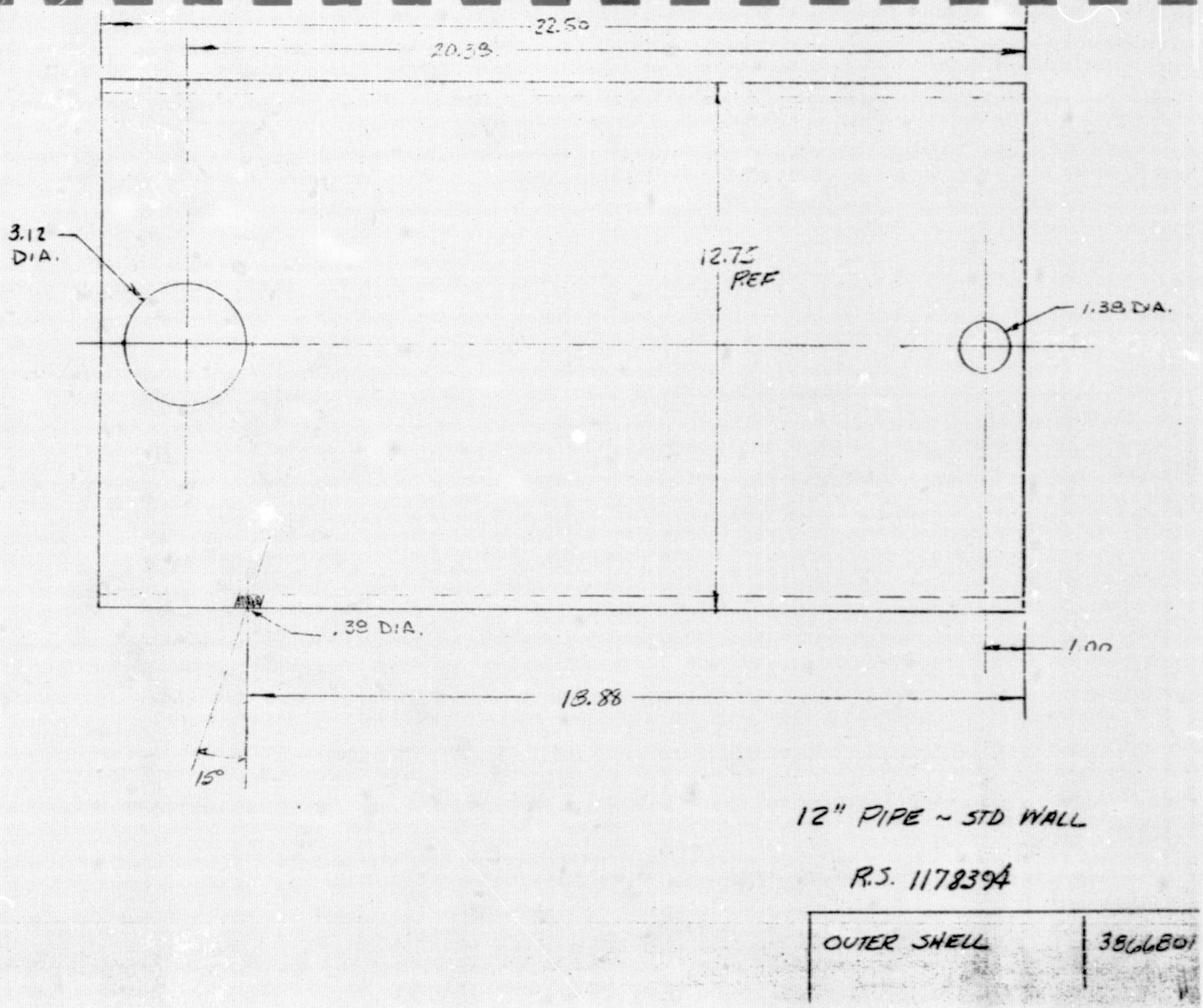
22.50
20.38
3.12
DIA.
12.75
REF
1.38 DIA.
.38 DIA.
1.00
18.88
15°
12" PIPE ~ STD WALL
R.S. 1178394
OUTER SHELL
3866801

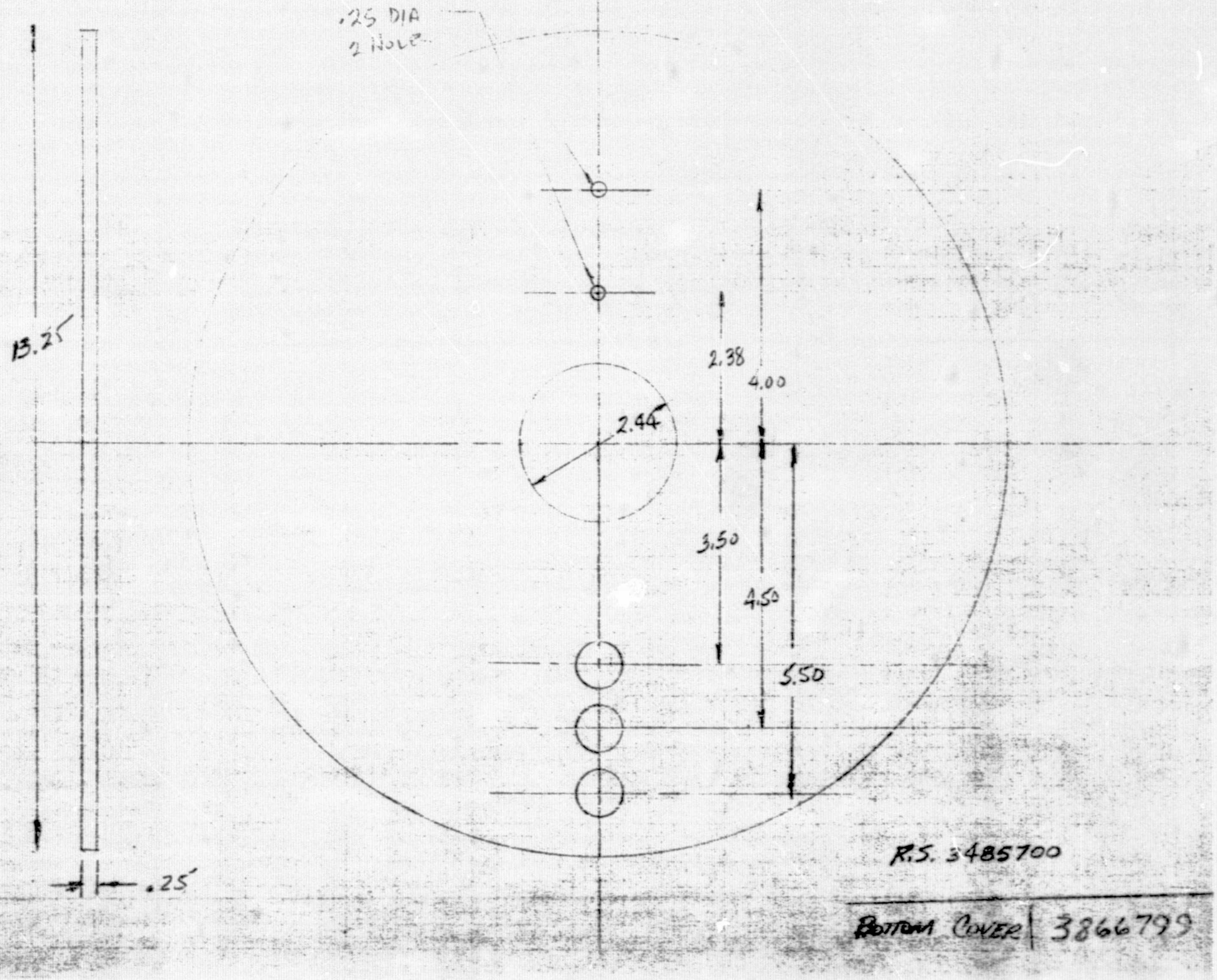
.25 DIA
2 HOLE
13.25
.25
2.44
2.38
4.00
3.50
4.50
5.50
R.S. 3485700
BOTTOM COVER
3866799

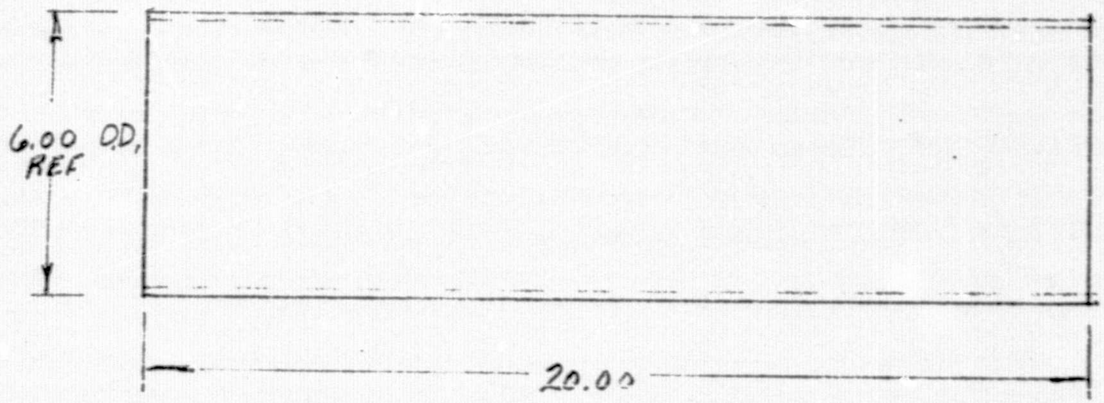

ENDS TO BE SQUARE
WITH AXIS ± 15 MIN

6" O.D. STEEL TUBING X .125 WALL
(ROUND MECHANICAL TUBING)

STANDPIPE	3866798

2 REQ'D

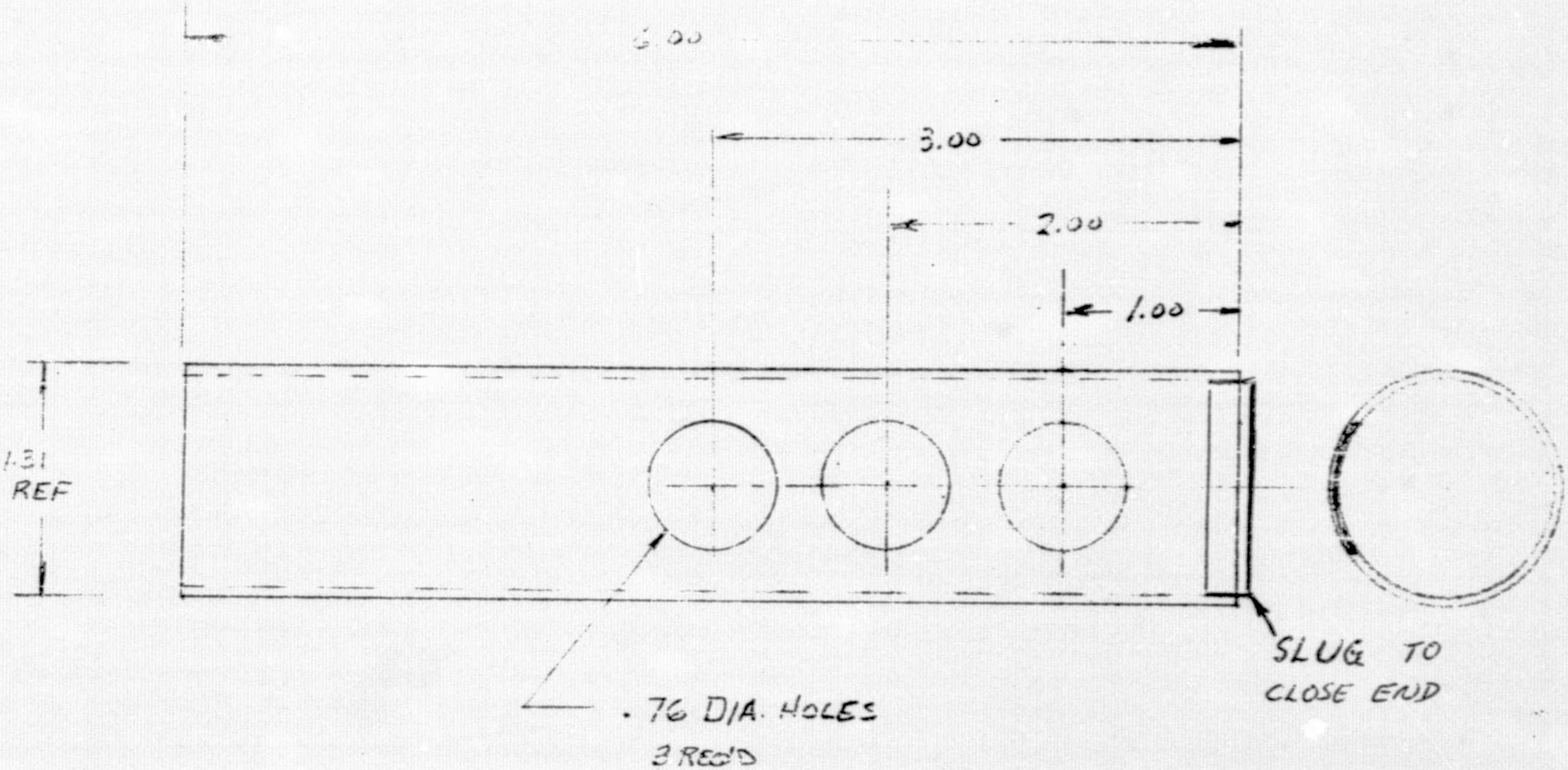

1" BLK IRON PIPE
STD WALL (SCH. 40)

MAKE FROM 3866804

HEADER.	3866803

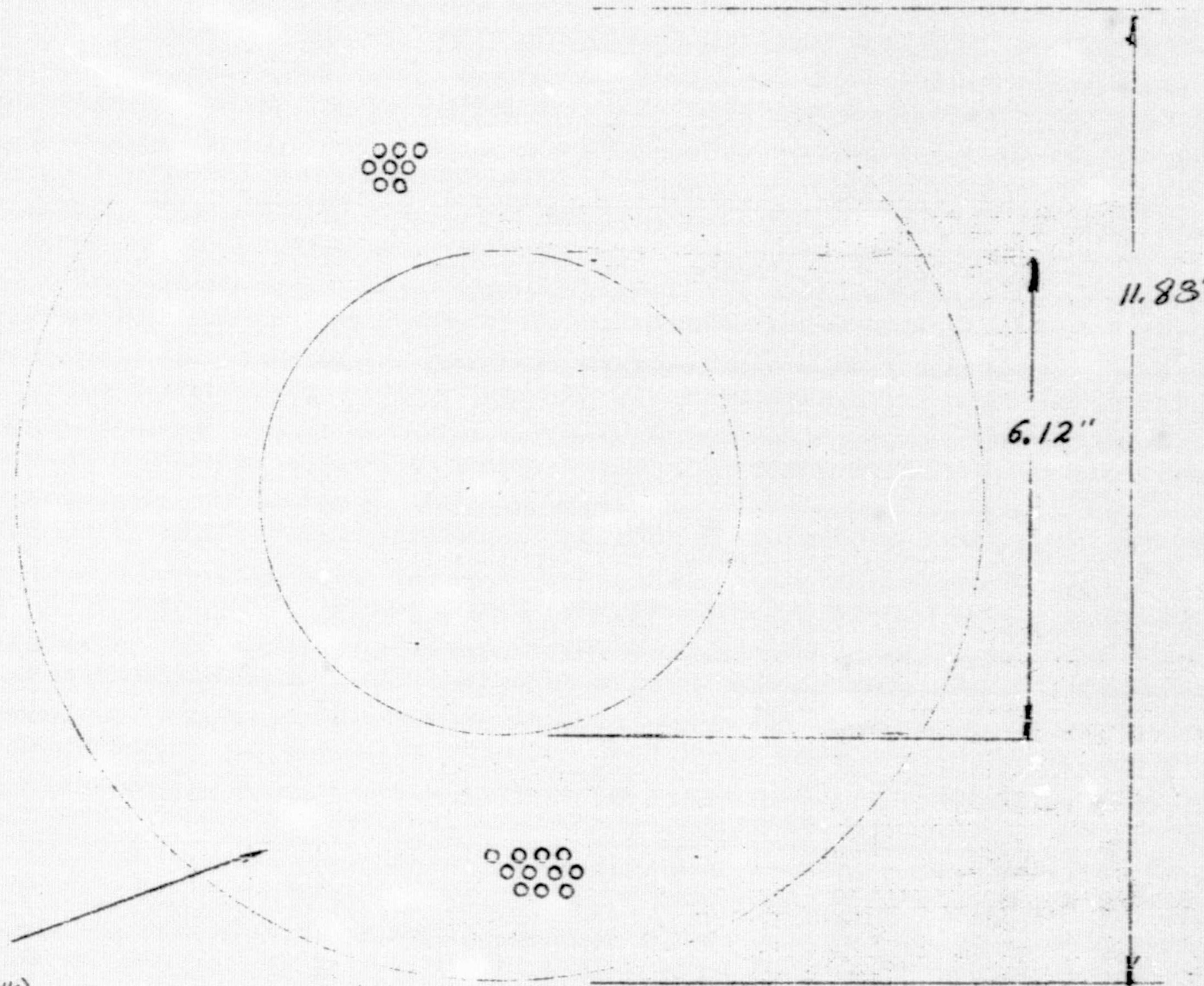

PERFORATED
METAL (1/8 THK)
3/32 DIA. HOLES STAGGERED ~ 5/16 CENTERS
33% OPEN

MAKE FROM 1178285

PERFORATED BAFFLE	3366790

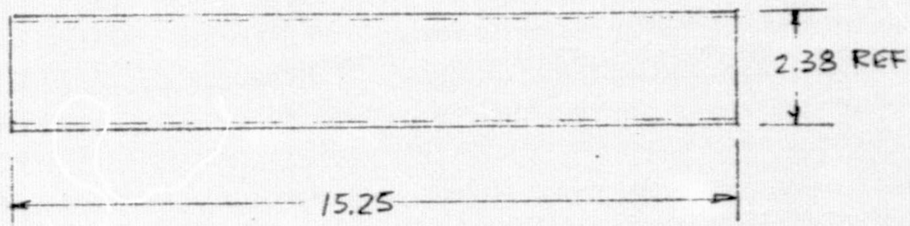

2" BLK. IRON PIPE
STD WALL (SCH. 40)

PIPE- SOLUTION OUTLET	3866797

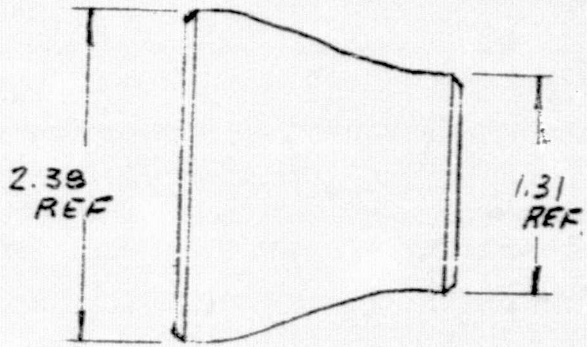

2x1 STEEL PIPE REDUCER
CONCENTRIC
STD. WEIGHT.

REF. SOURCE: TUBE TURNS
CAT. NO. 90

REDUCER 2x1	3866805

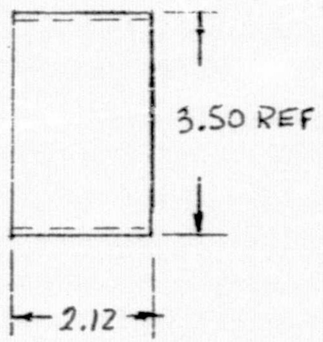

3" BLK IRON PIPE
STD WALL (SCH. 40)

PIPE-EXTENSION VAPOR OUT	386679.

3 REQ'D

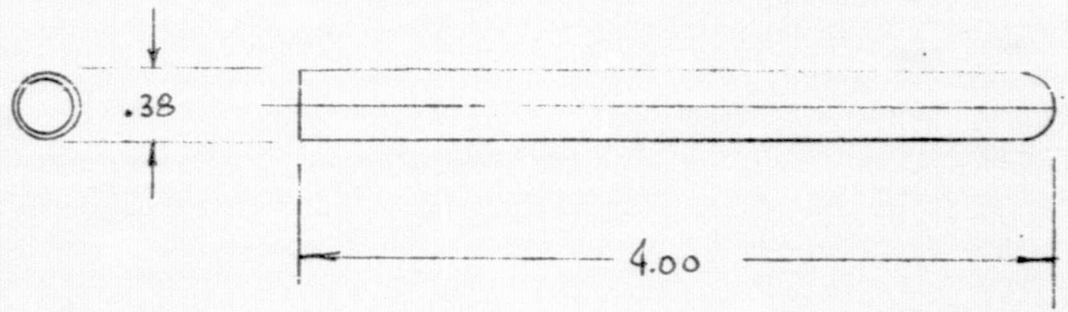

SPUN & BRAZED
TO SEAL END

MATERIAL: 3/8 x .049 BUNDY WELD
R.S. 2818829

THERMOMETER WELL	3866795

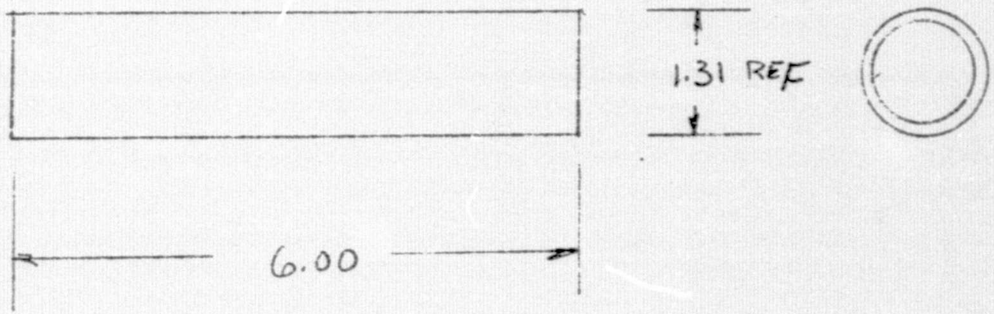

1" BLK IRON PIPE
STD. WALL (SCH. 40)

R.S. 2022050

1" PIPE x 6" LONG.	3866804

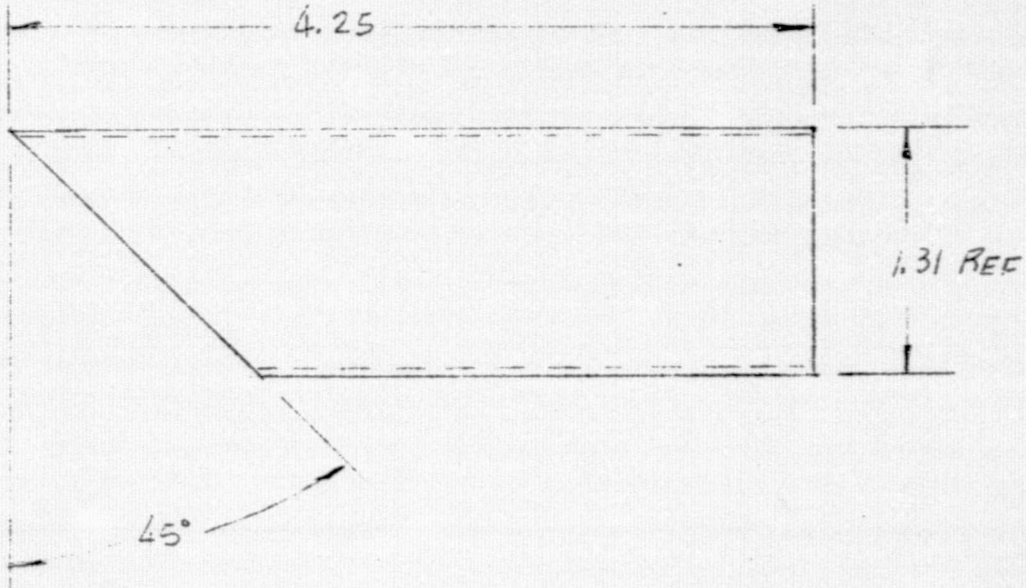

1" STD BLK PIPE
(SCH. 40)

R.S. 2022050

INLET PIPE	3866794

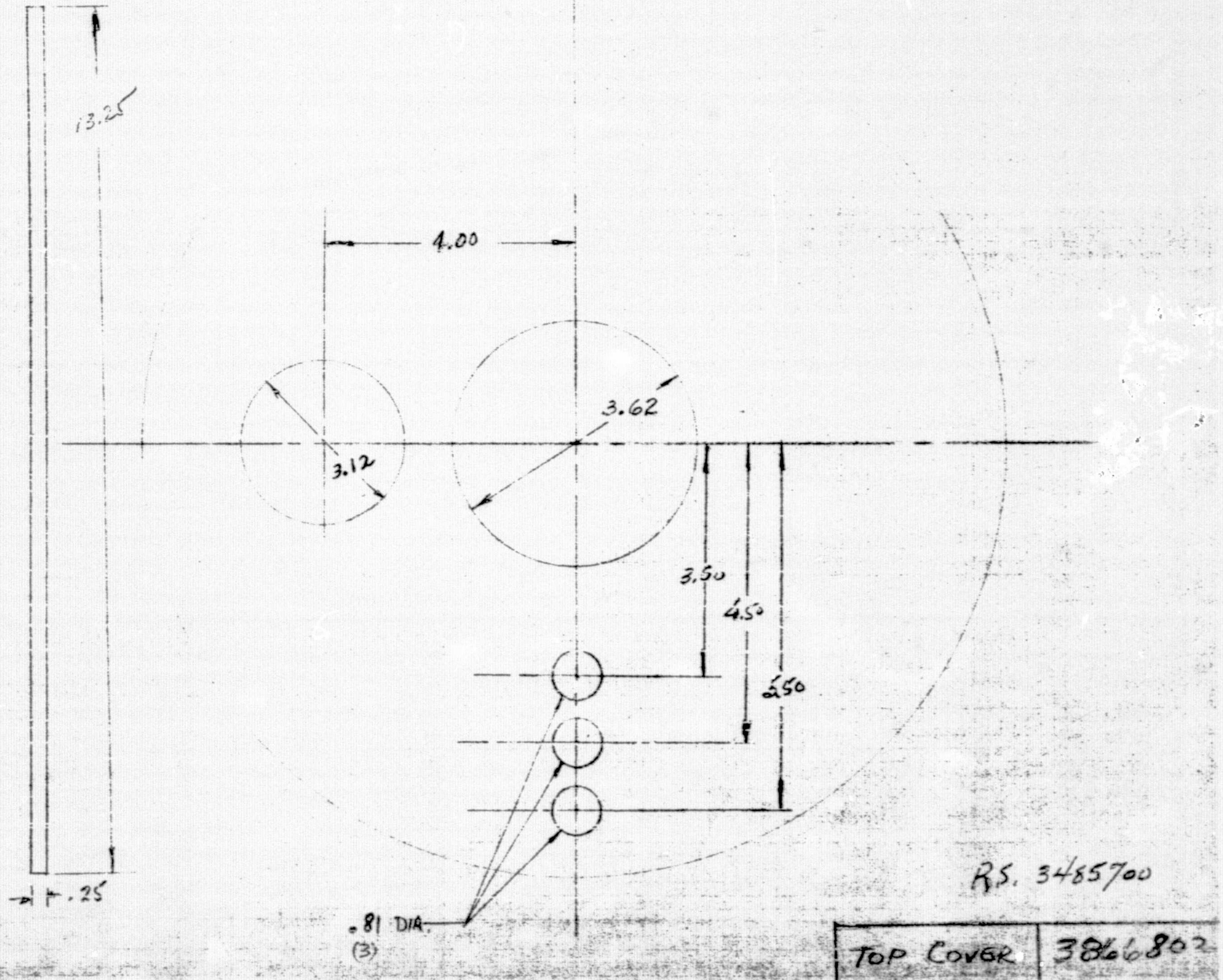
13.25
4.00
3.62
3.12
3.50
4.50
5.50
.25
.81 DIA.
(3)
R.S. 3485700
TOP COVER
3866802

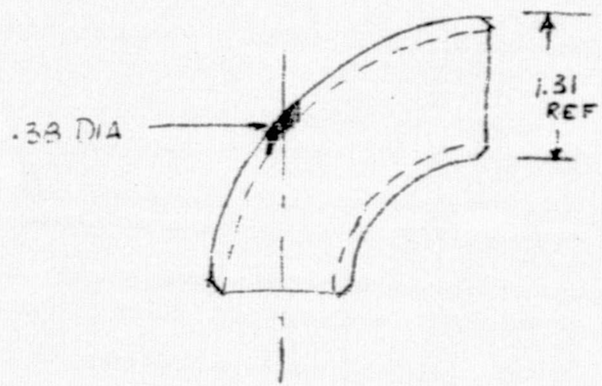

90° STEEL ELBOW

1" PIPE SIZE - STD WT.

REF. SOURCE: TURN TURNS PART NO. 3 OR EQUIV.

ELBOW - 1"	3866806

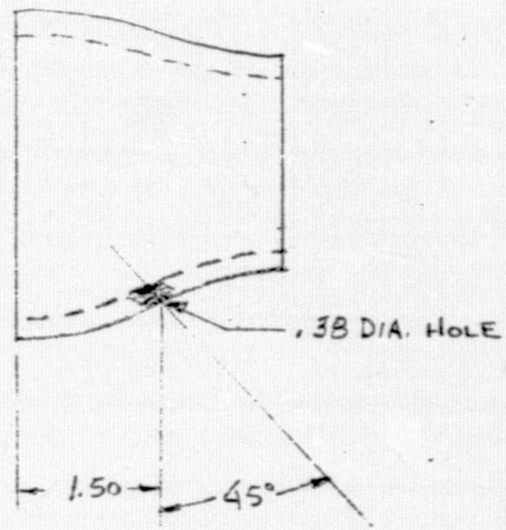

3x2 STEEL REDUCER
MAKE FROM 3866807

REDUCER - GAS OUTLET	3866793

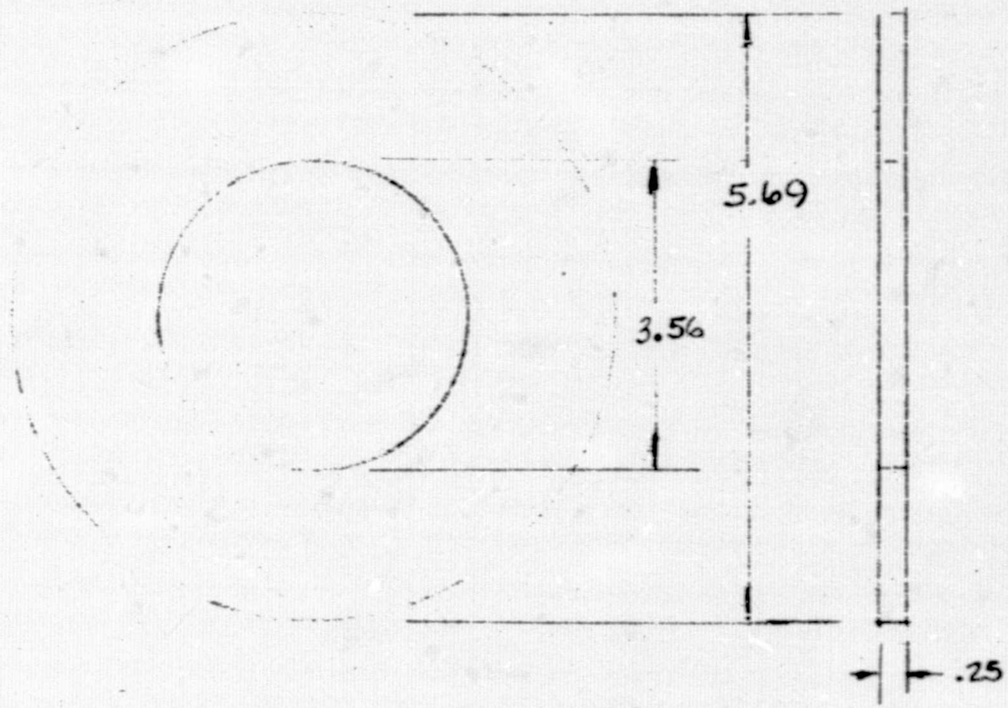

H.R. STEEL (MS 66)
R.S. 1178550

STANDPIPE WASHER	3866789

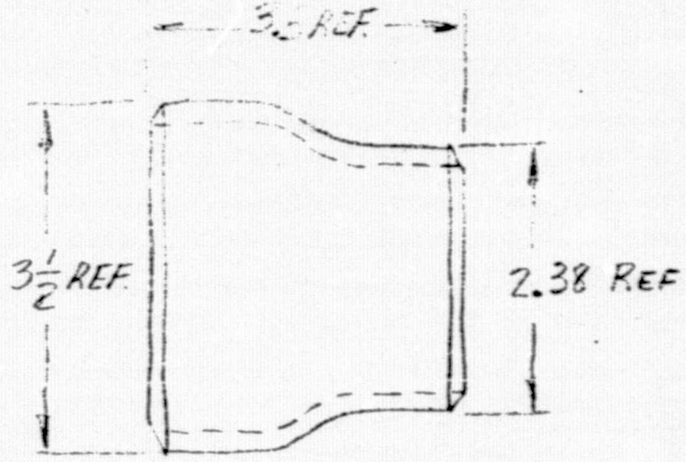

3 x 2 STEEL PIPE REDUCER

STD. WEIGHT

REF SOURCE: TUBE TURNS
PART NO. 90

REDUCER 3 x 2	3866807

TOLERANCES, UNLESS OTHERWISE SPECIFIED:

FRACTIONS ±   DECIMALS ±

ANGLES ±   DO NOT SCALE PRINT

3525301

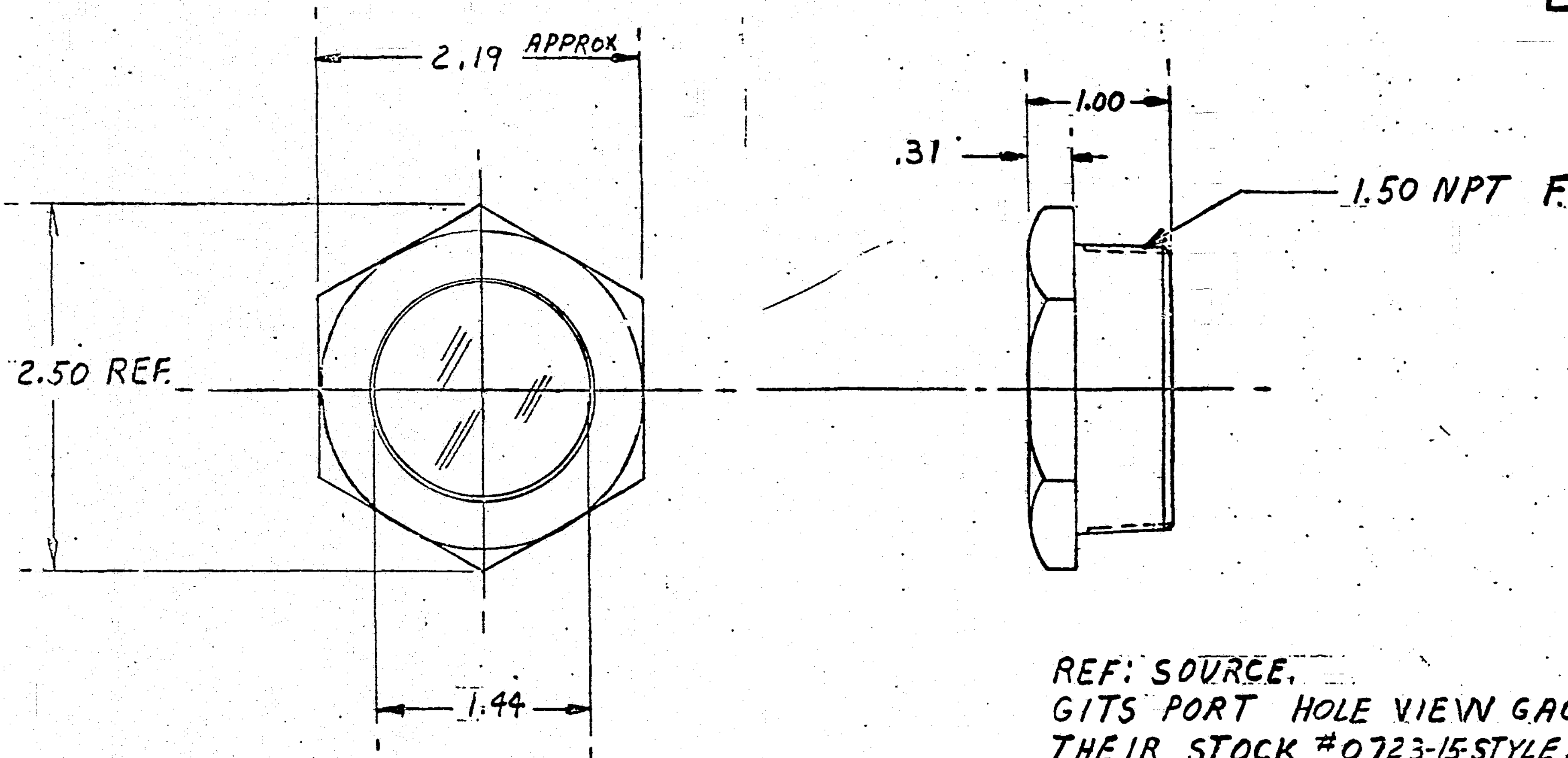

REF: SOURCE.
GITS PORT HOLE VIEW GAGE
THEIR STOCK #0723-15-STYLE BW
50

LET.	REVISION	JOB NO.	DATE	DR.	CK.	R.	LET	REVISION	JOB NO.	DATE	DR.	CK.	R.
								RELEASED FOR PROD.	3364	1/9/70	[signature]		

DATE DWN.	DWN. BY	CHKD. BY	DSGN. APPR.	LAB. APPR.	MTL. APPR.
10-30-69	TB	JMS	[signature] 1-8-70		

AIRTEMP DIVISION — CHRYSLER CORPORATION

SCALE ~

MTL. ~ ANAL. ~ PROC. ~

NAME: SIGHTGLASS 1½ NPT

PART NO. 3525301

84-203-8112

DAYTON, OHIO 43404

(6)

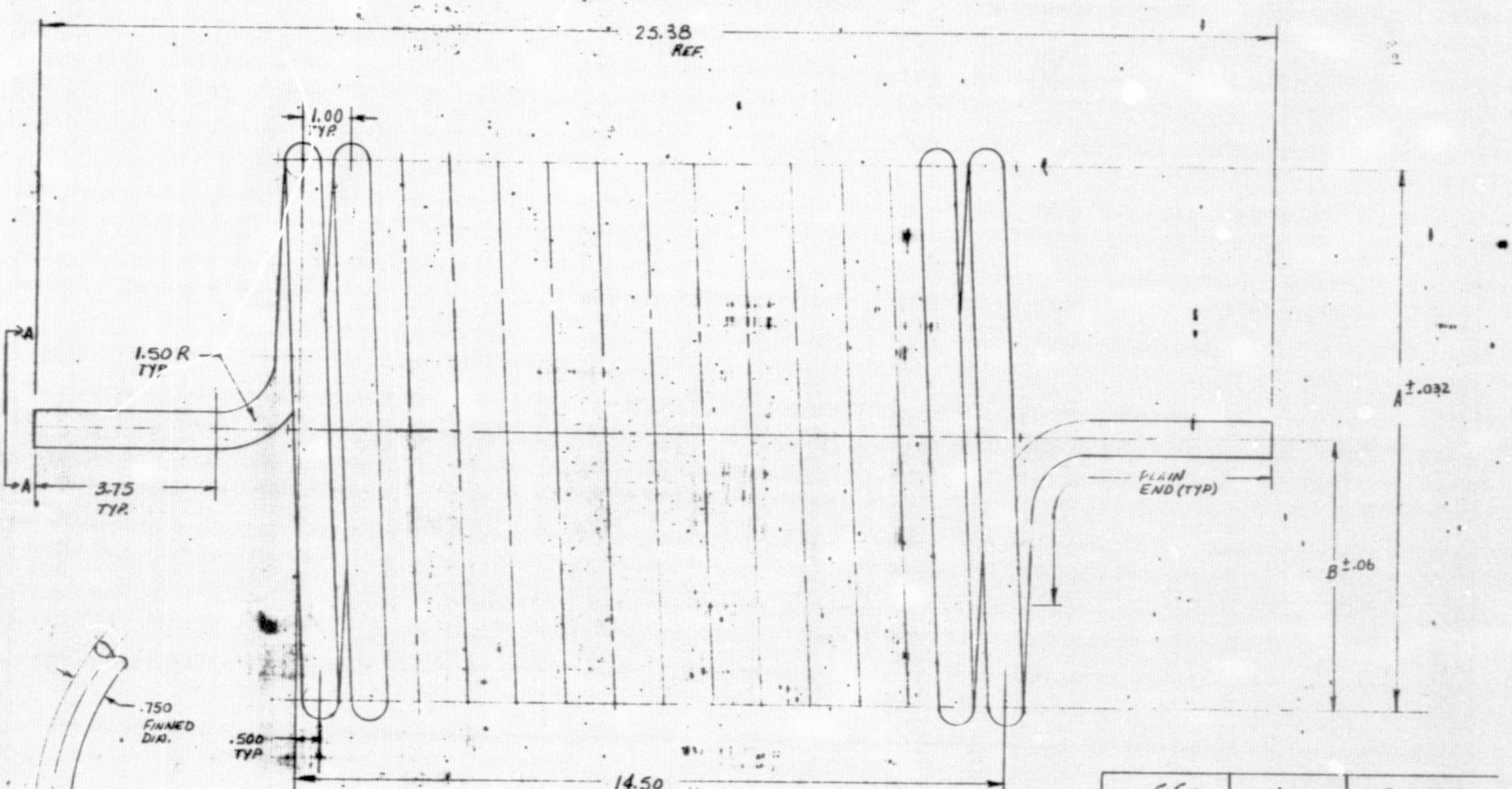

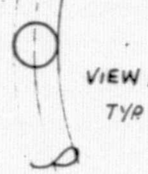

VIEW A-A
TYP -(BOTH ENDS)

MATERIAL: WOLVERINE TRUFIN (S/T)
19 FINS/IN.
90/10 CU-NI
CAT. NO: 60-195035-53

5.50	11.00	3865939
4.50	9.00	3865938
3.50	7.00	3865937
B	A	PART. NO.

APPENDIX G

GENERATOR LOCATION ANALYSIS

Reynolds Number, Rey $= \dfrac{4\mu}{\pi D \mu}$

Where W = Flow Rate
D = Diameter, Internal
μ = Viscosity

$W = \dfrac{Q}{h_{fg}}$ where h_{fg} = Refrigerant Latent Heat
Q = Heat load

$$W = \frac{36000}{1065} \frac{BTU}{HR} \frac{LBM}{BTU} \times \frac{HR}{3600\ Sec}$$

$W = 0.0093897$ LBM/Sec

From Keenan & Keyes, Thermodynamic Properties of Steam:

Viscosity μ (@ 32°F) $= 2.0 \times 10^{-7}$ LBF-SEC/FT^2
(@200°F) $= 2.7 \times 10^{-7}$

Interpolating @ 170°F, $= 2.575 \times 10^{-7}$ LBF SEC/FT^2
$= 8.29 \times 10^{-6}$ LBM/FT-SEC

For D = 2 inch

$$Rey = \frac{4}{\pi} \times \frac{12}{2} \times \frac{0.0093897}{8.29 \times 10^{-6}}$$

Rey = 8653.

PLAN VIEW OF ABSORPTION MACHINE SHOWING GENERATOR LOCATION CANDIDATES

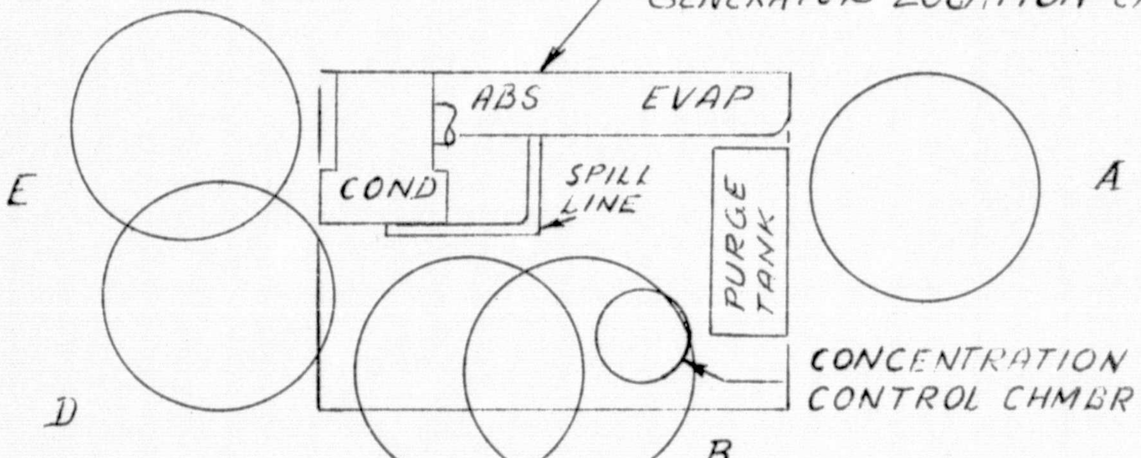

From Ref. 3, p. A-24.

For Rey = 8653, f = 0.032 where f = friction factor.

Pressure drop in vapor line

$$\Delta P = \frac{\rho f \; L \; V^2}{144 \; D \; 2g} \; \text{PSI X} \; 51.75 \; \frac{\text{mm } H_g}{\text{PSI}}$$

Where ρ = Density of vapor
L = Length of Flow
V = Velocity of flow
g = Gravitational constant

Since $V = \frac{W}{\rho A}$ and $V = \frac{Wv}{A}$ where v = specific volume,

then $\Delta P = \frac{51.715}{144 \text{ X } 2g} \frac{fL}{D} \frac{W^2 v}{D^4} \frac{16}{\pi^2}$

From Keenan & Keyes, Table 3 - Superheated Vapor Specific Volume:

psia	160	180°F
1	368.6	380.6
2	184.01	190.04

By linear interpolation:

v (@ 1.5 psia, 170°F) = 280.8 FT^3/LBM

For D = 2/12 FT,

ΔP = 0.055692 L mm Hg

From Reference 3, p. A-27.

For 90° Bend $\frac{L_B}{D}$ = 12 minimum

From Reference 3, p A-26. Entrance Loss, K = 0.78

Exit Loss K = 1.00

Where $K = f \frac{L}{D}$

Equivalent Length, $L_E = (1.78) \left(\frac{1}{0.032}\right) \left(\frac{2}{12}\right)$

= 9.27 Ft. for entrance and exit.

For each 90° Bend, equivalent length L_B is

$$L_B = 12 \times \frac{2}{12} = 2 \text{ Ft.}$$

Then $\Delta P = 0.055692 (L + 2B + 9.27)$ mm Hg

Where B = Number of bends
L = Length of tube

Gen Posn	No Bends	L*	(L+2B+9.27)	ΔP (mmHg)
A	1	31.6/12	13.9	0.774
B	2	26.0/12	15.4	0.858
C	2	20.4/12	15.0	0.835
D	3	29/12	17.7	0.986
E	3	27/12	17.5	0.976

*Allows for 6 inch riser from Gen. Exit.

Conclusion:

At constant concentration of LiBr, and at generator operating conditions, there is approximately 0.7°F increase in boiling temperature per millimeter of mercury increase.
Therefore, based on the pressure drops estimated above, there is little practical difference among the various possible generator locations.

APPENDIX H

SOLUTION VOLUME

Estimates for the solution-filled components are shown below. They form the basis for the initial charge.

GENERATOR:

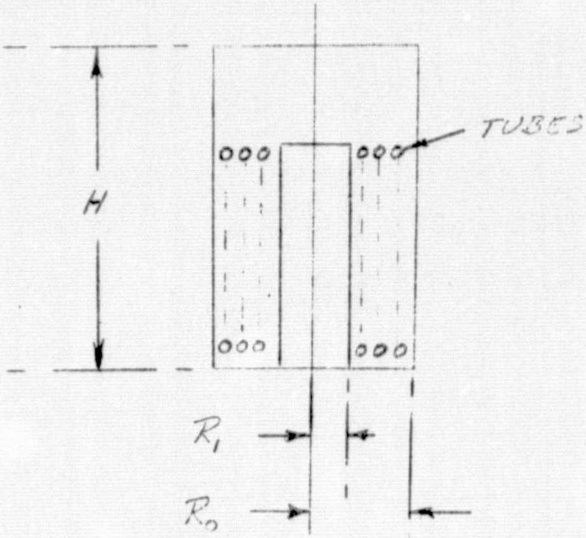

H = (20 in) 50.8 cm
L = (100 ft) 30.48 m
R_o = (6 in) 15.24 cm
R_1 = (3 in) 7.62 cm
R_T = (0.330 in) 0.838 cm

$$V_{GEN} = H\pi(R_o^2 - R_1^2) - V_{Tubes}$$

$$= H\pi(R_o^2 - R_1^2) - \pi R_T^2 L$$

$$V_{GEN} = 21.2\ dm^3\ (5.6\ Gal)$$

LIQUID HEAT EXCHANGER: (consider both shell side and tube side simultaneously)

$$V_{HX} = WT(H_1 + H_2)$$

H_1 = (6 in) 15.24 cm
H_2 = (19 in) 48.26 cm
T = (3 1/4) 8.26 cm
W = (11 in) 27.94 cm

$$V_{HX} = 14.8\ dm^3\ (3.9\ Gal)$$

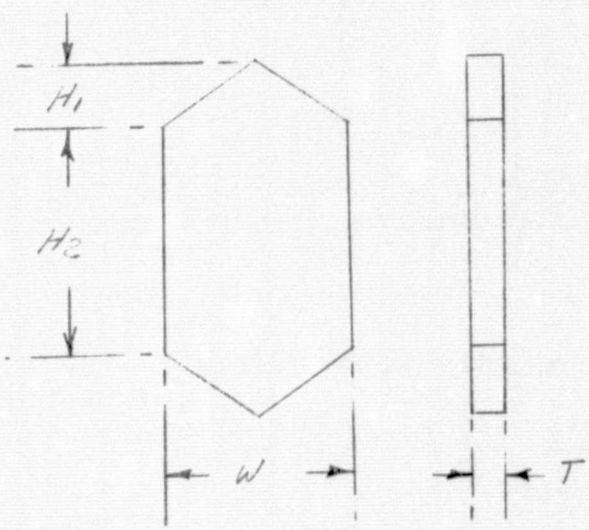

An additional 4.4 dm^3 (1 gal) is allowed for the solution-filled lines and the refrigerant which is accumulated in the condenser and evaporator.

Total Initial Charge: $V_{Total} = 21.2 + 14.8 + 4.4 = 40.4\ dm^3$ (10.6 gal).

APPENDIX I

PHASE II

CALCULATION PROCEDURE

This calculation procedure is to determine the evaporator heat load QEVAP, when the tower heat load QTWR and generator heat load QGEN are known. It is based on having constant ratios for QGEN/QABS and QCOND/QEVAP. Accuracy is verified by calculating an overall heat balance QTWR/(QEVAP + QGEN).

The QGEN/QABS ratio is examined by first writing steady-state heat balances for the absorber, liquid heat exchanger, and generator. Incoming heat or flow is taken to be positive.

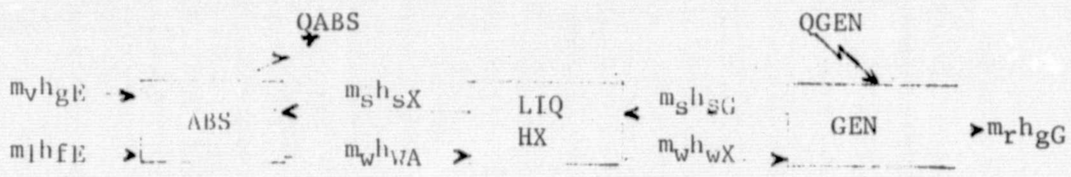

h_{fE}	Enthalpy of liquid leaving the evaporator
h_{gE}	Enthalpy of vapor leaving the evaporator
h_{gG}	Enthalpy of vapor leaving the generator
h_{sG}	Enthalpy of strong absorbent leaving the generator
h_{sX}	Enthalpy of strong absorbent leaving the heat exchanger
h_{wA}	Enthalpy of weak absorbent leaving the absorber
h_{wX}	Enthalpy of weak absorbent leaving the heat exchanger
m_l	Mass Flow, liquid leaving the evaporator
m_r	Mass Flow, refrigerant leaving the generator
m_s	Mass Flow, strong absorbent
m_v	Mass Flow, vapor leaving the evaporator
m_w	Mass Flow, weak absorbent
QABS	Absorber heat load
QGEN	Generator heat load

$\Sigma Q = 0$ for steady state

(1) Absorber: $-QABS - m_w h_{wa} + m_s h_{sX} + m_v h_{gE} + m_l h_{fE} = 0$

(2) Liq HX: $m_w h_{wA} - m_w h_{wX} + m_s h_{sG} - m_s h_{sX} = 0$

(3) Generator: $QGEN + m_w h_{wX} - m_s h_{sG} - m_r h_{gG} = 0$

From (1) and (3):

(4) $$\frac{QGEN}{QABS} = \frac{m_s h_{sG} + m_r h_{gG} - m_w h_{wX}}{m_s h_{sX} + m_v h_{gE} + m_l h_{fE} - m_w h_{wA}}$$

From (2): $m_s h_{sG} - m_w h_{wX} = m_s h_{sX} - m_w h_{wA}$

Combining with (4) leads to:

$$\frac{QGEN}{QABS} = \frac{m_s h_{sX} - m_w h_{wA}' + m_r h_{gG}}{m_s h_{sX} - m_w h_{wA} + m_v h_{gE} + m_1 h_{fE}}$$

In the range of interest, consider h_{gG} for superheated vapor. The Steam Tables, Keenan and Keyes, 1953, Table 3, show that "h" is approximately independent of pressure in the 1 to 2 psia range. The Mollier Chart shows the following data:

$$\begin{aligned} h\ (200°F,\ 1.2\ psia) &= 1150\ BTU/Lb \\ h\ (180°F,\ 1.2\ psia) &= \underline{1141.5}\ BTU/Lb \\ &\quad\ 8.5\ BTU/Lb < 0.75\%\ \text{difference} \end{aligned}$$

Similarly for saturated vapor in the 40 to 55°F range for h_{gE}:

$$\begin{aligned} h\ (\text{Sat. Vapor, } 40°F) &= 1079.3\ BTU/Lb \\ h\ (\text{Sat. Vapor, } 55°F) &= \underline{1085.8}\ BTU/Lb \\ &\quad\ -6.5\ BTU/Lb = 0.6\%\ \text{difference} \end{aligned}$$

Furthermore, since m_1 is low, and h_{fE} is of the order of 10 to 25 BTU/Lb, QGEN/QABS can be considered to be constant.

The QGEN/QABS ratio was calculated from test data to be 1.05. Thus QABS=QGEN/1.05, where QGEN is calculated from the measured hot water flow rate and inlet and outlet water temperatures. Then the condenser heat load QCOND is calculated from QCOND= QTWR-QABS, and the evaporator heat load $QEVAP=\frac{QCOND}{1.05}$ which is an approximation based on low spillage from the evaporator.

Finally, the overall heat balance QTWR/(QEVAP + QGEN) is calculated as an overall check. QTWR and QGEN are measured and calculated directly, whereas only QEVAP is calculated from the above approximations. The overall heat balance differed from unity by no more than 3% in all cases by utilizing this procedure, which indicates good accuracy.

APPENDIX J

SEPARATOR DRAWINGS

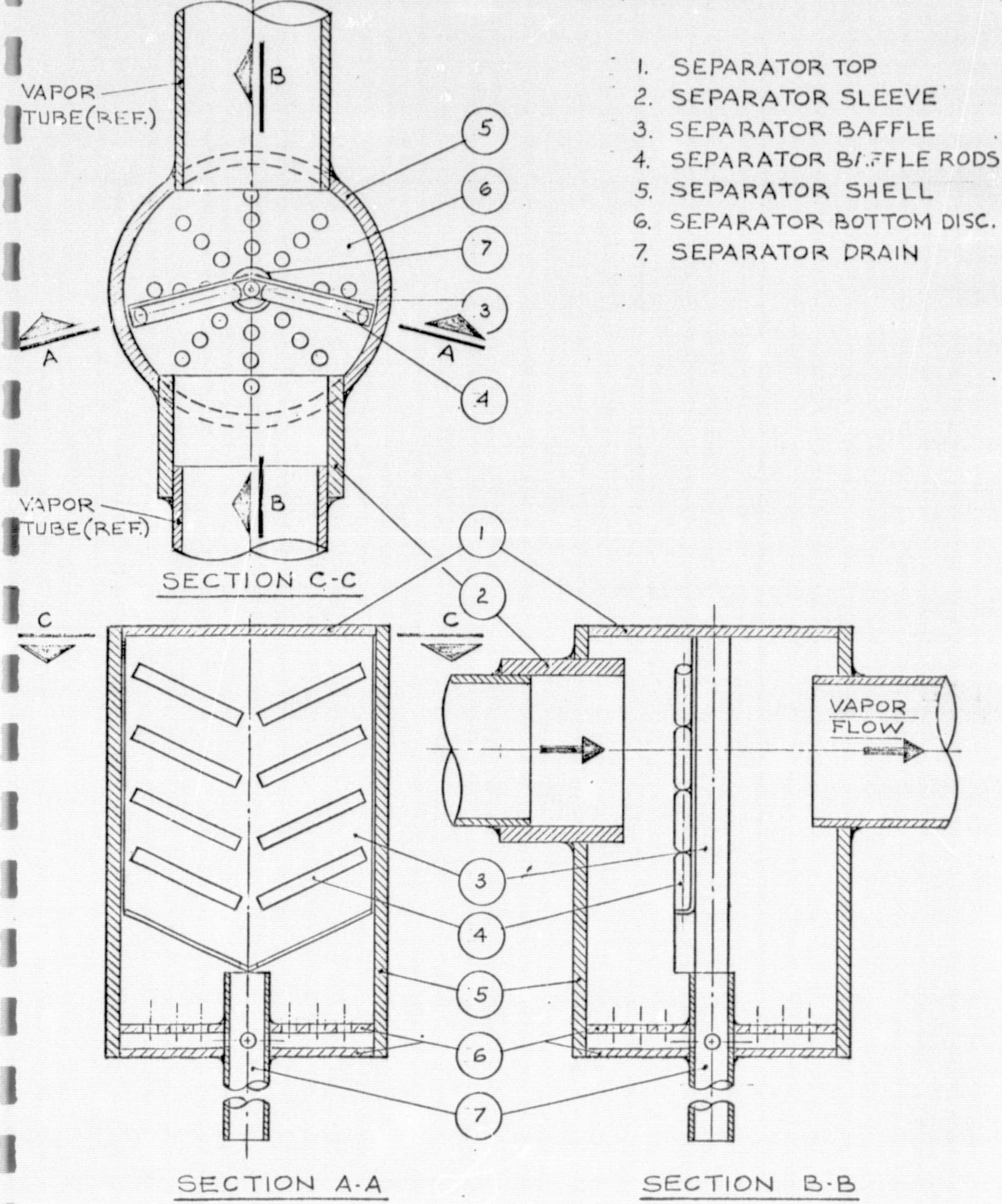
1. SEPARATOR TOP
2. SEPARATOR SLEEVE
3. SEPARATOR BAFFLE
4. SEPARATOR BAFFLE RODS
5. SEPARATOR SHELL
6. SEPARATOR BOTTOM DISC.
7. SEPARATOR DRAIN
VAPOR TUBE (REF.)
VAPOR TUBE (REF.)
B
B
A
A
C
C
1
2
3
4
5
6
7
VAPOR FLOW
SECTION C-C
SECTION A-A
SECTION B-B

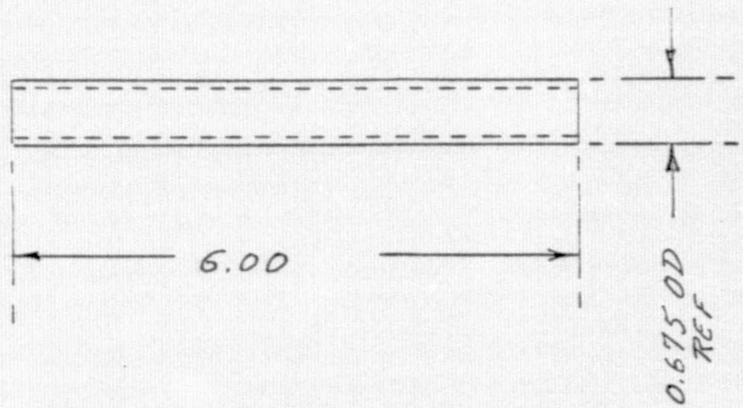

3/8" PIPE STD WALL - BLK IRON

ENDS TO BE DEBURRED AND SQUARE WITH AXIS ± 15 MIN

HALF SCALE

ONE REQUIRED

SEPARATOR DRAIN

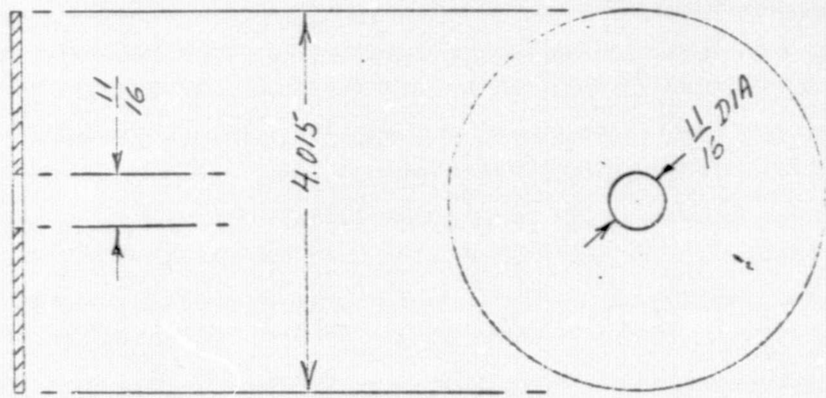

12 GUAGE SHEET STEEL
TWO REQUIRED
HALF SCALE

SEPARATOR BOTTOM DISCS

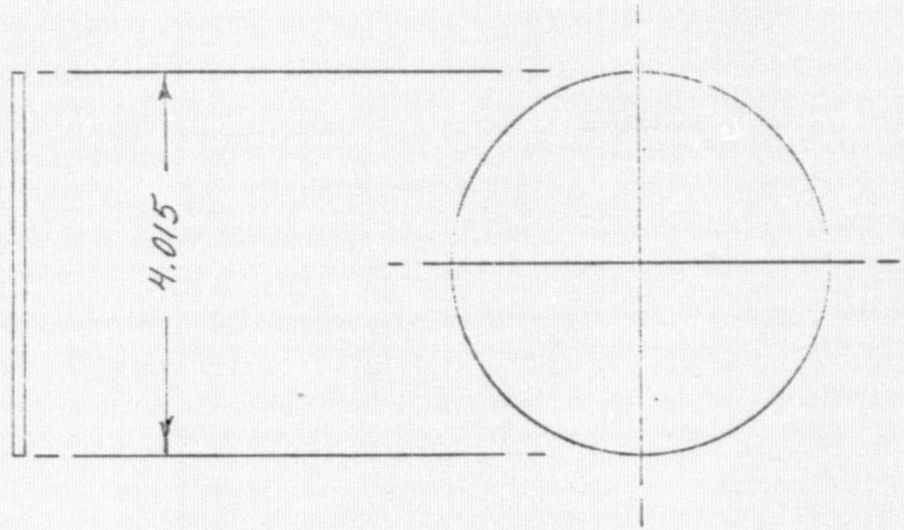

12 GUAGE SHEET STEEL
ONE REQUIRED
HALF SCALE

SEPARATOR TOP.

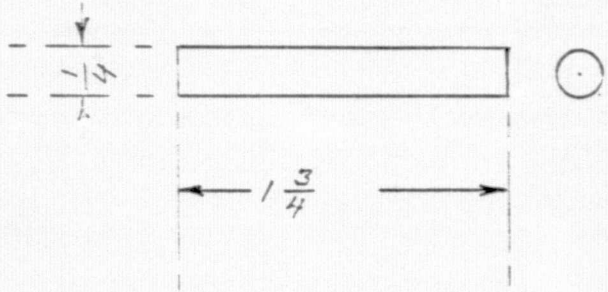

1/4" SOLID STEEL ROD (OR TUBING)
FULL SCALE
EIGHT REQUIRED

SEPARATOR BAFFLE RODS

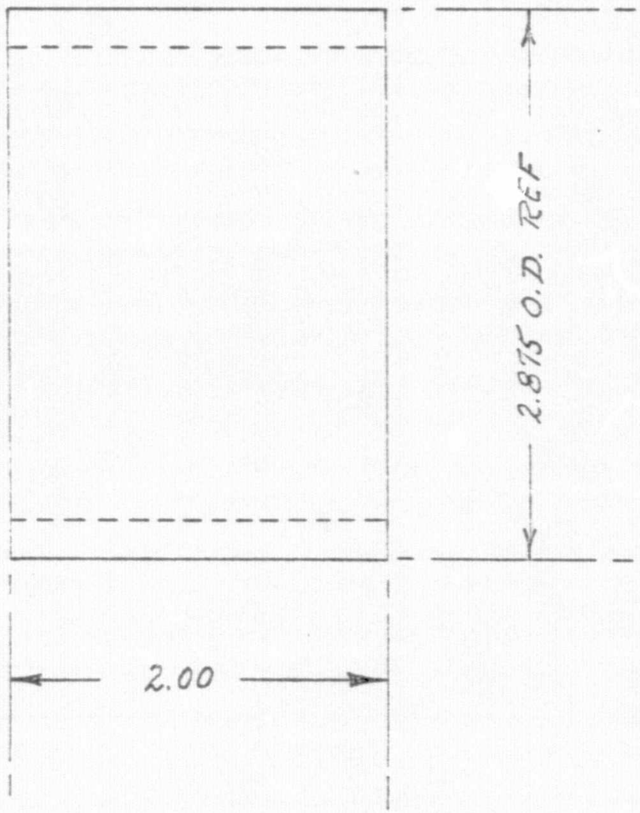

$2\frac{1}{2}$" PIPE STD WALL - BLK IRON
ENDS TO BE SQUARE
WITH AXIS ± 15 MIN
FULL SCALE
ONE REQ'D

SEPARATOR SLEEVE

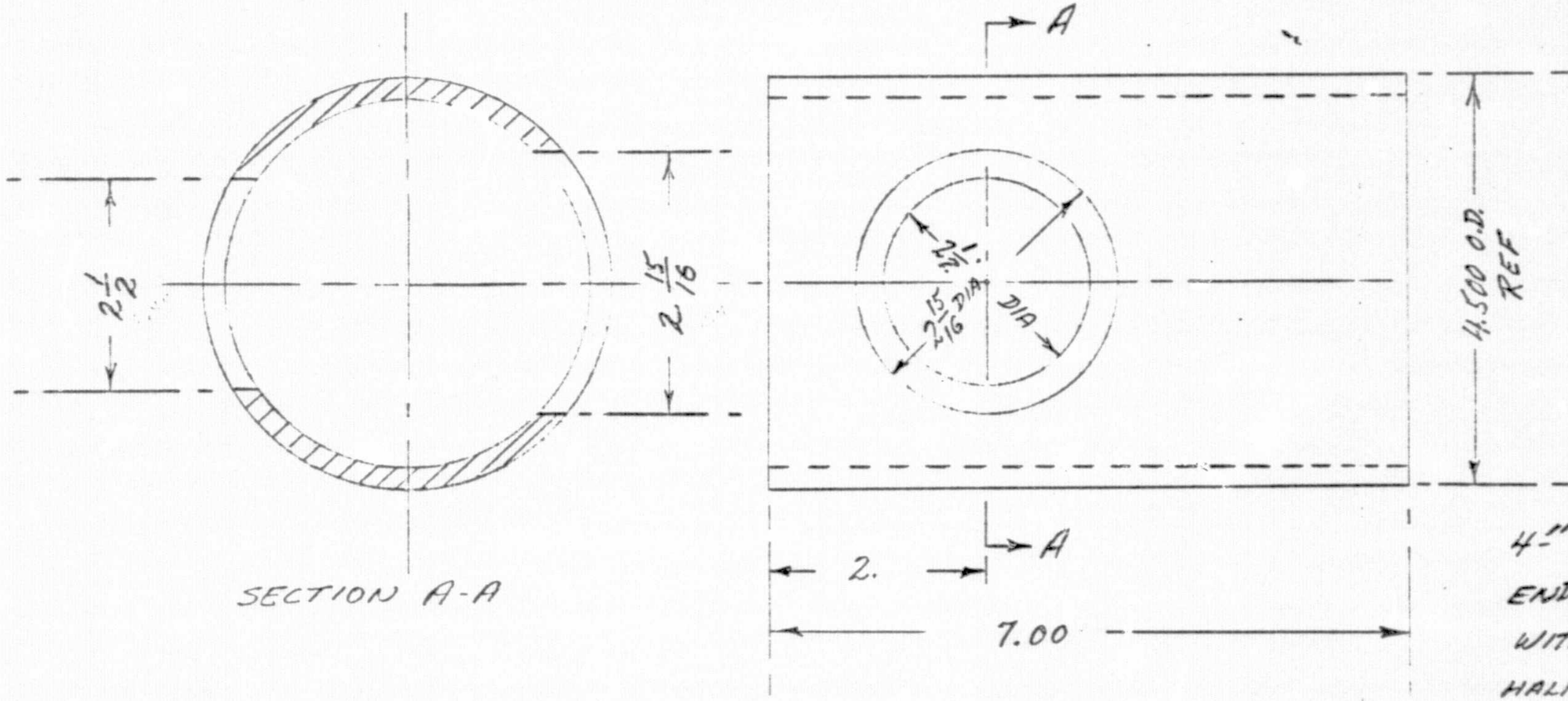

4" PIPE STD WT
ENDS TO BE SQUA
WITH AXIS ±15 MI
HALF SCALE

SEPARATOR SHELL - ONE REQD
D.J.L. 1-7-76

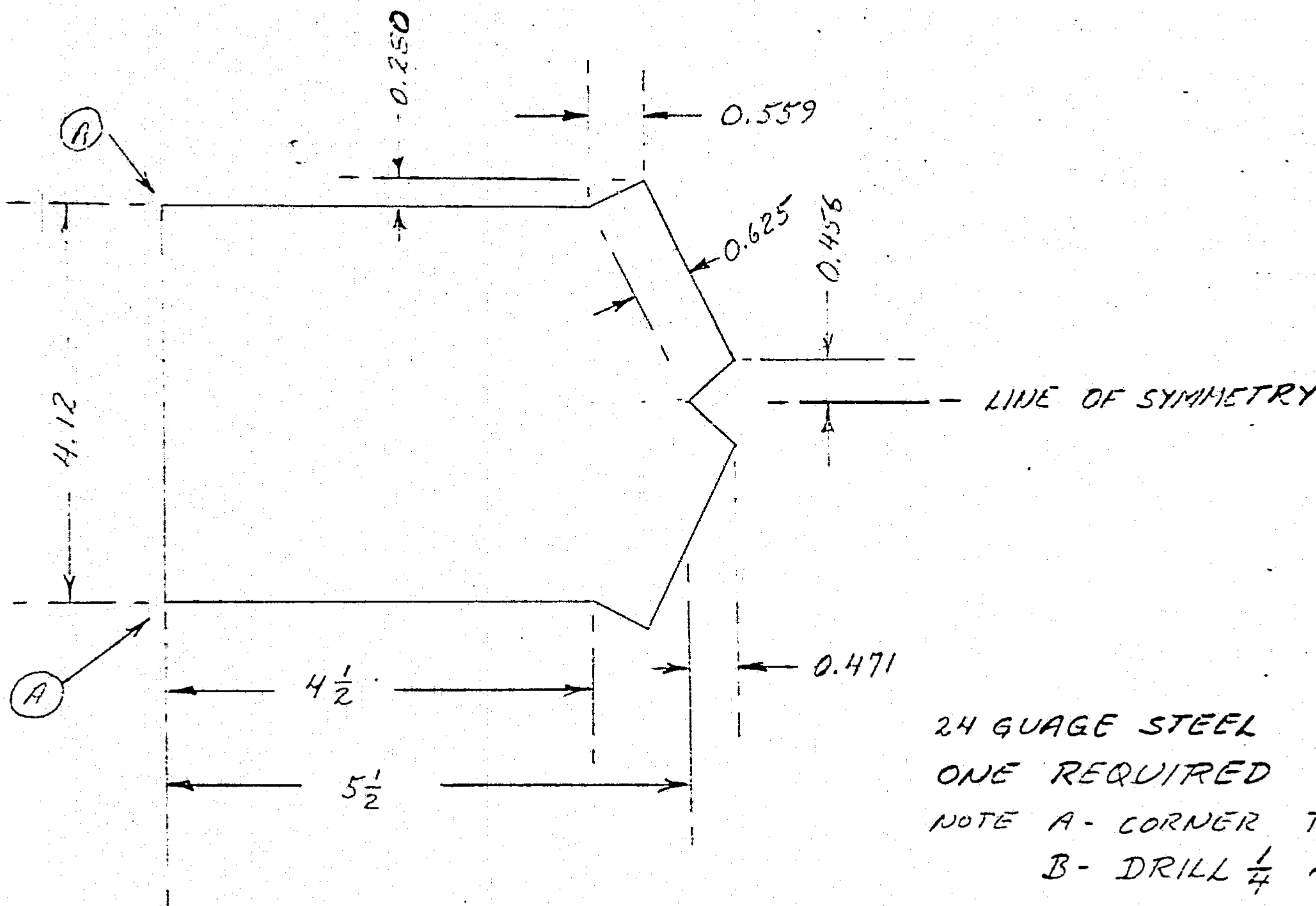

24 GUAGE STEEL
ONE REQUIRED
NOTE A - CORNER TO BE SQUARE ± 1/2 DEGREE
B - DRILL 1/4 AFTER BENDING

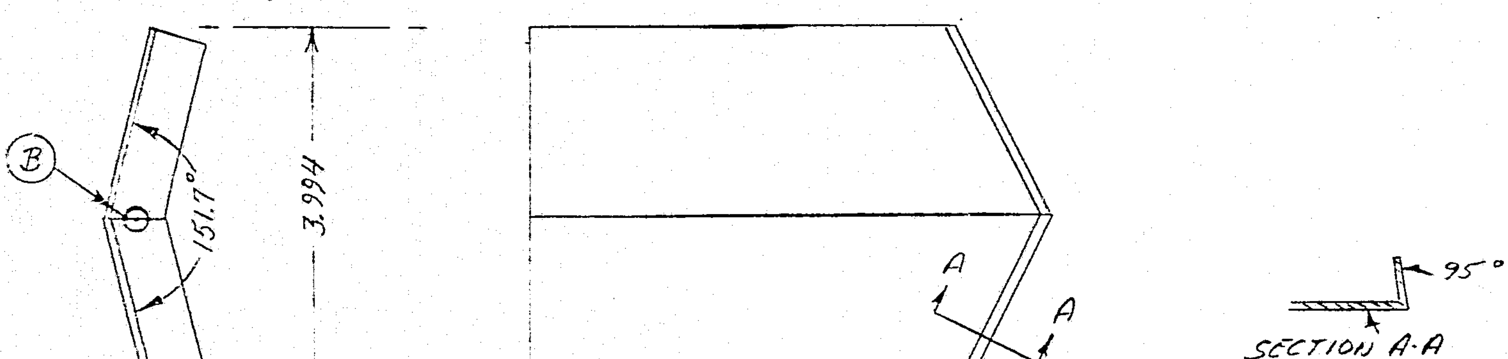

SEPARATOR BAFFLE